CHALMERS

Flexural Strengthening of Glued Laminated Timber Beams with Steel and Carbon Fiber Reinforced Polymers

Master's Thesis in the International Master's Programme Structural Engineering

JOBIN JACOB

OLGA LUCIA GARZON BARRAGÁN

Flexural Strengthening of Glued Laminated Timber Beams with Steel and Carbon Fiber Reinforced Polymers

Master's Thesis in the International Master's Programme Structural Engineering

JOBIN JACOB

OLGA LUCIA GARZON BARRAGÁN

Flexural Strengthening of Glued Laminated Timber Beams with Steel and Carbon Fiber Reinforced Polymers
Master's Thesis in the International Master's Programme Structural Engineering
JOBIN JACOB
OLGA LUCIA GARZON BARRAGÁN

Cover: Moment-Curvature diagram showing the nonlinear behaviour due to compressive plastification, Stress state in the cross section when timber plastifies in the compressive zone, Experimental setup for testing strengthened glulam beams at Chalmers University of Technology

Flexural Strengthening of Glued Laminated Timber Beams with Steel and Carbon Fiber Reinforced Polymers
Master's Thesis in the International Master's Programme Structural Engineering
JOBIN JACOB
OLGA LUCIA GARZON BARRAGÁN

Department of Civil and Environmental Engineering
Division of Structural Engineering
Steel and Timber Structures
Chalmers University of Technology

ABSTRACT

Composite construction methods are becoming more and more popular in construction industries with the introduction of newer construction materials and technical know how of integrating different materials for achieving desired engineering properties. Timber industry is also getting more and more adapted to composite technologies with the introduction of the so called 'highly engineered wood products'. The present study is an effort to investigate the viability of using Steel and Carbon fiber reinforced polymer as reinforcements in glued laminated timber beams. This thesis specifically focuses on the investigation of different configurations to come up with an optimum reinforcement arrangement which maximises the stiffness/strength properties.

The present study includes modelling using Matlab, an FE Model using I-deas and also experimentation on full-scale specimens. A nonlinear model was prepared in Matlab to simulate the behaviour of the beam under flexural loading. The FE model investigates the development of interfacial shear stresses in the glue line between timber and the reinforcement and predicts the possibility of de-lamination or de-bonding by failure of adhesive in shear. Full scale beams were prepared based on the results of analysis and were tested in bending for confirmation with the model.

The Nonlinear model developed in Matlab considering the plastification of timber in the compressive zone as well as the yielding behaviour of metallic reinforcements was able to predict the global behaviour of the beam under flexural loading. It could be seen that a configuration with 25% of reinforcements in the compression side and the rest 75% in the tension side performs well in terms of stiffness and ultimate strength. The FE model verifies that the shear stress in the adhesive is not high enough to cause adhesive failure in the glue-line under short term loadings. The experiments confirm the viability of the reinforcing schemes and the working procedures. The results from experiment showed very good agreement with the nonlinear model. A stiffness increase of 80% to 107% and a moment increase of 57% to 96% were achieved in the laboratory tests.

Key words: Nonlinear Modelling for strengthened Glulam, compressive plastification of timber, yielding of metallic reinforcements, interfacial shear stresses, testing of reinforced glulam, timber strengthening,

II

Contents

Preface

This master thesis was carried out at the Division of Steel and Timber Structures, Department of Structural Engineering, Chalmers University of Technology, Göteborg, Sweden, as a partial fulfillment of our International Masters Degree in Structural Engineering.

This project have been carried out with the support from Moelven Töreboda AB, manufacturer of glulam, as well as Sika Group Ltd., manufacturer of fiber reinforced polymer composites and adhesives. We would like to extend our thanks for their support in terms of raw materials and financial assistance.

We would like to extend our immense gratitude to Dr. Mohammad Al-Emrani, the examiner of our master thesis, for his valuable advices, constant support and dedicated guidance.

We would like to thank our supervisor from university, Dr. Marie Johansson, for her unconditional support and supervision all along the course of our thesis.

We also thank our supervisor from industry, Dr. Roberto Crocetti, Moelven Töreboda AB, for his advises and valuable time with us. With him, a person from industry, we always had a chance for expert advice regarding industrial implications.

Special thanks to our opponent group Silvio Formolo and Roland Ganström for their cooperation and suggestions throughout this work.

We would like to dedicate this work to our families and friends back home whose constant support and intercessions has always been a source for inspiration. They all are thousands of miles away, but have contributed in their on ways through their wishes and prayers to make this work possible.

Last but not the least; we would like to thank all our colleagues for their help during difficulties, discussions, inspiration and all lighter moments.

Göteborg, February 2007

Jobin Jacob

Olga Lucia Garzon Barragan

Notations

a	Distance of load application from end supports
b_{gl}	Width of Glulam
d_t	Depth till centre of tensile reinforcement from beam top
d_c	Depth till centre of compressive reinforcement from beam top
d_{t_fail}	Depth at which failure is considered
h_{gl}	Height of glulam
y_{el}	Depth of Neutral Axis in the linear elastic phase
y_{pl}	Depth of Neutral Axis in the plastic phase
A_{rc} , A_{lc} , A_{frp_c}	Area of compressive reinforcement
A_{rt} , A_{lt} , A_{frp_t}	Area of tensile reinforcement
E_{gl}	E-modulus of glulam
E_r , E_{frp} , E_{steel}	E- modulus of Reinforcement (FRP, Steel)
EI_{ef}	Stiffness of effective cross section
F_c	Sectional Compressive Forces in glulam
F_t	Sectional Tensile Forces in glulam
F_{frp_t}	Forces in tensile Reinforcement
F_{frp_c}	Forces in Compressive Reinforcement
I_{ef}	Moment of Inertia of effective cross section (transformed)
L_{beam}	Length of the beam
M_u , M_r	Ultimate moment resistance
P	Point Load applied on the beam
Z_c	Distance of compressive reinforcement from compression edge

Z_t	Distance of tensile reinforcement from tension edge
Z_p	Depth of Compressive plastification
ε_c	Compressive strain in outermost compressive glulam fiber
ε_t	Tensile strain in outermost tensile glulam fiber
ε_{rc}	Strain at middle of compressive reinforcement
ε_{rt}	Strain at middle of tensile reinforcement
$\varepsilon_{el\_c\_gl}$, ε_{c_gl}	Elastic compressive strain limit in glulam
$\varepsilon_{el\_t\_gl}$, ε_{t_gl}	Elastic tensile strain limit in glulam
$\varepsilon_{pl\_c\_gl}$	Plastic compressive strain limit in glulam
$\varepsilon_{pl\_t\_gl}$	Plastic tensile strain limit in glulam
$\varepsilon_{pl\_c\_st}$	Plastic compressive strain limit in steel
$\varepsilon_{pl\_t\_st}$	Plastic tensile strain limit in steel
$\varepsilon_{el\_c\_frp}$, ε_{frp_c}	Elastic compressive strain limit in FRP
$\varepsilon_{el\_t\_frp}$, ε_{frp_t}	Elastic tensile strain limit in FRP
f_{cu}, f_{cu_gl}	Ultimate compressive strength of glulam
f_{tu}, f_{tu_gl}	Ultimate tensile strength of glulam
f_{cu_frp}	Ultimate compressive strength of FRP
f_{tu_frp}	Ultimate tensile strength of FRP
f_{cu_st}	Ultimate compressive strength of Steel
f_{tu_st}	Ultimate tensile strength of Steel
$f_{y\_c\_r}$	Yield strength of reinforcement under compression
$f_{y\_t\_r}$	Yield strength of Reinforcement under tension
τ	Shear stress

σ_c	*Compressive stress*
σ_t	*Tensile Stress*
δ	*Mid-span Deflection*
$\delta_{\lim}$	*Deflection limit*
σ_{rc}	*Stress in the compressive reinforcement*
σ_{rt}	*Stress in the tensile reinforcement*
Φ	*Curvature*

Abbreviations

Glulam	*Glued Laminated Lumber*
FRP	*Fiber Reinforced Polymer*
CFRP	*Carbon Fiber Reinforced Polymer*
LVL	*Laminated Veneer Lumber*
GFRP	*Glass Fiber Reinforced Polymer*
NSM	*Near Surface Mounted*
FEA	*Finite Element Analysis*
LVDTs	*Linear Variable Differential Transducers*
FBD	*Free Body Diagram*
SG	*Strain Gauge*
MOR	*Moment of Resistance*

1 Introduction

Enhancing structural properties of building units by combining reinforcements with conventional building materials has been an age old concept used extensively in construction industry. For example, the combination of reinforcing steel and concrete, as a tailored macroscopic material system, has been the basis for a number of structural systems used for construction in the twentieth century. Designers and material experts continue to develop and adopt newer forms of materials that could be used in conjunction with conventional building materials like steel, concrete and timber which eventually would assist in the development of stronger, larger, more durable, energy efficient and aesthetic structures.

Wood has adequate strength both in tension and compression, comparable with strength properties of conventional quality concrete. But this high strength is usually accompanied with low stiffness properties, so that the design is usually controlled by deflection limitations. The purpose of reinforcing timber beams is to achieve better stiffness properties. Increased stiffness without a need of increasing the depth of the beam may result in substantial space savings along with material savings.

This thesis deals reinforcing of Glued Laminated Timber (GLULAM) beams with Steel and Carbon Fiber Reinforced Polymer (CFRP) composites to address the need for the development of material-adapted structural concepts and construction methods leading to an economic use of new materials and improving their competitiveness in comparison with conventional materials in construction.

1.1 Background

Because of its beauty, strength and ease of handling and assembly, wood has long been in demand as an important building material. But for precise structural applications, the variability in strength and stiffness properties of natural wood, caused by the presence of knots and due to variations in growing conditions, makes it difficult for engineers to predict their load responses. These natural variations could be, to some extent, minimised by using appropriate engineering interventions, which in turn led to the development of a new class of wood products known as 'Engineered wood products'.

Glued laminated timber (Glulam) is one of the most widely used engineered wood products in structural applications. Glulam is made by joining individual pieces of lumber, laminated together under pressure to form large timber elements. These large, laminated timbers can be fabricated in almost any straight or arched configuration for long-span conditions. This allows for the design of large, open spaces with minimal columns. These advances in the structural properties and behaviour of Glulam beams enable smaller wood members or members with lower grades of wood to be substituted for larger members made completely of wood.

The ability to utilize laminated wood members for massive structural applications is often limited by their relatively low bending strength and stiffness when compared to other materials such as concrete and steel. Moreover, long span applications usually call for the need of controlling deflections as well as limiting beam depths for manoeuvrability and aesthetic purposes. One possible way of addressing this problem

is reinforcing the section with some stronger and stiffer material. Earlier researchers focussed on using different materials as reinforcement for timber elements, of which metallic reinforcements like steel bars, steel cables, aluminium plates etc were among the first choices. The introduction of stiffer material in the cross section resulted in increased the overall stiffness of the beams which in turn resulted in lesser deflections.

Recent studies have shown the possibilities for incorporating fibre reinforced plastics in wooden beams in order to achieve better structural properties. Advances in fiber-reinforced plastics and increased availability of synthetic fibers have made fiber reinforced composites a viable alternative for reinforcing timber. Glulam beams reinforced with FRP materials, when designed to fail plastically, generally exhibit higher bending stiffness, bending strength, and ductility while also displaying a reduction in mechanical variability.

1.2 Objectives and Methodology

The aim of this thesis is to study the overall behaviour of reinforced Glulam beams loaded in flexure. The specific objectives can be described as follows.

- To investigate the possibility of decreasing beam depth and deflections in un-reinforced Glulam beams used as principal load bearing members in residential as well as in bridge structures.

- The main focus of this thesis had been on identifying effective interventions that for increasing the stiffness properties as well as increasing bending strength.

- To identify the possible failure modes and to propose adequate precautions in design.

- To study in comparison the strengthening effect of steel and CFRP.

- To optimise the reinforcement configuration and reinforcement distribution using modelling techniques for achieving maximum strength/stiffness properties.

The methodology used to attain the objectives is as follows:

- The study of overall behaviour of the beams with different configurations as well as optimisation of reinforcement configuration was done using a nonlinear model in Matlab.

- The effect of shear stress on the glue line between the reinforcement and Glulam has been investigated by a Finite Element Model.

- The optimised beam configurations have been fabricated and tested for conformity with the models.

1.3 Limitations

This study had been done in the frame of a master thesis, and is having the following inherent limitations

- This study considers the Glulam beams as a single cross section, ie, without considering the difference in material properties in each laminate.

- The glue lines between lumber laminates in Glulam are assumed to be providing perfect bonding between laminates, so that there is no slip between the laminates.

- The study does not consider any creep effects and other long term effects. The study also excludes the effects of moisture as well as fatigue loading on the structure.

- The number of beams tested was few, so the results lack good statistical control.

- The test considered only one beam cross section, the effect an increased/decreased cross sectional area is not considered.

- The effect of only short term loading was studied.

2 Literature Study

In the past few decades, studies have focussed on different methods for reinforcing timber in order to use them in heavily loaded civil structures. Researchers from different parts of the world have been working on different issues related to the production, application and maintenance of composite Glulam. Glulam industry, along with large number of researchers and institutions are actively trying to develop more viable and energy efficient products for civil infrastructure.

This chapter intends to put on record the previous studies that have been conducted in the field of reinforcing Glulam beams.

2.1 Composite Glulam- Material Components

This section is indented to provide the reader an acquaintance with the materials used and the different methods of reinforcements. The mother material is Glued Laminated Lumber and the reinforcements are Steel and Carbon Fibre Reinforced Polymers. Different types of adhesives used for bonding the reinforcements to the beams are also discussed.

2.1.1 Glued Laminated Lumber (GLULAM)

Glulam can be defined as an engineered, stress-rated timber product assembled from selected and prepared wood laminations bonded together with adhesives with the grain of the laminations approximately parallel in the longitudinal direction. Glulam is fabricated using individual pieces of high strength, kiln-dried lumber, laminated together under pressure to form large timber elements that retain the traditional beauty of wood along with engineered strength, extraordinary fire resistance, thermal efficiency, and dimensional stability. Individual pieces of lumber are usually finger jointed in the longitudinal direction in order to obtain laminates of desired length. Glued laminated timber is considered as a highly engineered wood product due to its unique production process which allows the use of material with desired properties at desired cross section, along with integral quality control. These large, laminated timbers can be fabricated in almost any straight or arched configuration for long-span conditions.

Glulam is typically manufactured using soft-woods and in Europe, the most common species used are Norway spruce and Silver Fir. *Figure 2.1* show two typical Glued Laminated (Glulam) beams.

Figure 2.1 Glued laminated beams of different sizes.

Long-length glulams are appropriate for complete structural systems in many types of buildings including churches, gymnasiums, auditoriums and recreational spaces. Everyday uses in smaller buildings include ridge beams, garage door headers, door and window headers, long-span girders, stair treads and stringers, and heavy timber trusses. *Figure 2.2* shows different standard shapes of Glulam beams.
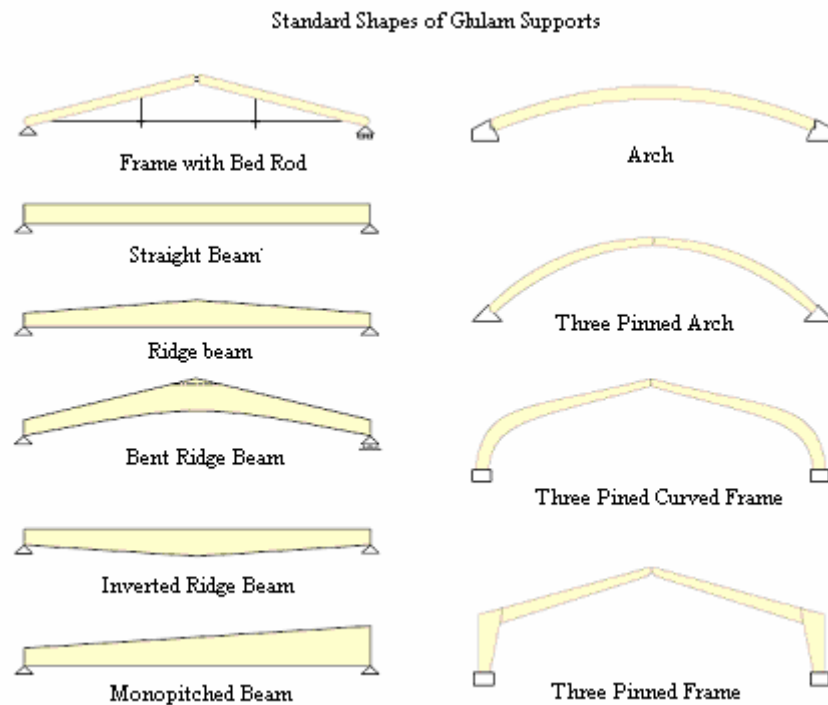
Figure 2.2 Standard Beam profiles. (Courtesy Moelven Töreboda AB)

Advantages of Glulam

Glulam inherits all the advantages of timber like ease to work with, easily joinable, can be planed, nailed, sawn and polished. It has a very good fatigue response just like wooden members. But glulam, as an engineered wood product, incorporates the following special advantages. The literature in this section is taken from Moelven's website *www.moelventoreboda.se.*

- *Versatility:* Glulam can be made to almost any size and used for arches and portals, roof, lintel and floor beams, for columns, rafters and 'A' frames, cross wall purlins and joists. Members can be of uniform or varying depth. They can be straight or curved to suit aesthetic requirements or to provide more structurally efficient designs than can be achieved with straight members. This scope makes Glulam suitable for every type of building.

- *Large Spans:* Glulam can be used over spans of more than 50 metres. Size, length and shape are limited only by the capacity of the various manufacturing plants or, more usually, by restrictions governing the transportation to site.

- *Energy Efficiency:* Glulam is also energy efficient in use. The well known insulation property of timber eliminates the risk of cold bridging where the frame may penetrate external elements of the structure. Its low thermal mass helps reduce fuel bills by absorbing little space heating energy.

- *Good Strength to weight Ratio:* Glulam is one of the strongest structural materials per unit weight. Compared with structural steel or concrete it can produce a lighter superstructure with a consequent economy in foundation construction. A structural steel beam may be 20% heavier and a concrete beam 600% heavier than an equivalent Glulam beam.

- *Superior Fire Performance:* Glulam has a high and predictable resistance to fire. Unlike steel and reinforced concrete it will not twist or spall in fire and, in some countries Glulam beams attract lower fire insurance premiums than steelwork

- *Corrosion Resistance:* Timber and the synthetic adhesives used in bonding Glulam have a remarkable resistance to chemical attack and therefore Glulam is often chosen as the preferred structural material for buildings such as salt barns, water treatment plants, etc.

- *Aesthetics:* The natural appearance of Glulam is sufficiently attractive to make it eminently presentable with no cladding - indeed, used as exposed beams, Glulam adds to the aesthetic appeal of a structure.

- *Reduced variability:* the laminating process randomly disperses the strength-reducing characteristics (SRC), such as knots, throughout the member. This random dispersal of SRCs, results in reduced variability in material properties and increased strength characteristics.

- *Formability:* Glulam is easily formable, which allows the manufacture of beams and other structural members with even shapes and curves

- *Economical:* A direct cost comparison shows that it is competitive with other structural materials; and the lower weight of glulam leads to savings on foundations, transport and erection.

Applications of Glulam

The first experiments with the lamination of timber were carried out some 100 years ago. During the ensuing decades improvements in adhesives have opened up great possibilities for creating exciting timber structures by incorporating laminated glulam beams and trusses and structural laminated arches and curves. The applications range from ordinary residential buildings to large timber bridges. The variety of shapes and curves makes glulam famous among architects. Glulam finds its application as major structural elements in religious buildings, indoor stadiums, monumental buildings, factory buildings etc.

In Scandinavia, Glulam is used in major Civil engineering infrastructures such as bridges, large auditoriums, public buildings and so on. Given that Scandinavia is a region blessed with plentiful forests, it is not surprising that glulam finding favour as a structural material for a growing number of structural applications. *Figure 2.3* shows some constructions in Scandinavia using Glulam beams.

Figure 2.3 Glulam Constructions: (1) Bridge over Vihantasalmi, Finland; (2) Maria's Chappel Levi, Finland; (3) Leonardo Bridge Aas, Norway; (4) Universeum, Gothenburg, Sweden

Glulam Manufacturing

Glulam manufacture is carried out in almost the same way regardless of manufacturer or country. Prior to glulam fabrication, all lumber is visually graded for strength properties and mechanically evaluated to determine the modulus of elasticity (E). These two assessments of strength and stiffness are used to determine where a given piece will be situated in a beam or column. Once graded, the individual pieces of laminates are end joined into full length laminations of constant grade and each end-joint is proof tested (moisture content in the laminates 8—15%). Then, the laminated lengths are arranged according to the required grade combination for the product being manufactured. Each laminations then moves through a glue applicator and the pieces are reassembled into the desired configuration at the clamping area. Hydraulic or manually activated clamps are placed around the member, and are brought into contact with steel jigs which have been pre-anchored to supports to provide the desired curvature or pattern. As pressure is applied, the laminations are adjusted for proper alignment .Once full clamping pressure is reached; the member is stored at a controlled temperature until the glue is fully cured.

The difference in moisture content between adjacent laminates may not exceed about 5%. The strength of the glue line will then be optimal and the moisture content in the finished construction will be balanced, avoiding troublesome splitting.

Figure 2.4 shows schematically, the manufacturing process at Moelven Töreboda AB. 2003.
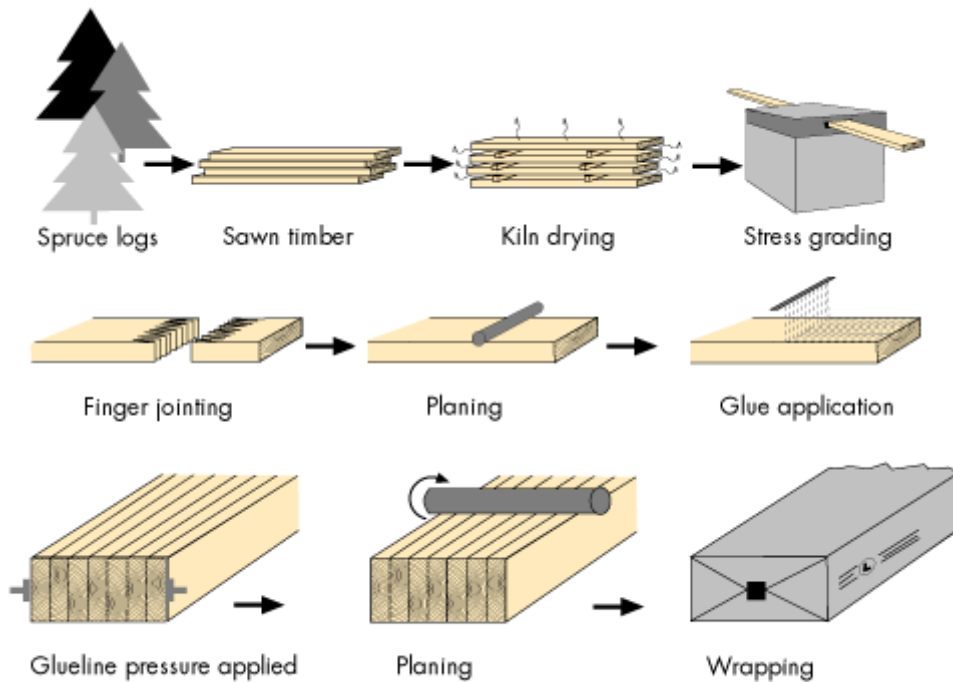
Figure 2.4 Glulam Manufacturing. (Courtesy Moelven Töreboda AB)

The cross-section of the Glulam can be built up of laminates with approximately the same strength, resulting in a "homogeneous Glulam" (*Figure 2.5* a) To utilize the strength of the timber to best advantage, however, it is customary to use timber of higher quality in the outer laminates of the cross-section, where stresses normally are highest, yields a "combined Glulam" (*Figure 2.5* b).
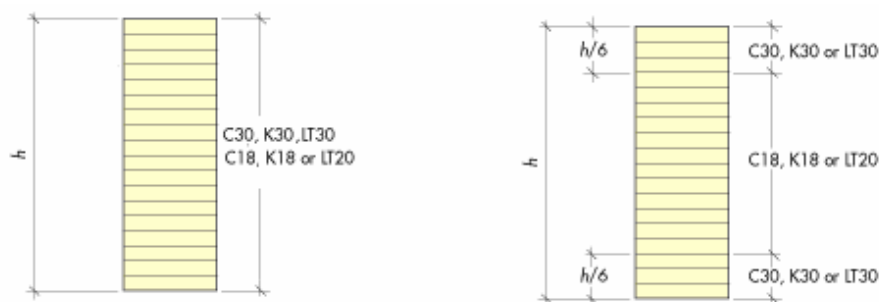
Figure 2.5 Lay-up of Homogeneous Glulam and Combined Glulam. (Courtesy Moelven Töreboda AB)

Individual pieces of timber are first stress graded. The strength grades required for a particular cross section is decided. These individual pieces of timber are finger jointed to form laminates. The laminates are cut to the required length and placed on top of each other. For combined Glulam, attention must be paid to the placing of the inner and outer laminates. To reduce internal stresses the laminates are turned so that the core sides face the same way throughout the cross-section. The outermost laminates

are however always turned with the core side outwards. *Figure 2.6* illustrates a finger joint used in Glulam beams.
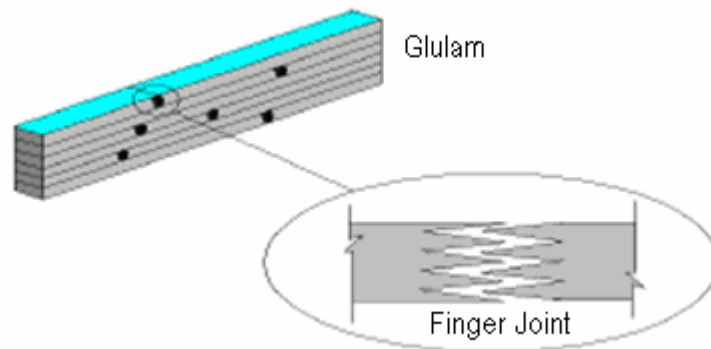
Figure 2.6 Finger joints in Glulam Beams.(Hernandez et al., 1997)

In prEN 1194 (September 1993) five strength classes for glulam are defined, as it is described in *Table 2.1*.

Table 2.1 Strength classes for glued laminated timber (Anon. 1995a)

Strength class		GL 20	GL 24	GL 28	GL 32	GL 36
$f_{m,g,k}$	(N/mm^2)	20	24	28	32	36
$f_{t,0,g,k}$	(N/mm^2)	15	18	21	24	27
$f_{t,90,g,k}$	(N/mm^2)	0,35	0,35	0,45	0,45	0,45
$f_{c,0,g,k}$	(N/mm^2)	21	24	27	29	31
$f_{c,90,g,k}$	(N/mm^2)	5,0	5,5	6,0	6,0	6,3
$f_{v,g,k}$	(N/mm^2)	2,8	2,8	3,0	3,5	3,5
$E_{0,mean,g}$	(N/mm^2)	10 000	11 000	12 000	13 500	14 500
$E_{0,05,g}$	(N/mm^2)	8 000	8 800	9 600	10 800	11 600
$\rho_{g,k}$	(kg/m^3)	360	380	410	440	480

2.1.2 Steel

Steel is the most common metallic reinforcement used in reinforcing timber. The most important attraction of steel reinforcement is its availability and comparatively lesser cost. Also steel reinforcements were used in conjunction with other materials such as concrete and were proved effective as a reinforcing element.

2.1.3 Fiber Reinforced Polymers (FRP)

Fibre reinforced polymer (FRP) matrix composites developed primarily for the aerospace and defence industries (Fletcher 1994) are a class of materials that present immense potential as a construction material in civil infrastructure, both for the rehabilitation of existing structures as well as for the construction of new facilities. The results of the research efforts in composites, initiated nearly a decade ago in several countries, are now being incorporated into core civil engineering and marine

infrastructure applications. The past few decades have seen outstanding advances in the use of composite materials in structural applications. There can be little doubt that, within engineering circles, composites have revolutionised traditional design concepts and made possible an unparalleled range of new and exciting possibilities as viable materials for construction.

An extensive review on the different applications of FRP was made by Fletcher (1999). The facts in the text below relating to FRP are taken from this review unless otherwise stated. *Figure 2.7* illustrates the wide range of applications of fiber reinforced plastics in Structural design.

```
                    ┌──────────────────────┐
                    │ Fibre Reinforced Composites │
                    │         (FRP)        │
                    └──────────────────────┘
                                │
        ┌───────────────────────┼───────────────────────┐
 ┌──────────────┐      ┌──────────────┐        ┌──────────────┐
 │ New construction │      │    Repair    │        │  Structural   │
 └──────────────┘      └──────────────┘        │ rehabilitation │
                                               └──────────────┘
                                                      │
                                              ┌──────────────┐
                                              │ Structural design │
                                              └──────────────┘
```

- High Specific Strength and Stiffness
-Enhanced Fatigue life
-Corrosion Resistance
-Controllable Thermal properties
-Part Integration
-Faster field installation
-Tailored Properties

Advantages of FRP

Disavantages of FRP

- Higher initial material cost
-Additional labor input
-Manufacturing process
-Reduced architectural appearance

Concrete
(i.e. Bridges, Column, beams, I-girder and box beam repair)

Timber Strutures
(Glulam beams, Timber joints, Bridges, Shear walls)

Steel
(Steel beam, Strengthening of steel-concrete configuration)

Marine Structure
Sandwich panel, FRP-plywood.

Figure 2.7 Classification, advantages and disadvantages of Fibre-reinforced materials in structural design, Fletcher (1999),

Fiber reinforced polymers are a group of high strength composite materials which acquires its extraordinary strength capabilities through the synergistic combination of fibers in a polymer resin matrix, wherein the fiber reinforcements carry load in pre-designed directions (taking advantage of anisotropy). (Lopez-Anido, 2000); Fiber Reinforced Polymers encompass a wide variety of composite materials with a polymer resin matrix that is reinforced (combined) with fibers in one or more directions. With their high strength and stiffness, the fibers carry the loads imposed on the composite, while the resin matrix distributes the load across all the fibers in the structure. By aligning fibers in one direction in a thin plate or shell, called lamina, layer, or ply, the maximum strength and stiffness of the unidirectional lamina can be obtained. Random orientation of fiber in the matrix results in a more isotropic behaviour.

The properties of the FRP material are not just predicted by simply summing the properties of its components. The fibers and resin matrix acts complementary to provide desirable properties of both the components. Most polymer resins are weak in tensile strength but are extremely tough and malleable, while the thin fibers have high tensile strength but are susceptible to damage. It should be emphasized that properties of FRP composites depend on the properties of material constituents (i.e., reinforcing fiber, matrix, and fillers), their corresponding volume fractions, their orientation and dispersion, and so on. Based on carbon fiber properties, carbon fibers can be grouped into the following categories.

- Ultra-high-modulus, type UHM (modulus >450Gpa)

- High-modulus, type HM (modulus between 350-450Gpa)

- Intermediate-modulus, type IM (modulus between 200-350Gpa)

- Low modulus and high-tensile, type HT (modulus < 100Gpa, tensile strength > 3.0Gpa)

- Super high-tensile, type SHT (tensile strength > 4.5Gpa)

Constituents of Fibre reinforced Polymer reinforcements

For using Fibre reinforced polymers as reinforcements in timber structures, it is essential to have a clear understanding of its constituents. The strength of the composite is basically determined by the fibers within them. The strength stiffness and volume fractions of the fibers used will reflect on the overall behaviour of the composite. The binder material, usually a polymeric resin, does not have much to do with the strength properties; rather, it holds the whole system together, to act as a composite member. The orientation of the fibers controls the properties of the composite in the three directions. A random distribution of fibre strands results in an isotropic composite, while a more oriented fibre distribution will result in more anisotropic composites.

The following sections detail the comparisons of the different reinforcement fibers and resin matrices that are commonly used in the FRP industry. The different FRP fabrication processes are also discussed. An extensive review o the subject of FRP was made by Fletcher (1994) and the facts in the text below related to FRP are taken form this review unless otherwise stated.

a. Fibers

There are three main types of fiber reinforcements used in polymer matrix: glass fibers, carbon/ graphite fibers, and synthetic polymer fibers (such as Kevlar and Aramid). The majority of the fibers used in the composite industry are basically glass. The basic building blocks for these fibers are carbon, silicon, oxygen, and nitrogen, each of which is characterized by strong covalent inter-atomic bonds, low density, thermal stability, and relative abundance in nature. Depending on the fiber type, filament diameter, sizing chemistry, and fiber form, a wide range of properties and performance can be achieved.

1. Glass Fibers: The commonly used glass fibers are E-glass (E for electrical), S-glass (S for strength), and C-glass (C for corrosion). Other types of glass fibers include D-glass (D for dielectric) and A-glass or AR-glass (AR for alkaline resistant). E-glass is the most commonly used glass fiber because it is the most economical for composites, offering sufficient strength at a low cost.

2. Carbon/Graphite Fibers: Carbon fibers, also called graphite fibers, are strong, lightweight, and chemically resistant. Generally, carbon fibers are produced using the following three types of raw materials or precursors: polyacrylonitrile (PAN), pitch, and rayon $(C_6H_{10}O_5)_n$. However, the major advantage of rayon fibers is that they possess superior qualities when used as the reinforcement in metal matrix composites. They are slightly denser compared to PAN and pitched fibers. Carbon fibers made from PAN precursors are much stronger than those made from rayon.

3. Polymer Fibers: Polymer fibers, sometimes called organic fibers, are made by a process of aligning the polymer chains along the axis of the fiber. They can also exhibit very high strength and stiffness, good chemical resistance, and low density if a suitable process is used for its manufacture.

Table 2.2 shows the major properties of some commonly used reinforced fibers.

Table 2.2 Properties of different types of fibers

Fiber type	Diameter [μm]	Density y[g/cm2]	Tensile Modulus [GPa]	Tensile Strength [GPa]	Elongation [%]	Coefficient of thermal expansion [$10^6/°C$]
E-Glass	8-14	2.54	72.4	3.45	1.8-3.2	5.0
C-Glass	-	2.49	68.9	3.16	1.8	7.2
S-Glass	10	2.49	85.5	4.59	5.7	5.6
D-Glass	-	2.14	55.0	2.5	4.7	3.1
PAN Carbon	7-10	1.67-1.9	228-5.7	1.72-2.93	0.3-1.0	-0.1to-1.0
Pitch Carbon	10-11	2.02	345	1.72	0.4-0.9	-0.9to-1.6
Rayon Carbon	6.5	1.53-1.66	41-393	0.62-2.20	1.5-2.5	-
Kevlar-29	12	1.44	62	2.76	3-4	-2
Kevlar-49	12	1.48	131	2.80-3.79	2.2-2.8	-2
Kevlar-149	-	1.47	179	3.62	1.9	-
Spectra 900	38	0.97	117	2.58	4-5	-

b. Polymer Matrices

The polymer matrix generally accounts for 30–40% of a FRP composite material. The purposes of the matrix material is to hold the fibers together and maintain the fiber orientation, transfer the load between fibers during the FRP composite application, and carry transverse and inter-laminar shear stresses within the FRP composites. The polymer matrix also protects the fibers from the environment and mechanical abrasion. The following are the most commonly used matrices. *Table 2.3* lists the properties of the most commonly used polymer matrices.

1. *Polyester.* Polyesters are the most widely used class of thermo-sets in the construction market. They have a relatively low price, ease of handling, and a

good balance of mechanical, electrical, and chemical properties. The unsaturated polyester resin has a low viscosity and can be dissolved in a reactive monomer, such as styrene, divinyle benzene, or methyl methacrylate.

2. **Vinyl Ester**. Vinyl ester offers a transition in mechanical properties and cost between the easily processed polyesters and higher-performance epoxy resins which are described in the following paragraph. Vinyl esters are synthesized from an unsaturated carboxylic acid (usually methacrylic acid) and an epoxy resin. Different vinyl ester resins are available for applications.

3. **Epoxy.** Epoxy resins are widely used in applications such as honeycomb structures, airframe and missile application, and tooling because of their versatility, high mechanical properties, high corrosion and chemical resistance, and good dimensional stability. Compared to polyester, epoxy resins shrink less and have higher strength / stiffness at moderate temperatures. They also cure slowly and are quite brittle after they are fully cured. Epoxy resins typically are twice the cost of vinyl esters.

4. **Phenolics**. Phenolic resins are the predominately used adhesive system for the wood composite industry. Therefore, as a reinforcement of wood composites, FRPs manufactured using phenolic resin should be more compatible with the wood composite materials. Phenolic resins are usually dimensionally stable to temperature. They have excellent physical and mechanical durability. They also have a good adhesive property, low smoke production, and low flammability. Phenol-resorcinol formaldehyde (PRF) resins are very popular as a resin matrix for FRP and as a binder in many other applications.

Table 2.3 Properties of the commonly used Resin Matrices in FRP.

Resin Matrix	Density [g/cm³]	Tensile Modulus [GPa]	Tensile Strength [MPa]	Compressive Strength [MPa]	Elongation [%]	Coefficient of thermal Expansion [%]	Shrinkage on Curing [%]	Glass Transition Temp [⁰C]
Polyester	1.1-1.5	1.2-4.5	40-90	90-250	2-5	60-200	4-12	50-110
Vinyl ester	1.15	3.0-4.0	65-90	127	1-5	53	1-6	100-50
Epoxy	1.1-1.4	2-6	35-130	100-200	1-1.85	45-70	1.5	50-250
Phenolic resin	1.25-1.4	-	55	-	1.8	-	1.1	-

Manufacturing FRP

FRP is manufactured by incorporating reinforcement fibers in appropriate polymer matrices. The fibers are placed either unidirectional or randomly and is encapsulated in matrices which hold them together as a composite material. The manufacturing processes vary so much according to the required properties of the final product.

The manufacturing process basically incorporates different methodologies for introduction of resin in liquid form in between fibres, which on solidification forms a strong substrate for the fibers which holds them together. During the solidification processes, it passes from the liquid state to the solid state by copolymerization with a

monomer that is mixed the resin - the phenomenon which leads to hardening. This can be done using either a chemical (accelerator) or heat.

The main steps in manufacturing include wetting of the reinforcements with the resin (which is in liquid form), forming (shaping) into required shapes/ dimensions, compaction, and curing. Each of these steps can be done in verity of ways, depending upon the type of matrices (thermo set/thermoplastic), type of fiber (continuous/ chopped), orientation of fibers (unidirectional/multidirectional), level of quality control required(aerospace applications require high quality control), and so on. A variety of methods are used according to the end item design requirements.

The major manufacturing processes are resin transfer moulding, vacuum injection moulding, wet lay-up, tape lay-up, spray-up, vacuum bag process, press moulding, pultrusion etc.

The following figure represents the major steps used in all manufacturing processes.
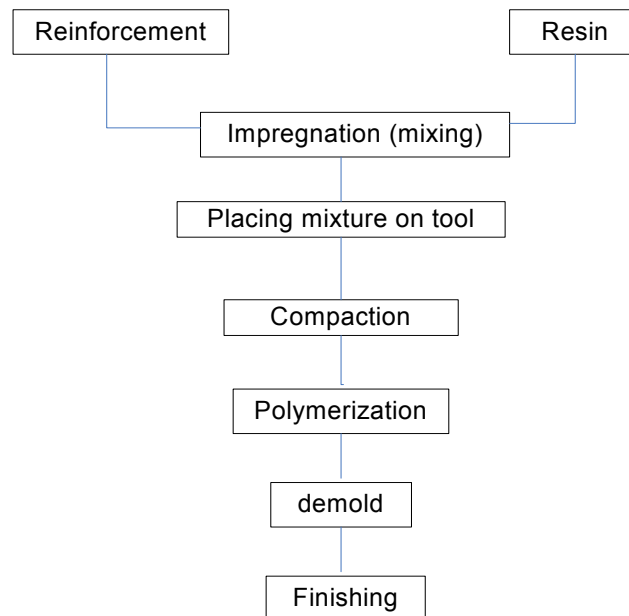
Figure 2.8 Major steps in FRP manufacturing.

In this thesis, the CFRP used falls in the category of Pultruded plates. The process of pultrusion is explained briefly in the following section.

Pultrusion Process. Pultrusion is a continuous, automated closed-moulding process that is cost effective for high volume production of constant cross section parts. Due to uniformity of cross-section, resin dispersion, fibre distribution & alignment, excellent composite structural materials can be fabricated by pultrusion. The basic process usually involves pulling of continuous fibres through a bath of resin, blended with a catalyst and then into pre-forming fixtures where the section is partially pre-shaped and excess resin is removed. It is then passed through a heated die, which determines the sectional geometry and finish of the final product. The resin gets polymerised in the process of curing. This continuous and uniform method ensures consistency throughout the entire product length, therefore eliminating the possibility

of weak spots. The profiles produced with this process can compete with traditional metal profiles made of steel and aluminium for strength and weight.

The rate of production varies between 0.5 and 3 m/minute, depending on the nature of the profile. In *Figure 2.9* schematically represents the Pultrusion Process.
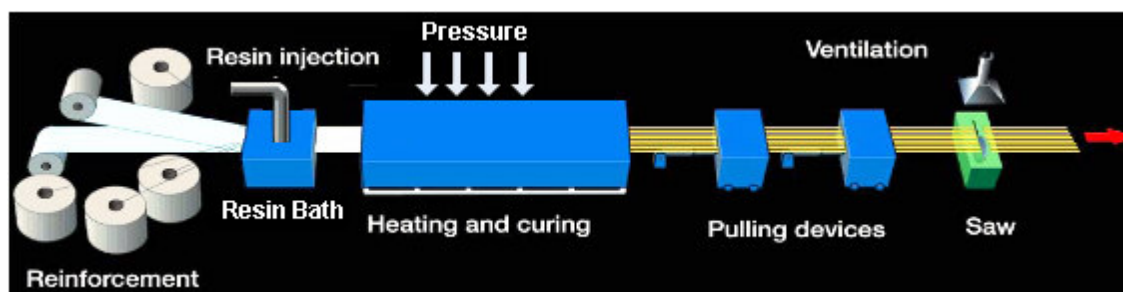
Figure 2.9   Pultrusion process (Fiberline Composites)

2.1.4 Adhesives

The bonding of an adhesive to an object or a surface is the sum of a number of mechanical, physical, and chemical forces that overlap and influence one another. As it is not possible to separate these forces from one another, we distinguish between a) mechanical interlocking, caused by the mechanical anchoring of the adhesive in the pores and the uneven parts of the surface, b) electrostatic forces, as regard to the difference in electro-negativities of adhering materials, c) adhesion mechanisms based on with intermolecular and Chemical bonding forces that occur at the interfaces of heterogeneous systems.

Table 2.4 shows different adhesives which are used in construction industry.

Table 2.4 Adhesives

Name of Product	Type	Manufacturer
Sikadur-30	Epoxid	Sika Chemie GmbH
Ispo Concretin SK 41	Epoxid	Ispo GmbH
Collano Purbond HB 110	Polyurathane	Ebnöther AG
Dynosol S-199 with H-629	Resorcin	Dyno Industries

2.2 Composite Timber Structures

Composite or hybrid timber structures are those timber structures which incorporates reinforcing elements within them incorporating the advantages both timber and reinforcing elements to the structure. Timber structures are now-a-days combined with different reinforcing materials to enhance their strength and stiffness properties, which allows them to be used as structural members in more massive constructions. The composite action allows better utilization of the cross section, as the reinforcement prevents premature failure of weak zones. The high strain capacity of the reinforcements allows the fibers in compression to fail plastically upon reach of their ultimate compressive strains, and the fibers in tension to reach their ultimate

tensile capacity. More over the variability in strength properties of reinforced timber seems to be very less compared to un-reinforced ones.

Earlier investigations considered the use of metallic reinforcements in timber structures. Steel and aluminium were the most important metallic reinforcements. The results were quite satisfactory, with an average increase of 40-50% in stiffness as well as strength values for reinforcement ratios as low as 1% (Sliker, 1962). Various adhesive systems and mechanical fasteners were also investigated for connecting the metal reinforcements to the timber elements.

Recent studies about reinforcing timber bring out the possibility of using polymer based fibre composites as reinforcement in timber structures. Different types of fibre–matrix combinations were used with different material as well as different loading configurations. Different fibers such as carbon fibers, glass fibers, aramid fibers and even different natural fibers such as jute, cotton etc were used as primary reinforcing elements in combination with appropriate polymer matrices. *Figure 2.10* is a schematic representation of the methods and applications of reinforcing timber structures (Steiger, 2004).
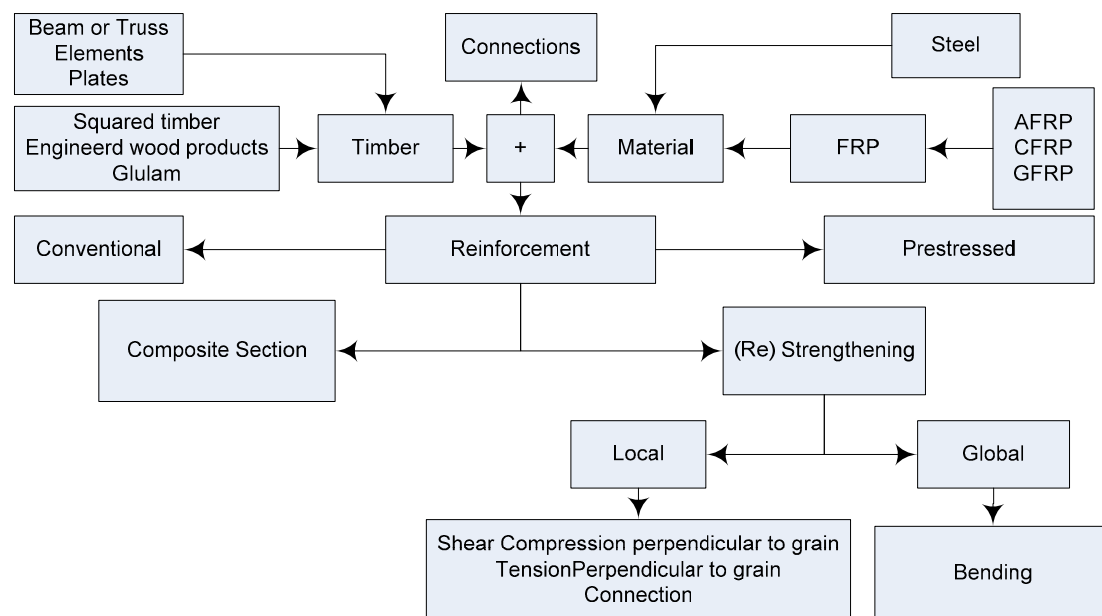
Figure 2.10 Reinforcing Timber sections- applications (Steiger, 2004).

2.3 Flexural Strengthening of Glulam Beams

Glulam has been successfully used as a structural building material in Europe since the 1890's. In the United States, it has been used in buildings since approximately 1935. The introduction of wet use adhesives in the mid 1940's allowed the uses of glulam to be expanded to include exposed applications such as highway and railway bridges, transmission facilities and other structures.
Introduction of Glulam in larger structures like bridges, stadiums, auditoriums etc has resulted in the need for reinforcing them for limiting depth of beam and controlling deflections. With any given amount of reinforcement, the gain in stiffness is influenced by the elastic moduli and allowable stresses of the component materials.

The higher the ratio of strength or stiffness between the component materials are, the greater the gain in global strength/ stiffness.

Variability in timber is the biggest problem which makes it so unpredictable in designs-due to the fact that each tree grows in its own environmental condition, which has very big influence in the introduction of strength reducing factors in timber. *Figure 2.11* represents strength characteristics as well as scatter in strength characteristics in wood, Glulam and in reinforced Glulam (This representation has not been realized experimentally) (Alann André, 2006). By comparing the characteristics of timber, Glulam and FRP reinforced Glulam, we can expect that FRP reinforced glulam should provide less scatter in mechanical properties. The design value is also improved, which means that it could be possible to construct wooden structures with FRP reinforced Glulam that can sustain higher loads.
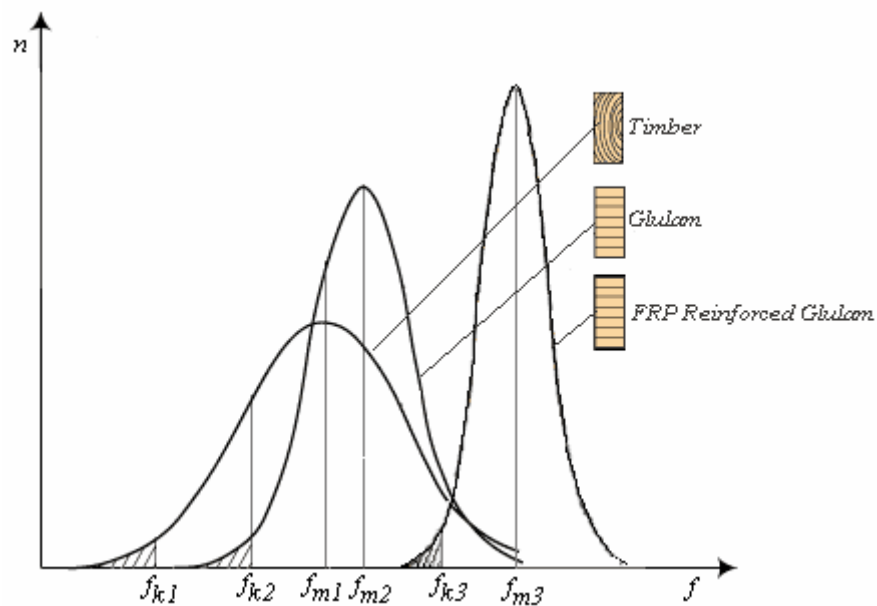
Figure 2.11 Characteristics of timber, Glulam and FRP reinforced Glulam, (Alann André, 2006) (f_k represents characteristic values and f_m mean values)

Reinforcing with Steel

Reinforcing Glulam with steel has been a focus of study for long time, and has been in practice since decades. The old flitch-beam idea, where a metal plate is sandwiched between two joists-so that the three acts together as one unit-was known in the last century. Dagher et.al have documented the historical evolution of the metallic reinforcement in detail. The following discussion regarding the past usage of steel reinforcements in timber is mostly based on his study unless otherwise stated. The first attempt to use steel more rationally was reported by Granholm(1954). He used square steel rods placed in grooves cut into the tom and bottom surfaces. Mark (1961) studied the effects of bonding aluminium to the compression and tension faces of wood core-sections of eight different wood species. Sliker (1962) bonded aluminium sheets between various layers of laminated wood beams. Lantos (1970) reinforced rectangular laminated wood beams with steel rods. Stem and Kumar (1973) studied the effect of steel plate reinforcement for vertically laminated timber beams. Coleman and Hurst (1974) reinforced southern pine beams with light gage steel reinforcement.

Hoyle (1975) tested members composed of nominal dimension lumber with toothed steel plates between lumber pieces. Bulleit, Sandberg, Woods (1989) reported on Spruce-Pine-Fir Glulam beams reinforced in the tension zone with special steel-reinforced tension laminations..

Reinforcing with Fiber Reinforced Plastics (FRPs)

The principal disadvantage of using metallic reinforcements in timber structure was the incompatibility between the wood and the reinforcing materials. More over, the difference in the hydro-expansion properties and stiffness characteristics between wood and metallic reinforcements are so different that it results in the failure in the glue line between them which eventually causes de-lamination.

A possible method for avoiding such problems is to use high strength fiber reinforced plastic (FRP) to reinforce timber glued laminated timber (Glulam) members. A new process of reinforcing Glulam with plastic fiber is rapidly altering the structural timber market by creating stronger, stiffer lighter and smaller structural members using lower grade lumber at significant cost savings over conventional Glulam.

Prior to 1990, a number of studies on wood beams reinforced with fiber and FRP materials were also conducted. Wangaard, (1964) and Biblis, (1965) studied the effect of bonding unidirectional fiberglass/epoxy reinforced plastic to the compression and tension faces of wood cores of various species. Theakson (1965) studied the feasibility of strengthening both laminated and solid wood beams with fiberglass. Krueger and Sandberg (1974 b) studied laminated timber reinforced in the tension zone with a composite of high-strength bronze coated woven steel wire and epoxy. Krueger and Eddy (1974 a) carried out research similar to that of Kruegar and Sandberg (1974 b). Spaun (1981) studied finger-jointed western hemlock cores reinforced with wood veneers and fiber-glass rovings.

In the nineties, research on wood beams reinforced with fiber and FRP materials has increased. Plevris and Triantafillou (1992) studied the effect of reinforcing fir wood with carbon/epoxy fiber reinforced plastics. Plevris and Triantafillou (1995) also discussed the creep behaviour of FRP-reinforced wood. Triantafillou and Deskovic (1992) studied the effect of pre-stressed carbon/epoxy FRP (CFRP) reinforcement bonded to European beech lumber. Davalos, Salim, Munipalle (1992) discussed the response of small yellow-poplar glulam beams reinforced on the tension side with glass/vinylester FRP. Tingley and Leichti (1993) discussed glulam made from lower grade ponderosa pine reinforced in the tension zone with pultruded kevlar and carbon FRP. Abdel-Magid, Dagher, and Kimball (1994) studied nominal 2x4 hemlock beams reinforced tension with carbon/epoxy and Kevlar/epoxy FRP. Sonti, Davalos, Hernandez, Moody, and Kim (1995) discussed yellow-poplar glulam reinforced with pultruded glass/vinylester FRP.

Importance of Ductility

Ductile structural elements allow redistribution of internal forces, dissipation of energy from impact or seismic actions which induces increased structural safety, as well as warning of possible structural failures/overloads. This is possible because of the presence of large plastic or inelastic deformations before failure.

Reinforcing with steel elements imparts ductility to the system, because the steel starts yielding before the timber starts failing. Despite the great potential of FRP materials, they remain largely unexploited by designers and builders due to inappropriate design codes and guidelines and certain properties that still hinder the widespread acceptance of new FRP constructions by structural engineers who are familiar with conventional construction materials like steel or reinforced concrete. One of these disadvantages is the lack of inherent ductility in FRP materials. A second disadvantage is the difficulty of joining structural FRP components due to the brittle fibrous and anisotropic character of the materials.But by using proper reinforcement arrangement of the reinforcement, the problem with lack of ductility in the reinforcement material can be managed. Thanks to the plastic behaviour of timber when loaded in compression. So by using proper reinforcement scheme- i.e. with proper distribution of tension and compression reinforcement- we can induce ductility in the global behaviour of the reinforced beam.

Comparison between Steel and FRP as reinforcements for Glulam members

This thesis deals with the study of the reinforcing effect of two basic types of reinforcements (metallic and FRP) on glulam beams. The following section gives a comparison between the two reinforcement materials used in this thesis.

Table 2.5 Comparison between steel and CFRP

CFRP	Steel
Light weight (lesser strength/weight ratio)	*Comparatively heavy (higher strength/weight ratio)*
More resistant to corrosion	*Prone to rusting and chemical corrosion*
Poor fire resistance	*Better fire resistance*
Low axial coefficient of thermal expansion, so lesser problems in alternating weather	*Thermal expansion coefficient is high, which causes incompatibility in alternating weather*
Favourable creep, relaxation characteristics	*Problems with relaxation in highly stressed elements*
Electromagnetic neutrality	*Electromagnetically active*
Low resistance to concentrated(punching) loads	*More resistant to point loads*
No Ductility(brittle failure)	*Highly ductile*
Higher costs	*Comparatively cheap*
Need expertise in handling and installation	*Conventional material, need lesser expertise(or there exists many experts)*
Difficult to join	*Easier connection/joints*

2.3.1 Configurations and Design Models

Different materials and configurations have been used by researchers all around the world. This section intends to give an overview of the different configurations, materials and methodologies used by different researchers in order to reinforce Glulam sections.

a. Reinforced only on tension side

Glulam beams tested in bending usually fail in the tension side at knots, near to defects, at finger joint positions or at maximum stressed zone. Glulam are commonly reinforced at the tension side to enhance the tensile properties which in turn results in increased flexural strength and stiffness, and to get a compression failure mode, more predictable and more plastic, and thus increasing the evacuation time of a failing wooden structure. *Figure 2.12* shows a liner elastic- elastic plastic model which includes the nonlinear behaviour in compression.
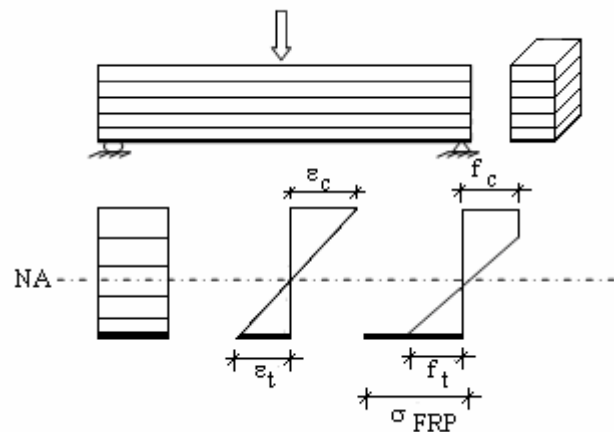
Figure 2.12 Linear elastic, elastic plastic model, Hernandez et al., 1997

The tension failure in wood in bending is brittle, random and difficult to predict (John and Lacroix, 2000). As a result, reinforcement of timber or Glulam beams with FRP layers bonded in the tension side of the beam has been very "popular" the last years and the involved in many investigations (John and Lacroix, 2000; Hernandez et al., 1997; Blaß and Romani, 1998-2000; Fiorelli et al., 2003; Borri et al., 2005; Romani and Blaß, 2001).

Johns and Lacroix (2000) investigated the length effect of CFRP (Epoxy) bonded onto the tension side of timbers (CFRP layer on the full length or on the constant moment area only). It was reported a strength increase between 40 to 70 % if compared to the un-reinforced control beams. A more narrow distribution has also been observed, which indicate a higher strength of the fifth percentile for CFRP reinforced timbers. Most failures occurred in the compression side, which indicated a more ductile behaviour.

Fiorelli et al. (2003) reinforced Pinus Caribea timber beams by using external bonding of FRP sheets on their tension sides. GFRP (1% of the volume of timber) and CFRP

(0.4% of the volume of timber) were used as reinforcement and were compared. The failure process occurred in two stages, were the first failure was due to the crushing of the timber in the compression side followed by shear or tensile failure of the timber, which correspond to a more ductile failure mode. The flexural stiffness increased by 15 to 30%.

Borri et al. (2005) bonded CFRP (epoxy) sheets with different density in the tension area of timber beams. Some beams were reinforced with pre-stressed CFRP sheets. It was reported a maximum load increase around 40 and 60% and a stiffness increment by 22.5 and 29.2% for the un-reinforced beams with lower and higher CFRP density respectively (if compared to the control). Pre-stressing of the CFRP sheets did not lead to any significant improvement compared to the non pre-stressed reinforcement

Blaß and Romani (2001) reported a great increase of the flexural properties with CFRP as reinforcement. Failure at knots or finger joints have however been observed for all specimens at the tension side above the reinforcement.(*Figure 2.13.*)
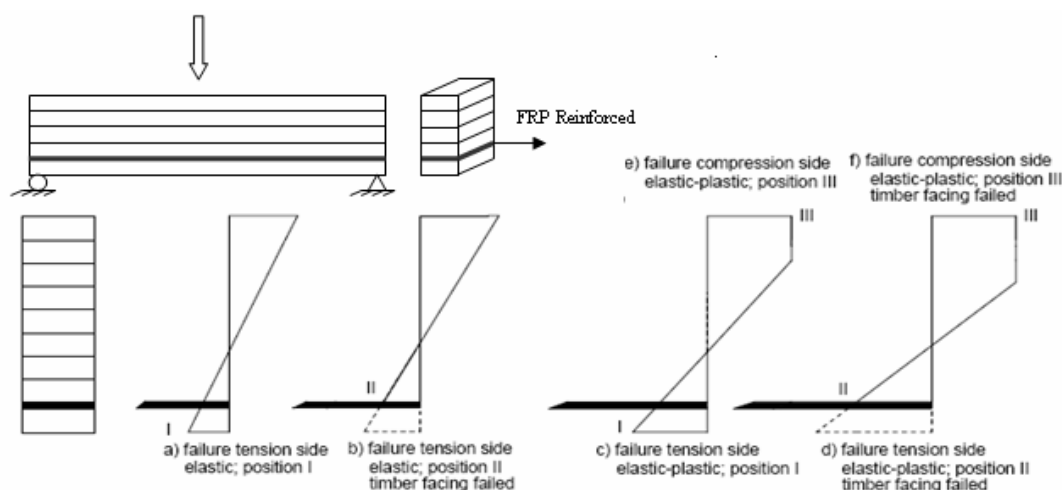

Figure 2.13 Failure Modes, Blaß and Romani , 2001)

Dagher et al. (1996) studied FRP reinforced eastern hemlock Glulam beams. Eastern hemlock was chosen because the authors believed that FRP reinforced Glulam or timber can be used with great results to reinforced inexpensive and low mechanical properties wood like eastern hemlock. Low, medium and high graded Glulam beams were reinforced with FRP (Two different volume ratios: 1.1 and 3.1 %).

Increasing flexural properties have been reported in all cases, but the greatest enhancements have been registered with the lower grades of wood. The flexural strength of the medium grade Glulam beams were affected by increasing the volume ratio of FRP (+33% to +55%, if compared to the un-reinforced beams). However, no significant improvement of the flexural strength was reported with high grade Glulam beams bonded with FRP.Galloway et al. (1996) reinforced southern pine glued-laminate timber with non stressed and pre-stressed aramid (Kevlar) FRP layers. It was shown that the Glulam beams reinforced with the pre-stressed AFRP does not show significant increase of the flexural strength. Most of the beams failed at finger joints in the tension side. Shear strength tests of Kevlar/wood interface showed a decrease of the bonding between wood/Kevlar interfaces while increasing the pre-stressing level.

Blaß and Romani (1998-2000, 2001) bonded AFRP and CFRP layers between the two last lumbers of a glued-laminated timber. Most of the failure occurred above the reinforcement, but also under the reinforcement (tension failure) and at the compression side (Failure at finger joints mostly) for the AFRP and CFRP reinforced Glulam.

Hernandez et al. (1997) had been investigating the flexural strength and stiffness of yellow-poplar Glulam reinforced with GFRP (Vinyl ester). A reinforcement quantity of three percent by volume was added. Two layers were bonded on the tension zone. The small size of the piece could not give significant statistical comparison, but there was clear indication of higher flexural strength and stiffness with the reinforcement. They also observed catastrophic failure on the tension side with de-lamination failure of the GFRP layers.
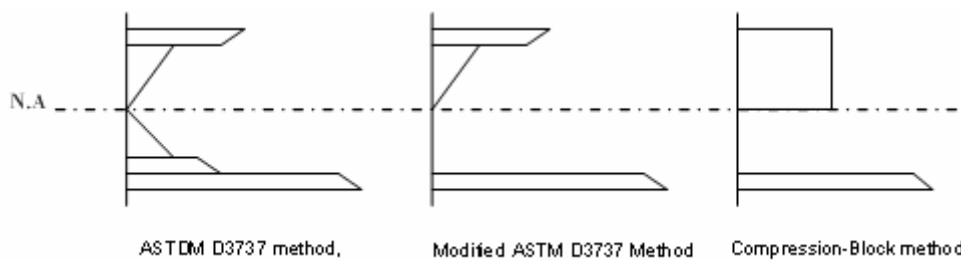
Figure 2.14 Design models for bilinear stress strain behaviour, Hernandez (1997)

b. Reinforced on the tension side as well as compression side

The timber or Glulam beam is reinforced with FRP sheets or layers in both compression and tension sides, based on the sandwich construction, with high mechanical properties skins and Glulam core. This reinforcement type is expected to increase the durability of the wooden members by providing environmental protection (Lopez-Anido and Xu, 2002).

Figure 2.15 Linear elastic-elastic plastic model (Lopez-Anido and Xu, 2002).

Hernandez et al. (1997) have investigated the flexural strength and stiffness of yellow-poplar Glulam reinforced with GFRP (Vinyl ester). Three percent by volume were added. One layer was bonded on the tension zone and one on the compression zone. The small size of the piece could not give significant statistical comparison but it was reported that the reinforcement gave higher flexural strength and stiffness. Tested beams failed catastrophically in tension and de-lamination of the fibres composite layers was observed.
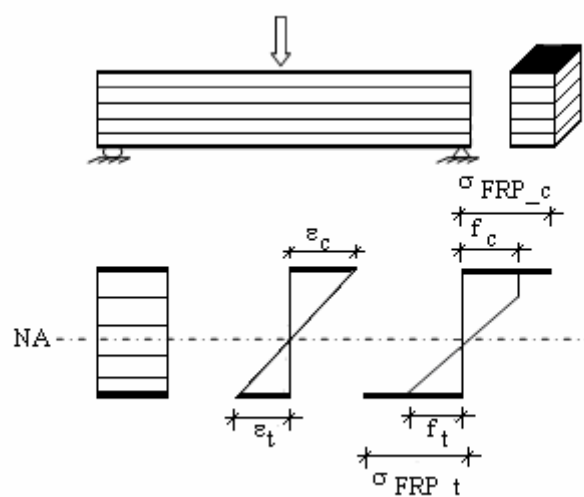
Lopez-Anido and Xu (2002) studied, as Dagher et al. (1996), the reinforcement of eastern hemlock Glulam. Vinyl ester and glass fibres were chosen for the reinforcement, and the volume ratio was 2.1%. Unidirectional laminates and ±45° laminates were used. The former reinforcement (UD laminates) showed an increase of the ultimate load by + 47% and it was observed a change of the failure mode with greater ductility. The second reinforcement (±45° laminates) does not improve the flexural properties and the failure mode was controlled by wood fracture in tension as in the case of un-reinforced beams.

Ogawa (2000) worked on the reinforcement of cryptomeria japonica and larch softwood Glulam timbers with CFRP (volume content between 0.08 and 1.3%). A new phenolic resin was used to give higher inter-laminar shear strength (ILSS) with CFRP to provide a good fire resistance. The flexural properties increased regardless of the kind of wood and the amount of CFRP bonded on the Glulam. Also, a lower variation and higher 5% lower limit value for the reinforced specimens was observed (A standard variation from 6 to 8% has been reported for CFRP reinforced Glulam, compared to 10 to 25% for un-reinforced Glulam). As mentioned earlier (Dagher et al., 1996), the most defects filled specimens showed the greatest flexural properties increase. It was shown that bonded CFRP sheets on both side of the Glulam provide good protection against fire (800°C under a constant load) since oxygen supply is stopped by the CFRP sheets. Hence the safer feature of CFRP reinforced Glulam (the use of the new phenolic resin fire resistant) is also an improvement compared to un-reinforced Glulam specimens.

c. Reinforced on the bottom face as well as part of the lateral faces.

 The timber beam is reinforced over the bottom timber laminate with FRP. This reinforcement is not common, and has been investigated by Borri et al. (2005) using CFRP. A maximum load increase of 55 % was registered and the stiffness was improved by 30.3 %, which is somewhat identical to the flexural properties of the beams reinforced with high density CFRP in the tension side
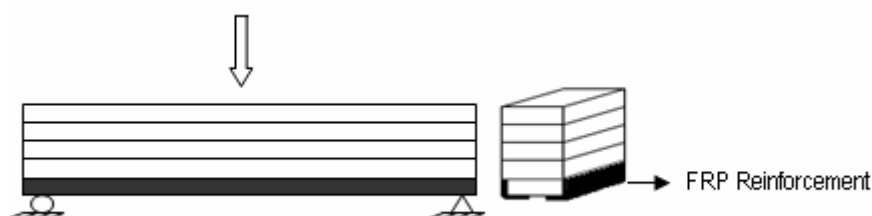

Figure 2.16 Glulam beam reinforced with FRP on lateral faces Borri et al. (2005)

d. Reinforced by Near Surface mounted re-bars

In this method to reinforce timber or Glulam beams, NSM (Near Surface Mounted) reinforcements have been positioned along the larger dimension of the beam. One or several grooves are made in the wood to put FRP bars in general. A resin is used to bond the FRP to the wood (e.g. epoxy).

Gentile et al. (2002) studied the effect of NSM reinforcement (GF/Epoxy) in 30 years old Douglas fir timber beams. Two bars (diameter 13 mm) have been introduced in each side of the timber in the tension zone. The volume ratio of reinforcement was 0.42%. An enhancement of the flexural properties was reported (up to 46%). Besides, 60% of the reinforced beams failed in flexural compression mode, which is more ductile and controllable than the brittle failure of the un-reinforced beams.
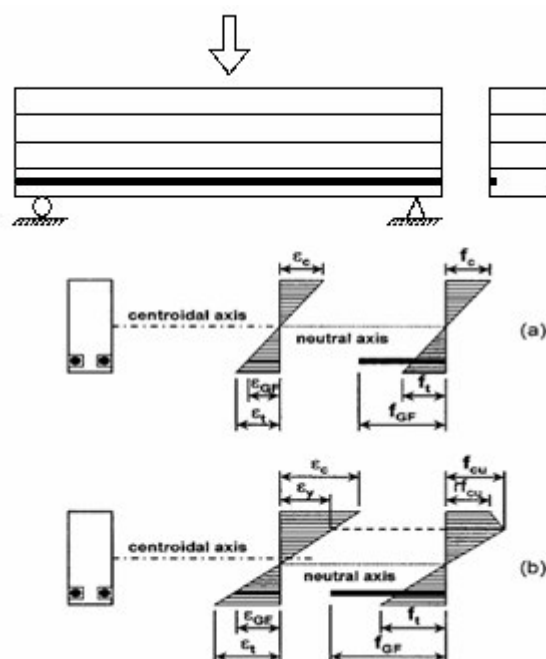

Figure 2.17 Distribution of stress and strain for bilinear stress-strain relationship. Gentile et al. (2002)

Amy and Svecova (2004) reinforced dapped Douglas fir timber beams. The stress concentration at dap in the timber stringers used in some timber bridges (e.g. in Manitoba, Canada) made them to investigated FRP reinforced dapped timber beams. GFRP/Epoxy bars of 12 mm in diameter were used for flexural strengthening. The control beams (un-reinforced but higher grade if compared to the reinforced beams) exhibits an average ultimate load of 121.3kN, and dap or shear failure mode were reported in all cases. The usage of flexural GFRP bars led to a slight increase of the average ultimate load (123.5kN), and dap or shear failures were observed. It was noticed that the flexural bars could not prevent from failure in shear or at the daps of the timbers.

The timber or Glulam is reinforced with the so-called NSM/FRP bars situated in the tension zone of the timber. One or several notches are made on the length of the wooden member. The bars are then put inside the notched and bond to the wood with a resin (epoxy, etc.)

Borri et al. (2005) used CFRP bars to reinforce timber beams. The bars were 7.5 mm in diameter. Two sets of reinforcement were selected:

- One CFRP bar in the centre in the tension side

- Two bars positioned symmetrically from the centre of the tension edge

In both cases, an enhancement of the maximum load and the stiffness has been reported (28.9 % and 22% for the first case, 52 % and 25.5% in the second case). The presence of two CFRP bars increase significantly the maximum load but, the same statement cannot be claimed for the stiffness. A less ductile behaviour was also observed if compare to the previous tests with CFRP sheets. It was suggested that the "bridge" effect for wood defects present with FRP sheets is lower with NSM/FRP bars. However, the aesthetic aspect is much better by using this method.

Gentile et al. (2002) studied the effect of NSM reinforcement (GF/Epoxy) in 30 years old Douglas fir timber beams. Four bars (diameter 13 and 10 mm) were introduced in the tension side area. The volume ratio of reinforcement was respectively 0.42% and 0.26%.Same phenomenon has been reported as in Johnsson et al. (2005) investigated the strengthening of spruce Glulam beams with CFRP rods (rectangular cross section, 10*10 mm). Epoxy resin was used. Three sets of reinforcement were selected:

- One CFRP bar in the centre of the tension edge

- Two bars positioned symmetrically from the centre of tension edge

- One shortened CFRP bar in the centre of tension side

All reinforced Glulam beams showed higher flexural properties if compared with the control beams. The increase in mean load capacity is between 44 and 63%. As in other studies (Gentile et al., 2002, etc.), ductile failure mode in compression side has been registered in reinforced Glulam beams.

2.3.2 Strengthening in other applications

a. Reinforced with FRP fabric wrapped all around the beam.

Buell et al. (2005) have investigated this single reinforcement. It consists in placing CFRP reinforcement at the bottom of the timber beam in the tension side far from the neutral axis to maximize the bending resistance. The shift of the CFRP has been achieved by positioning long piece of wood to the bottom of the beam. An additional carbon fabric was wrapped around the beam in the side and the tension area. It was reported a 69% increase of the bending strength if compared to the control beam and a compression failure mode. This reinforcement provided much higher strength in comparison to the other reinforced beams tested in bending by Buell et al (2005). It was also reported an increase of the stiffness by 18%.
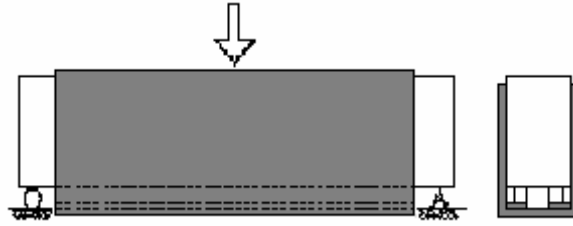
Figure 2.18 Reinforced with FRP fabric wrapped all around the beam, Buell et al.(2005)

b. Flexural reinforcement and joints with CFRP.

Joints of beams have to be stiff in order to prevent deflection. Steiger (2004) decided to test short and long term 4-point bending tests on beams cross sections of 120*180 mm and lengths of 2.80 m spliced at the centre figure 22, were carried out. The achieved strengths were satisfactory for all three splice lengths. The MOR was between 30 N/mm2 and 34 30 N/mm2 (referring to the cross section), which is adequate level when designing beam elements made of Glulam. The increase of deflection of the beams due to the splice was merely 6% to 12 % compared to specimens without joint, i.e the stiffness of the splice proved to be remarkable.
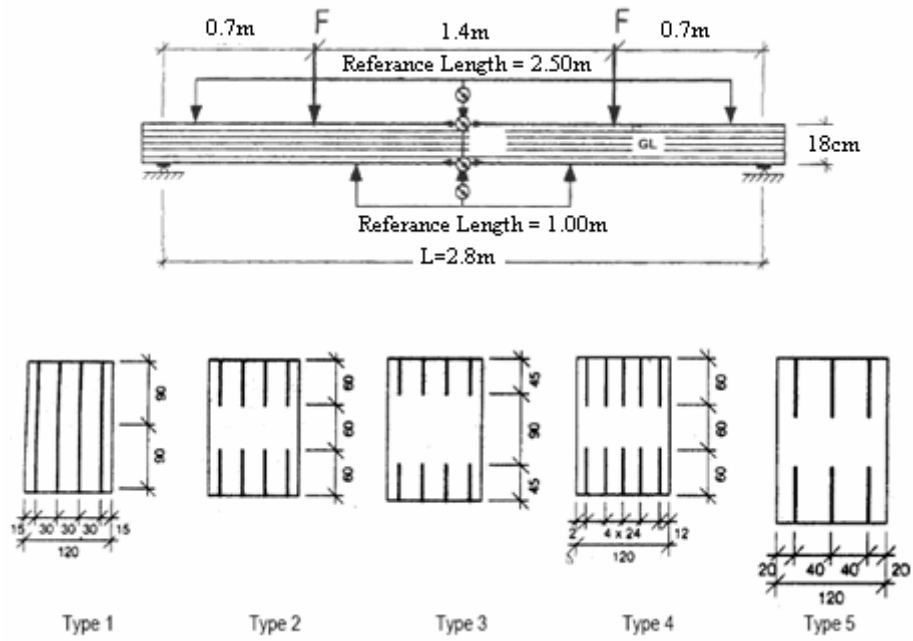

Figure 2.19 Retrofit structure, joint reinforced with FRP. Steiger(2004)

A first exploratory long-term bending test on a specimen with joint configuration type 2 according to the figure was carried out, increasing the bending stress up to 27.5 N/mm^2 over the time intervals of 28 days (first step) and 7 days (second step). At a stress level of 25 N/mm^2 the deflections increased significantly.

Micelli (2005), have tested a new flexural head-joint, that consist of inserting one or more drilled plates that are connected to the timber beams by steel bolts. *Figure 2.20.* The flexural stress is transferred to the connectors that are subjected to shear.
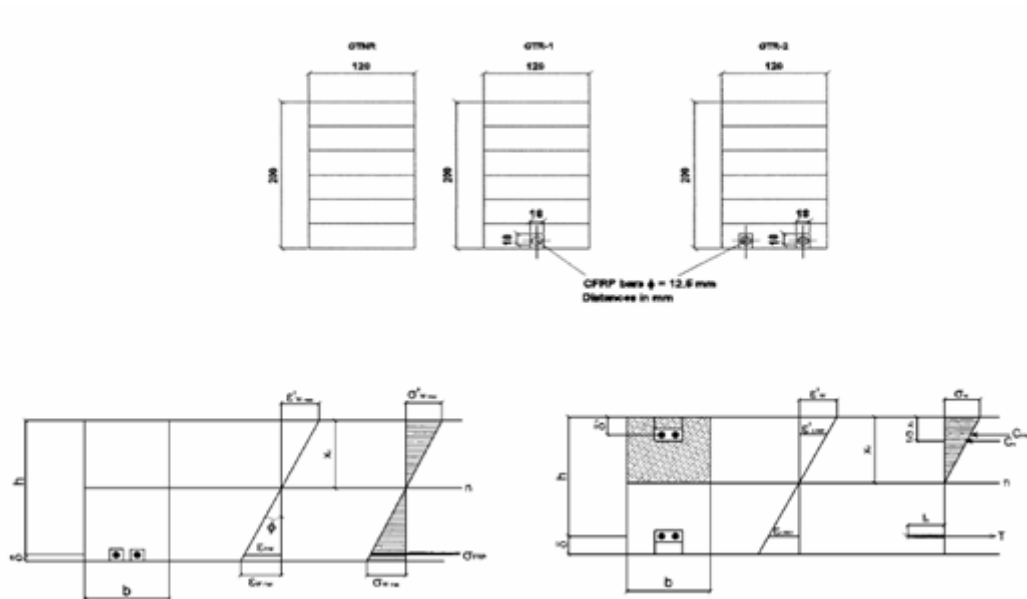
Figure 2.20 Stress-strain distribution. Micelli(2005).

Six Glulam beam specimens of European first-quality spruce were tested showing the failure modes were governed by the ultimate strain of the timber in correspondence to the maximum stress region in one section loaded in the constant moment zone. Collapse of the reinforced beams was also governed by the tensile strength of the timber.

3   MATERIAL DATA

3.1 Materials and Material Models

This section deals with the material properties and different material models used for the analysis as well as for the experiments. The material models are idealized for simplicity in modelling. The linear analysis explained in the following section uses only the linear part of the material models presented here. The presence of knots and other imperfections are not taken into consideration in the modelling. Individual material testing was not carried out during this thesis, the material data were rather obtained from the manufacturers.

3.1.1   Glued Laminated Timber (GLULAM)

The Glulam was made from Class 2 lumber, glued together in factory conditions according to Eurocode 5 (ENV 1995 -1-1; 1993). The strength values are mean values form glulam lot and are not charectoristic values.

Table 3.1 gives the major properties which we used in our modelling.

Table 3.1 Mechanical properties of beam specimen (Moelven Toreboda AB)

Property	Value
Compressive strength parallel to grain	*46 N/mm^2*
Tensile strength parallel to grain	*44 N/mm^2*
Modulus of elasticity parallel to grain	*13 500 N/mm^2*
Shear strength of Glulam in perpendicular direction	*7.0 N/mm^2*
Poisson's ratio	*0.2*

The model assumed an Idealized Stress- Strain relationship for timber. Tension behaviour is assumed to be linear-elastic, and failure occurs when the stress reaches the ultimate tensile strength f_{tu}, corresponding to strain ε_{tu}.

The model incorporated the plastic behaviour of the timber under compressive loading. A bilinear relationship is assumed for the compression behaviour, with a linear part up to limiting compressive strength f_{cu} and a corresponding strain ε_{cl}, and an ideal plastic behaviour till ultimate strain ε_{pl}. *Figure 3.1* shows the idealized stress strain relationship used in modelling.

The plastic strain limit in compression was assumed to be three times the elastic limit based on the studies done by Fiorelli and Dias (2003) on Spruce (see *Figure 3.2*). A pure compressive failure was assumed if the strain level in the outermost compression fiber reaches this limit.
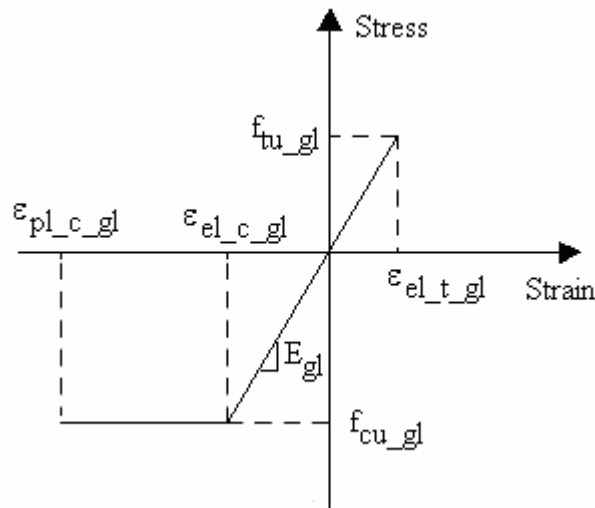
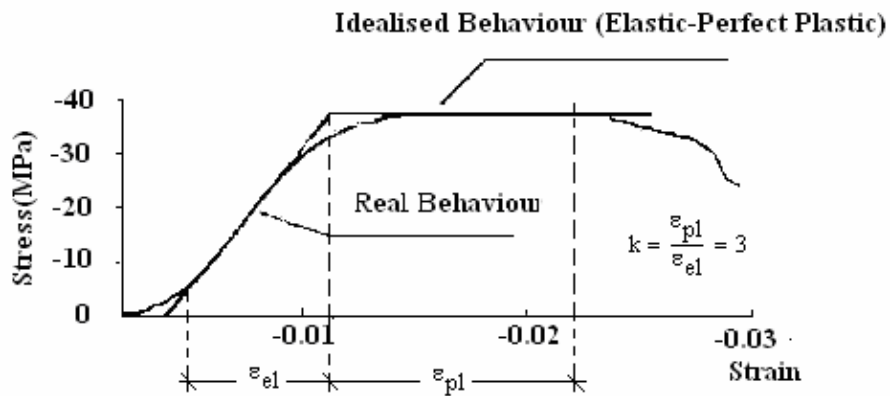*Figure 3.1 Idealized stress-strain relationship for timber.*

Figure 3.2 Idealization of compressive behaviour proposed by Juliano Fiorelli and Antonio Alves Dias(2003).

3.1.2 Carbon fibre reinforced polymer (CFRP)

Carbon Fiber-reinforced Polymer used in this test is identified as heavy-duty CFRP provided by Sika Group. Two types of CFRP Laminates were used in this test and are identified to be Sika CarboDur S614 with cross sectional dimension 60 x 1.4 mm^2 and Sika CarboDur H514 with 50 x 1.4 mm^2. Sika CarboDur is a pultruded carbon fiber reinforced polymer (CFRP) laminate designed for strengthening concrete, timber and masonry structures. Sika CarboDur is bonded onto the structure as external reinforcement using Sikadur 30 or sikadur 330 epoxy resins as the adhesive. The laminates consisted of unidirectional fibers aligned along the longitudinal direction with a fiber volume fraction greater than 68%. The densities of these reinforcements are in the range of 1.6 g/cm^3

Table 3.2 shows the properties of the CFRP reinforcements

Table 3.2 Technical and Physical Data of CFRP (Provided by Sika)

Sika CarboDur-Laminates

Colour	*Black*
Base	*Carbon fiber reinforced with an epoxy matrix*
Elastic Modulus	
Sika CarboDur S	*165,000 N/mm²*
Sika CarboDur H	*300,000 N/mm²*
Tensile Strength*	
Sika CarboDur S	*2,800 N/mm²*
Sika CarboDur H	*1,300 N/mm²*
Mean Value of Tensile*	
Strength at Break	
Sika CarboDur S	*3,050 N/mm²*
Sika CarboDur H	*1,450 N/mm²*
Elongation at Break	
Sika CarboDur S	*1,7%*
Sika CarboDur H	*0,45%*

* Mechanical values obtained from longitudinal directions of fibers

The CFRP laminates were idealized as linear-elastic with a brittle failure mode. The stress-strain relationship and nomenclature can be seen in *Figure 3.3*. The effect of failure of the laminate by fiber buckling was not taken into consideration within the scope of this thesis.
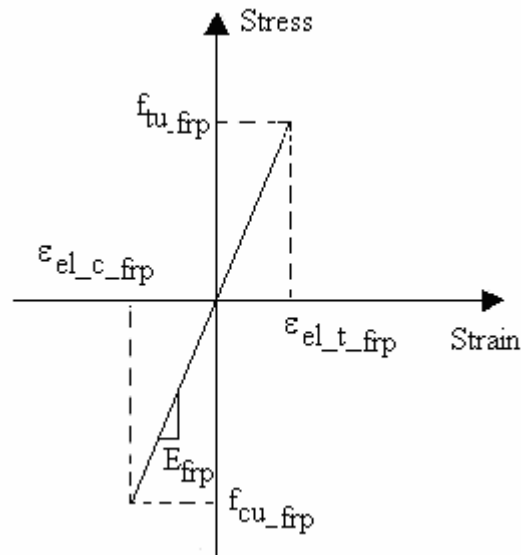
Figure 3.3 Idealized stress-strain relationship for FRP.

3.1.3   Steel

Metals including steel have a linear stress-strain relationship up to the yield point. Below the yield strength all deformation is recoverable, and the material will return to its initial shape when the load is removed. For stresses above the yield point the deformation is not recoverable, and the material will not return to its initial shape. This unrecoverable deformation is known as plastic deformation.

Steel plates were used in this study were having the cross area 4x30mm^2. The properties of the steel used in our analysis are given in the table below.

Table 3.3 Technical and Physical Data of steel

Property	Value
Yield Strength (fyk)	*186-350mm^2*
Tensile Strength (ftk)	*275-455mm^2*
Modulus of elasticity	*210 000 N/mm^2*

Steel is considered as plastic material for modelling purposes, and the behaviour idealised to be linear elastic-perfect plastic in both tension and compression. *Figure 3.4* shows the stress strain relationship.

The necking effect at the reach of yield strength is not considered in modelling.
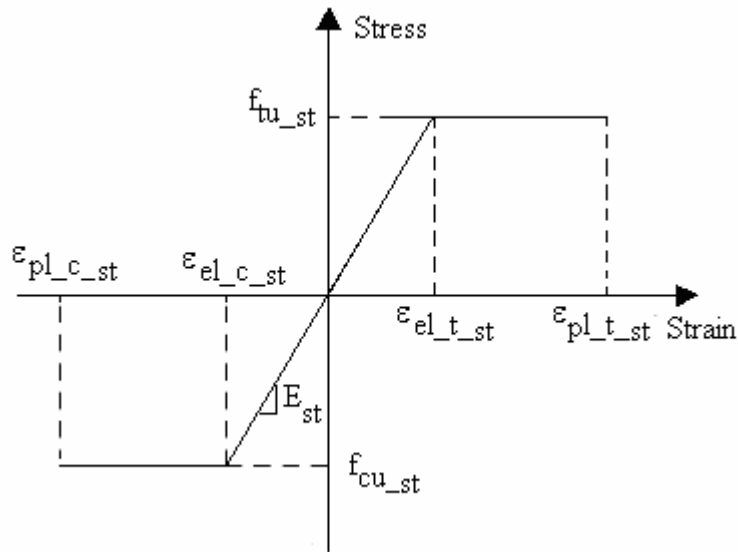
Figure 3.4 Idealized stress-strain relationship for Steel.

3.1.4 Adhesives

The adhesives have not been taken into account for the numerical modelling. In FE modelling the Two types of adhesive systems were used in the experiments.

a. Sikadur 30

Sikadur-30 is a thixotropic adhesive mortar based on a 2-component solvent free epoxy resin. Sikadur-30 is used primarily to bond structural reinforcements to other substrates. It can also be used to bond and fill a wide variety of building and construction materials.

Sikadur-30 is supplied in factory proportioned units comprising the correct quantities of Part A (Resin) and Part B (Hardener).

*Table 3.4 Technical and Physical Data of **Sikadur 30** (Provided by Sika)*

Appearance	Values
Part A	*White paste*
Part B	*Black paste*
Part A + B	*Light grey when mixed*
Mix Ratio	*A : B = 3 :1 (parts by weight & volume)*
Density	*1.77 kg/L (A + B)*
*Pot Life ***	*40 minutes (at 35°C)*
*Open Time**	*30 minutes (at 35°C)*

Sag Flow*	3 - 5mm (at 35°C)
Shrinkage	0.04%
Glass Transition Point*	62°C
Static E-Modulus*	12,800 MPa
Adhesive strength (wet)*	4 MPa
Shear strength*	15 MPa
Coefficient of Expansion	9 x 10-5 per °C (-10°C to 40°C)

*To F.I.P Federation Internationale de la Precontrainte

b. SikaDur 330

SikaDur 330 is a solvent free, cold cure, two component epoxy resin based product formulated specifically for the bonding of the **SikaWrap** structural strengthening fabrics using the "dry" application system.

*Table 3.5 Technical and Physical Data of **Sikadur 330** (Provided by Sika)*

| Properties	Values
Part A	White
Part B	Grey
Part A + B	Light grey when mixed
Mix Ratio	A : B = 4 :1 (parts by weight & volume)
Density	1.31 kg/L (A + B)
Pot Life	90 minutes (at 15°C)
	30 minutes (at 35 °C)
Open Time	30 minutes (at 35°C)
Viscosity	Paste like
Flexural E-Modulus	3800 MPa
Adhesive strength	> 1.5 MPa
Tensile strength	30 MPa
Application Temperature	5°C to 35°C (ambient and substrate)

4 MODELS

Using composite materials for reinforcing wood elements under bending loads require particular attention to several aspects. Firstly, it is very important to carefully plan the kind of interventions to be realized. In fact, there are quite a lot of techniques available for reinforcing wood elements - using different layouts of reinforcing elements, using different combinations of reinforcement ratios in compression and tension zones, using different reinforcing materials and so on - and each choice could potentially lead to different responses and failure modes. The second point is the selection of the most appropriate reinforcing materials. A wide range of products with different structural and mechanical properties are currently available in the market. For these reasons, the selection of appropriate configurations and reinforcements should be guided by accurate analysis in order to avoid ineffective interventions.

In the early stages of our study, the main focus was on finding an efficient reinforcement configuration which gives satisfactory strength and stiffness values. Due to economical reasons, it was not possible to test each and every configuration and find the optimum one. Also the number of tests to be done in order to have statistically reliable data is high due to inherent defects, which is characteristic for timber specimens. The lack of proper design codes and unified design procedures was also a problem. The peeling stresses and interfacial stresses in the adhesive layer are difficult to calculate by hand. For these reasons, the beams were modelled both numerically and also using Finite Element tools.

Dimensions used in modelling

The dimensions of the beams were selected and determined by MOELVEN Töreboda AB. *Figure 4.1* shows the dimension of the beam 115 x 200 mm^2.
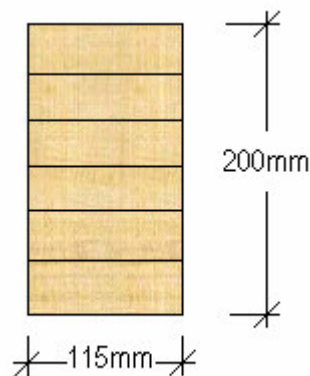
Figure 4.1 Cross sectional dimensions of the Glulam specimen

All the reinforcements were given the dimension of 1.4x50mm^2 (same as Sika CarboDur H514) for ease of comparison; even though the Sika CarboDur S614 has the dimension 1.4 x 60 mm^2. But actual dimensions were used for the validation of the model using experimental results.

4.1 Failure modes

The identification of different failure modes is important for both modelling and experimentation. Different failure modes were identified based on material properties, cross sectional distribution of reinforcements and loading configurations, and were incorporated in the model.

The failure modes are also affected by the presence of knots and other imperfection in the wood. But these factors were not taken into consideration while modelling. But for design situations, appropriate correction factors should be introduced to take into account the variability and presence of strength reducing factors.

The following sections deals with the most critical failure modes.

4.1.1 Tensile failure in timber

This is the most common failure mode in timber structures. This failure mode is brittle as the timber does not have plastic behaviour under tensile loads. This can even introduce cracks along the fiber direction which will result in catastrophic destruction of the cross section.

The timber's tensile limit state is considered to be attained when the maximum tensile stress is equal to its tensile strength. The beam is considered to be failed when the outermost fiber in tension exceeds tensile limit.

Two failure modes can be identified in the tensile zone based on the degree of plastification at the compression side.

The following are the global failure modes in tension side:

1. ***Failure of the timber on tensile zone while the cross section is in a linear-elastic state*:** This occurs when the stress in the outer most fiber in the tension zone reaches its tensile limit and the compression zone is still in the linear elastic range. This usually happens with un-reinforced beams whose tensile strength is lesser than the compressive strength. The failure is brittle.
2. ***Failure of the timber while the cross section is in a linear-elastic-ideal-plastic state:*** This occurs when the stresses in the outermost fiber in the tensile zone reaches the tensile limit only after some plastification in the compression side. But still the compressive zone has not reached the ultimate compressive strain. This is the most common type of failure and is typical to beams which are lightly reinforced in only tensile zone or in both tensile and compressive zones. Even though there is some ductility in the global behaviour, the fibers locally fails in tension which makes the failure mode brittle.

Figure 4.2 illustrates these failure modes and the corresponding stress/strain state.
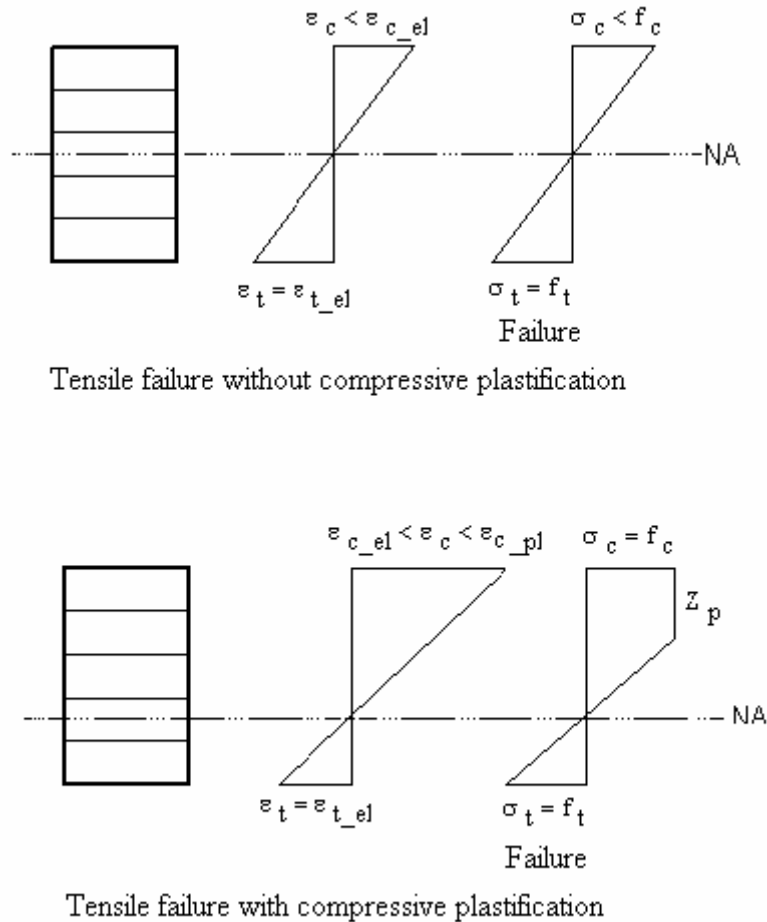
Figure 4.2 Tensile failure modes - stress/strain states

4.1.2 Compressive failure in timber

This failure mode is not very common in un-reinforced sections. But when the beam is reinforced in the tension side, this failure mode can occur. A detailed study of this phenomenon can be seen in the modelling part. The ultimate state of compression is considered to have been attained when the maximum strain in the compression zone reaches the value ultimate compressive strain. We can identify one failure mode in the compression side:

1. *Compressive failure before the timber fails in tension*: this usually happens in beams which are heavily reinforced in the tension side. The response of the beam is quite ductile due to plastic deformation in the compressive zone.

Figure 4.3 illustrates these failure modes and the corresponding stress/strain state.
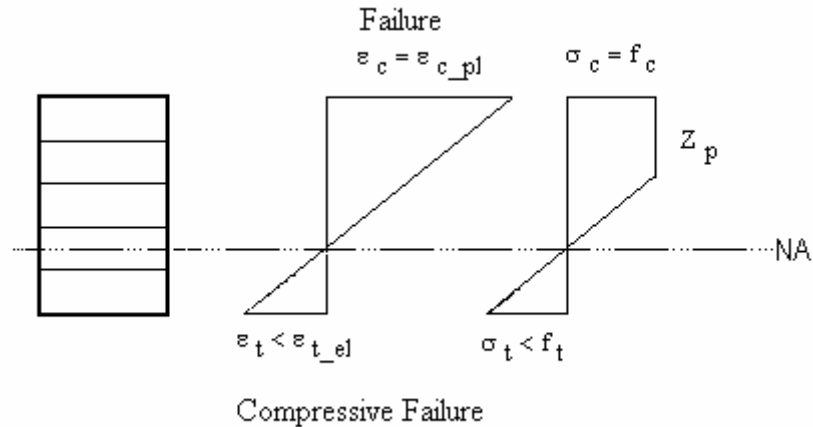
Figure 4.3 Compressive failure mode - stress/strain states

4.1.3 Shear failure in Timber

Shearing of timber is a common failure mode in reinforced timber. Usually the tensile and compressive capacity of the beam is taken care of by the reinforcement, and then the failure shifts to shear. This occurs when the shear stress in the cross section exceeds the limiting shear strength of the timber. The failure will be abrupt, as the crack propagates along fibre direction.

For the assumed stress distribution, the longitudinal shear stress equation for a rectangular section is

$$\tau = \frac{VQ}{Ib} = \frac{3V}{2bd}$$

Where:

τ = Shear stress [Pa];
V = Shear force [N];
b = Width of beam [m];
d = Depth of beam [m];
I = Moment of inertia [m^4];
Q = Statical moment of the area [m^3]

4.1.4 Yielding or Rupture of Reinforcement

The stresses in the reinforcement will be much higher than the stresses in timber due to the difference in E-modulus of reinforcement and timber (higher α value). The stiffer material attracts more stresses. Therefore the reinforcements may reach their yield/ultimate capacities well before the timber. Brittle reinforcements just fail abruptly at this point, while ductile reinforcements can still work in their plastic range.

4.1.5 Failure of Adhesive

The adhesive plays an important role in transferring the stresses from the timber to the reinforcement. Near to support where the forces are linked to the reinforcement, there

are chances of failure in the adhesive. Adhesive failure can also occur near to the first crack, when the forces need to be linked to the reinforcement abruptly.

4.2 Assumptions and simplifications

The E-modulus of timber is assumed to be same in both compression and tension

The stress strain relation is simplified to be linear- elastic in tension side, and linear-elastic-perfect- plastic in compression, ignoring the nonlinearities

It is assumed that the failure occurs when the outer most fiber reaches the maximum allowable stress or strain state. Or in another way, the decrease in cross sectional resistance due to reduction in cross sectional area resulting from yielding of outermost fibers is not taken into account.

The adhesive is assumed to act perfectly, or there exists no bond slip at joints, which in-turn results in a linear strain distribution.

The presence of knots and other imperfections in timber is not considered in the models.

The FRP laminates are assumed to have linear elastic material behaviour.

4.3 Analytical Modelling

Two models were prepared numerically using MathCAD and Mat lab. These models were used for finding out the best configuration of beam cross section and also to find the optimum distribution of reinforcement in the tension and compression sides taking care of the stiffness as well as resisting moment. The details of these two models are explained in the following sections

4.3.1 Linear Elastic Model

A linear model was prepared using MathCAD with linear elastic material properties for the Glulam as well as the reinforcements. The behaviour of the beam is assumed to be linear elastic till failure.

The main aim of this analysis was to find out an optimum configuration of the composite cross section and choose the best configuration from the different alternatives available. The linear model was intended to compare the different configurations geometrically alone. The linear material properties were deliberately chosen in order to avoid misinterpretations which can occur due interaction of material nonlinearities and geometric effects. So the linear model enables to have a more focused comparison of geometric configurations, excluding the effect of material nonlinearities.

Figure 4.4 shows the design model within linear elastic limits. The compressive strains in the timber are limited within elastic range. Also the nonlinearity due to yielding behaviour of reinforcement was also not taken into consideration in this model.
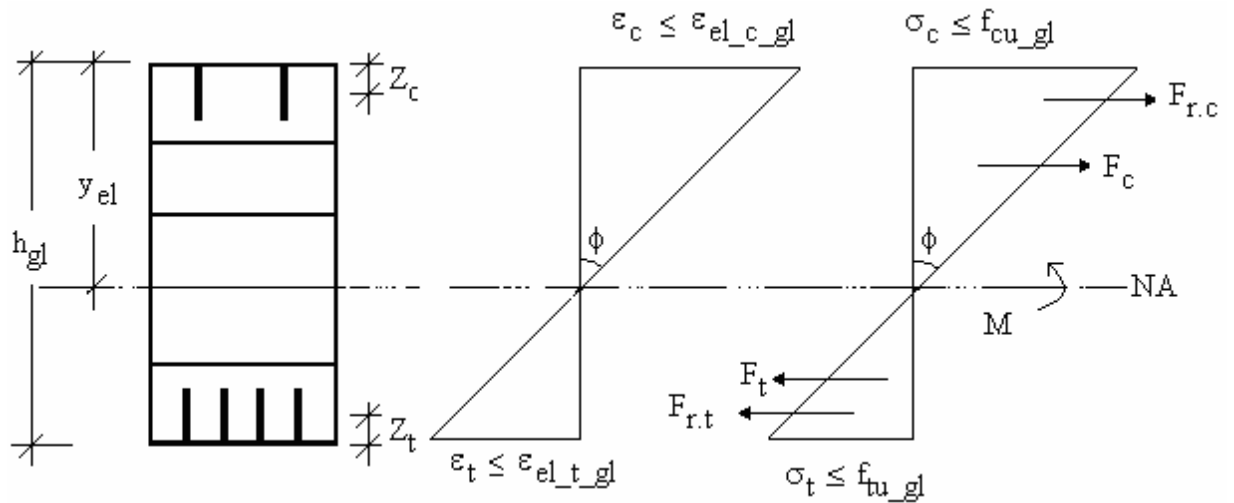
Figure 4.4 Linear Model

The model works on the simple bending theory in the linear elastic phase. The limiting values of tensile/compression stress/ strains are used to achieve a stress/strain distribution across the cross section as shown in *Figure 4.4*. The sectional forces are calculated based on the linear stress distribution. The sectional forces are then used for the calculation of moment resistance using appropriate lever arm values.It should be noted that the linear model result in a lower values of moment resistance as the post linear loading capacity is totally ignored.

The Mathcad file used for the calculations is given as APPENDIX 1.

Figure 4.5 shows the flow chart for the linear elastic model.

Start

Input Geometric data
Input Material properties(linear)

Calculating Neutral Axis and Moment of Inertia of the section

Checking the
governing
failure mode

Fixing the tensile strain in the outermost timber
fiber to elastic tensile limit strain

No   Checking if the
compressive strains
excced limiting values   Yes

Failure
is in
tension

Failure is in
compression

Recalculating
correponding
tensile strains

Achieving the Strain distribution
across the cross section

Calculating the
corresponding
Linear Stress
distribution

Force
Equilibirium

Strain
Compatablity

Calculating
Sectional forces
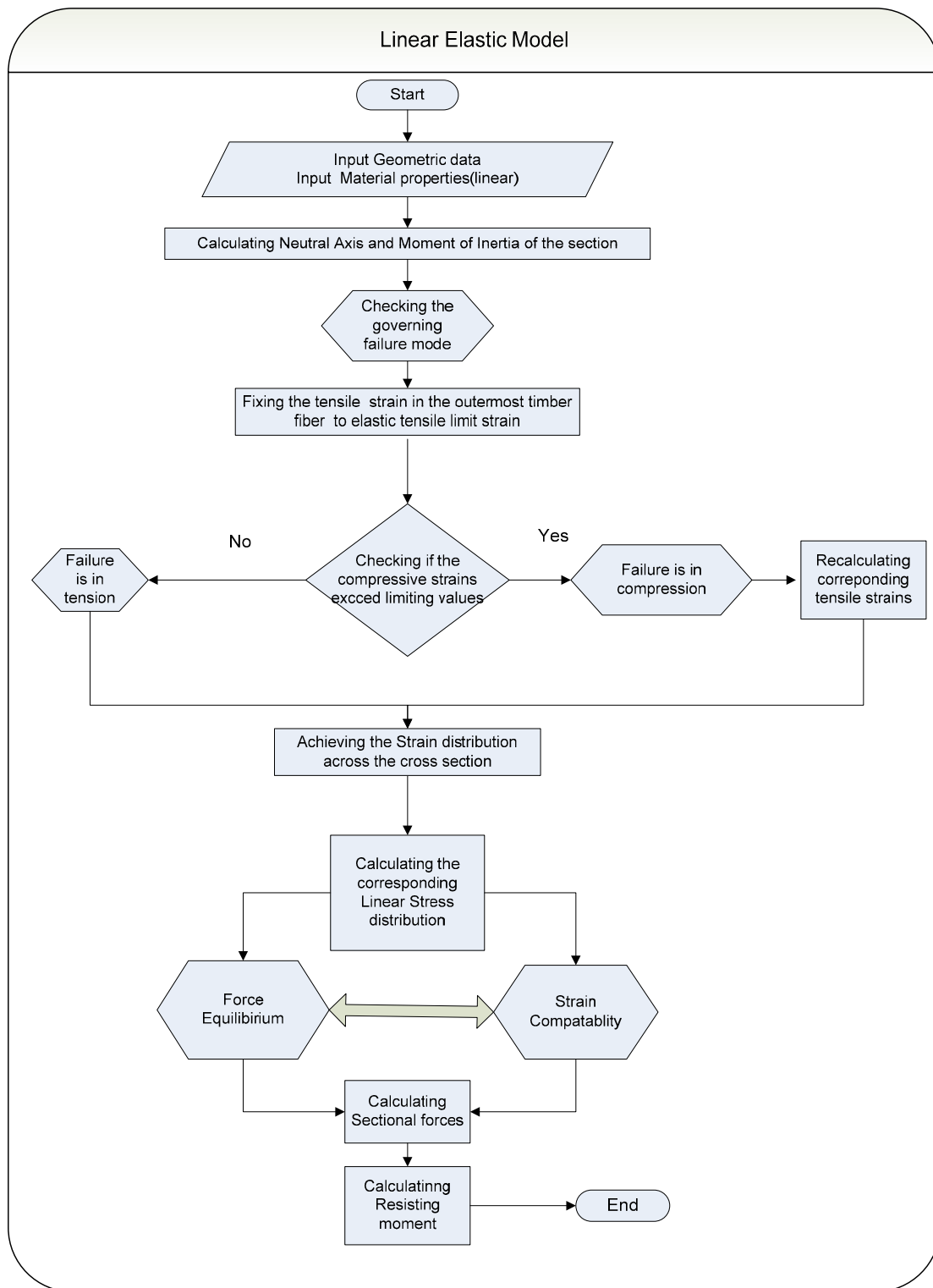
Calculatinng
Resisting
moment

End

Figure 4.5   Flow chart- Linear Model

The following section deals with the mathematical framework of the linear elastic model.

A transformed cross section is used for the calculation of the neutral axis while the whole cross section is in linear elastic phase.

Establishing the strain distribution across cross section,

Fixing the tensile strain just above the reinforcement to ε_{c_gl}

$$\varepsilon_{c\_gl} = \varepsilon_{el\_t\_gl}$$

$$\varepsilon_{c\_gl} = \frac{\varepsilon_{t\_gl}}{d_{t\_fail} - y_1} \times y_1$$

Checking if the corresponding compressive strains exceed limiting values

$$\varepsilon_{t\_gl} = \frac{\varepsilon_{t\_gl}}{y_1} \times (d_{t\_fail} - y_1) \quad \text{if} \quad \varepsilon_{c\_gl} > \varepsilon_{el\_c\_gl}$$

$$\varepsilon_{c\_Gl} = \varepsilon_{c\_Gl} \quad \text{if} \quad \varepsilon_{c\_Gl} > \varepsilon_{c\_elGl}$$

Establishing the stress distribution across the cross section

$$\sigma_c = \varepsilon_{c\_gl} \times E_{gl}$$
$$\sigma_t = \varepsilon_{t\_gl} \times E_{gl}$$

Force of equilibrium implies

$$F_{frp\_t} + F_t = F_{frp\_c} + F_c$$

Finding sectional forces

$$F_c = \frac{\sigma_c \times b_{gl} \times y_1}{2}$$

$$F_t = \frac{\sigma_t \times b_{gl} \times (d_{t\_fail} - y_1)}{2}$$

Finding Forces in the laminate,

Strain compatibility implies

$$\frac{\varepsilon_{frp\_t}}{d_t - y_1} = \frac{\varepsilon_{t\_gl}}{h_{gl} - y_1}$$

$$\varepsilon_{frp\_c} = \frac{\varepsilon_{frp\_t}}{d_t - y_1} \times (y_1 - d_c)$$

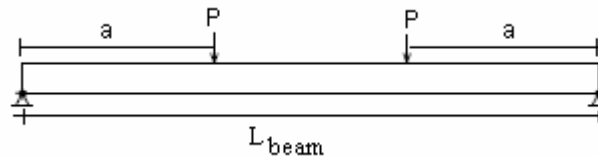$$\varepsilon_{frp\_t} = \frac{\varepsilon_{t\_gl}}{y_1 - d_c} \times (d_t - y_1)$$

$$F_{frp\_t} = \varepsilon_{frp\_t} \times E_{frp} \times A_{frp\_t}$$

$$F_{frp\_c} = \varepsilon_{frp\_c} \times E_{frp} \times A_{frp\_c}$$

The ultimate moment resistance is then calculated by the equation

$$M_u = -F_t \left[d_t - y_1 - \frac{2}{3} \times (h_{gl} - y_1) \right] + \left[F_{frp\_c} \times (d_t - d_c) + F_c \times (d_t - \frac{y_1}{3}) \right]$$

Checking Deformations

Limiting deformation

$$\delta_{\lim} = \frac{L_{beam}}{300}$$

$$\delta = \frac{P \times a \times (3 \times L_{beam}^2 - 4 \times a^2)}{24 \times EI_{ef}}$$

So the maximum load that can be applied with respect to deformation criterion is

$$P = \frac{\delta_{\lim} \times 24 \times EI_{ef}}{a \times (3 \times L_{beam}^2 - 4 \times a^2)}$$

Comparing with the ultimate load carrying capacity based on the ultimate moment resistance,

$$M_u = P \times a$$

$$P_{\lim it\_moment} = \frac{M_u}{a}$$

The ultimate moment resistance as well as stiffness of different reinforcement configurations were compared. The ultimate load bearing capacity was assessed with a four point bending configuration for a clear span of 4 m. The limiting load due to deformation criteria was also found out and compared with each other for different configurations. The areas of reinforcement as well as material properties were kept constant in all models.

The beam dimensions used in the analysis was 115mm x 200mm and the CFRP had the dimensions 1.4mm x 50mm. E- modulus for timber was taken to be 13500Mpa and that for CFRP was taken to be 300000Mpa.

The following section details the results from the linear analysis.

Results

Table 4.1 Results of Linear Analysis**

Configuration	CFRP Cross section mm²	I_{xx} x 10^6 mm⁴	EI_{eff} kNm²	P_{defor} kN	M_{ul} kNm	P_{ult} kN	Failure mode
		55.9	340.929	2.001	9.563	7.173	Tension
	2(50 x 1.4)	98.395	600.209	3.523	18.344	13.758	Compression
	2 (1.4 x 50)	79.153	482.838	2.834	15.365	11.526	Compression
	Bottom=1.4 x 50 Top= 50 x 1.4	98.35	599.959	3.521	16.162	12.121	Tension
	Bottom=50x 1.4 Top=1.4 x 50	99.19	605.058	3.551	17.472	13.104	Tension
	Bottom=50x 1.4 Top=50 x 1.4	111.66	681.151	3.998	19.144	14.358	Tension
	Bottom=1.4 x 50 Top= 1.4 x 50	86.41	527.129	3.094	14.541	10.906	Tension
	2(1.4 x 50)	69.89	426.356	2.503	12.348	9.261	Tension
	2 (50 x 1.4)	96.45	588.362	3.453	18.066	13.549	Compression

** I_{xx} is the second moment of inertia of the section, EI_{eff} is the effective stiffness of the transformed cross section, M_{ul} is the ultimate moment capacity, P_{ul} is the ultimate load carrying capacity and P_{def} is the load at deflection limit

Interpretations

It can be seen that the configurations with reinforcements parallel to the bottom edge showed high strength and stiffness values. The configurations with reinforcements perpendicular to the bottom face were comparatively giving lesser strength/ stiffness values. But in this analysis we decided to go further with the configurations with reinforcement perpendicular to the bottom face because of the following advantages in-spite-of a bit lesser strength/stiffness values.

a. This configuration is aesthetically appealing as the reinforcements are almost concealed.

b. The area for transfer of forces from reinforcement to the timber is more than twice compared to the other configurations. This will lead to lesser shear stresses in the glue-line and reduces the chances of de-lamination.

c. On the onset of a crack (may be due to a finger joint failing or a knot), this configuration gives a better stiffness, because the reinforcement is loaded in its strong axis. This will prevent excessive deflections which in other case will result in rapid propagation of crack in the fibre direction and will cause abrupt failure.

4.3.2 Non-linear Model

Timber is a material which shows nonlinear behaviour under compressive loading. The principal reason for developing a non-linear model was to incorporate this plastic behaviour that reinforced beams can have on compression side. The nonlinear model helps to study how the distribution of the reinforcement in the tension and compressive zones can affect the load bearing capacity as well as stiffness of the beam. This will finally lead to the best reinforcement configuration in order to maximise strength/stiffness properties.

The model considers two types of nonlinearities

1. The nonlinearity of timber in the compressive zone.

2. The nonlinear behaviour of metallic reinforcements due to ductility.

The model basically simulates the global behaviour under a stepwise strain increment. Initially a small strain in the outermost compressive fiber is assumed and the corresponding strain/ stress state across the cross section is achieved. The stress/strain state is calculated and compared with their limiting yield values, taking into consideration the effect of yielding of reinforcement as well as plasticity in timber. If this stress/strain state does not lead to failure of any component, a small increment in strain is introduced. This procedure is continued until failure occurs.

For the sake of simplicity, the modelling was implemented in two phases based on whether the timber is plastified or not. The nonlinearity due to the reinforcement yielding was then incorporated into both these phases. The following section deals with these two phases in detail.

1. Linear Elastic Phase

This phase considers the response of the beam when the timber is in linear elastic state. The reinforcement may be yielding or not yielding. Yielding of reinforcement affects the overall stiffness of the cross section and will result in the shift of neutral axis. The values of y_{el} are calculated based on whether the reinforcement is yielded or not.
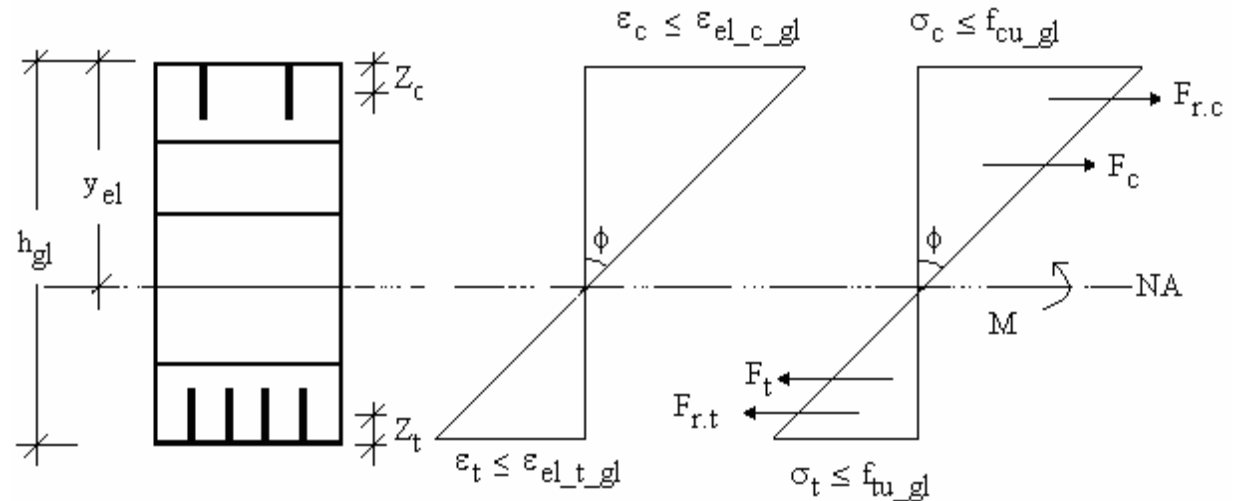
Figure 4.6 Linear Elastic Phase

Considering a small initial strain ε_c

Strain compatibility implies

$$\varepsilon_{rc} = \frac{(y_{el} - Z_c)}{y_{el}} \varepsilon_c$$

$$\varepsilon_{rt} = \frac{(h - y_{el} - Zt)}{y_{el}} \varepsilon_c$$

$$\varepsilon_t = \frac{(h - y_{el})}{y_{el}} \varepsilon_c$$

Force equilibrium implies

$$\sum F_t = \sum F_c$$

$$F_t + F_{rt} = F_c + F_{rt}$$

Four cases may be identified based on reinforcement yielding. The shift of neutral axis is calculated based on the modified stress state due to pastification.

a. *Nothing yields*

This is the case at low load levels. All the materials in the cross-section are in linear elastic state without any plastification. The global response of the beam is linear. The neutral axis may be found out using the conventional method of transformed cross section.

$$y_{el} = \frac{A_{lc}\alpha Z_c + A_{lt}\alpha(h_{gl} - Z_t) + \dfrac{b_{gl}h_{gl}^2}{2}}{\alpha(A_{lc} + A_{lt}) + b_{gl}h_{gl}}$$

b. *Only tensile reinforcement yields*

This case occurs in metal reinforced sections when the stresses in the tensile reinforcement (only) cross the yield stress value in tension. The neutral axis may be found out using the following equations.

$$\left[\varepsilon_c E_{gl} b_{gl}\right] y_{el}^2 + \left[\varepsilon_c E_{la} A_{lc} - \varepsilon_c E_{gl} h_{gl} b_{gl} - f_{t\_r} A_{lt}\right] y_{el} - \left[\varepsilon_c E_{la} A_{lc} Z_c\right] = 0$$

$$y_{el} = \frac{-b \pm \sqrt{b^2 - 4ac}}{2a}$$

c. *Only compressive reinforcement yields*

This case occurs in metal reinforced sections when the stresses in the compressive reinforcement (only) cross the yield stress value in compression. The neutral axis may be found out using the following equations.

$$\left[\varepsilon_c E_{gl} b_{gl}\right] y_{el}^2 + \left[f_{c\_r} A_{lc} - \varepsilon_c E_{gl} h_{gl} b_{gl} - \varepsilon_c E_{la} A_{lt}\right] y_{el} - \left[\varepsilon_c E_{la} A_{lt} h - \varepsilon_c E_{la} A_{lt} Z_t\right] = 0$$

$$y_{el} = \frac{-b \pm \sqrt{b^2 - 4ac}}{2a}$$

d. *Both tensile and compressive reinforcement yields*

This can happen at higher load levels in doubly reinforced sections (section which are reinforced both in tension and compression). At this stage both the tension and compression reinforcements are yielded and are not any more capable of taking more stresses. The neutral axis may be found out using the formula given below.

$$y_{el} = \frac{f_{t\_r} A_{lt} - f_{c\_r} A_{lc}}{\varepsilon_c E_{gl} b_{gl}} + \frac{h_{gl}}{2}$$

2. Plastic Phase

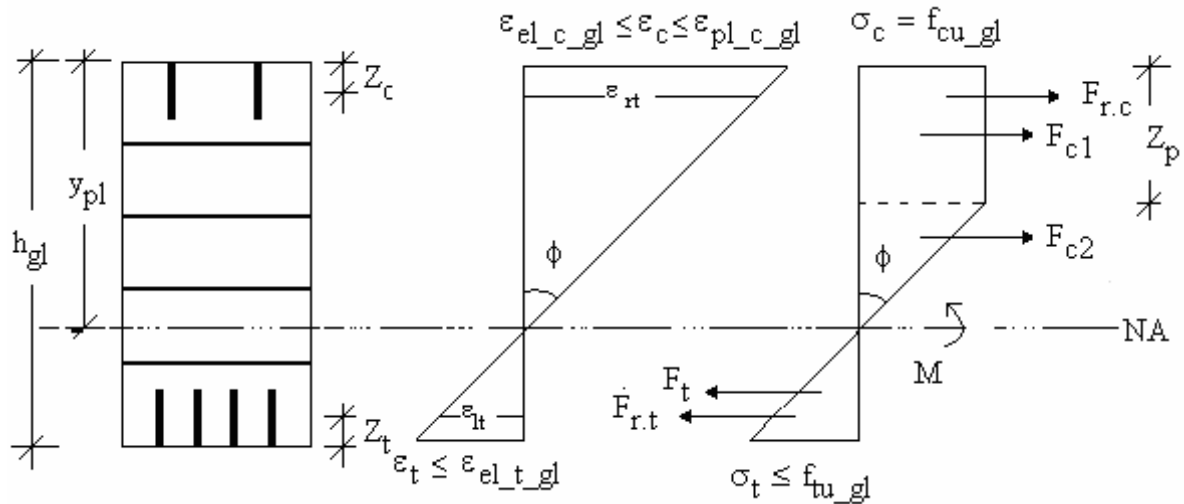This phase considers the response of the beam when the timber is in plastic phase(in compression)

Figure 4.7 Plastic phase

Figure 4.7 illustrates the design model for a Glulam beam reinforced both in tension and compression. The strain state corresponds to the post elastic phase, where compressive strains in timber are above elastic limit, but below the plastic limit. It should be noted that as the compressive strains crosses the elastic limit, plastification in the compressive zone occurs and the timber stresses cannot be increased anymore. This results in shift of the neutral axis so that the equilibrium condition holds good.

Considering a small initial strain ε_c

Strain compatibility implies

$$\varepsilon_{rc} = \frac{(y_{pl} - Z_c)}{y_{pl}} \varepsilon_c$$

$$\varepsilon_{rt} = \frac{(h - y_{pl} - Zt)}{y_{pl}} \varepsilon_c$$

$$\varepsilon_{t} = \frac{(h - y_{pl})}{y_{pl}} \varepsilon_c$$

The degree of plastification is found out using the following formula

$$Z_p = \frac{\varepsilon_c - \varepsilon_e}{\varepsilon_c} y_{pl}$$

Force equilibrium implies

CHALMERS, *Civil and Environmental Engineering*, Master's Thesis 2007:28

$$\sum F_t = \sum F_c$$

$$F_t + F_{rt} = F_{c1} + F_{c2} + F_{rt}$$

Substituting, and collecting terms for y_{pl}, we get

a. Only timber yields in compression

In this phase, only the timber in compression has crossed its plastic limit. The neutral axis was found out using the following equations

$$\left[f_{cu\_gl} b_{gl} \left(1 - \frac{\varepsilon_{el\_c\_gl}}{\varepsilon_c} \right) + \left(\frac{f_{cu\_gl} b_{gl}}{2} \frac{\varepsilon_{el\_c\_gl}}{\varepsilon_c} \right) - \frac{\varepsilon_c b_{gl}}{2} E_{gl} \right] y_{pl}^2 +$$

$$\left[\varepsilon_c E_r A_{rc} + b_{gl} \varepsilon_c E_{gl} h_{gl} + \varepsilon_c E_r A_{rt} \right] y_{pl} +$$

$$\left[\varepsilon_c E_r A_{rt} Z_t - \varepsilon_c E_r A_{rc} Z_c - \varepsilon_c \frac{b_{gl} h_{gl}^2}{2} E_{gl} - h_{gl} \varepsilon_c E_r A_{rt} \right] = 0$$

$$y_{pl} = \frac{-b \pm \sqrt{b^2 - 4ac}}{2a}$$

b. Tension reinforcement yields along with timber failing in compression

This is the phase where the reinforcement is the tension side has yielded along with the timber in compression. The shift in the neutral axis may be calculated by using the following equations

$$\left[f_{cu\_gl} b_{gl} \left(1 - \frac{\varepsilon_{el\_c\_gl}}{\varepsilon_c} \right) + \frac{f_{cu\_gl} b_{gl}}{2} - \left(\frac{f_{cu\_gl} b_{gl}}{2} \frac{\left(\varepsilon_c - \varepsilon_{el\_c\_gl}\right)}{\varepsilon_c} \right) - \frac{\varepsilon_c b_{gl}}{2} E_{gl} \right] y_{pl}^2 +$$

$$\left[\varepsilon_c E_r A_{rc} + b_{gl} \varepsilon_c E_{gl} h_{gl} - f_{t\_r} A_{rt} \right] y_{pl} +$$

$$\left[-\varepsilon_c \frac{b_{gl} h_{gl}^2}{2} E_{gl} - \varepsilon_c E_r A_{rc} Z_c \right] = 0$$

$$y_{pl} = \frac{-b \pm \sqrt{b^2 - 4ac}}{2a}$$

c. Compression reinforcement yields with timber failing in compression

This phase corresponds to the situation when the compression reinforcement has been yielded and the timber has reached its plastic stage. The neutral axis is calculated by solving the following nonlinear equation.

$$\left[f_{cu\_gl} b_{gl} \left(1 - \frac{\varepsilon_{el\_c\_gl}}{\varepsilon_c}\right) + \frac{f_{cu\_gl} b_{gl}}{2} - \left(\frac{f_{cu\_gl} b_{gl}}{2} \frac{(\varepsilon_c - \varepsilon_{el\_c\_gl})}{\varepsilon_c}\right) - \frac{\varepsilon_c b_{gl}}{2} E_{gl} \right] y_{pl}^2 +$$

$$\left[f_{c\_r} A_{rc} + b_{gl} \varepsilon_c E_{gl} h_{gl} - \varepsilon_c E_r A_{rt} \right] y_{pl} +$$

$$\left[-\varepsilon_c \frac{b_{gl} h_{gl}^2}{2} E_{gl} - \varepsilon_c E_r A_{rt} \left(h_{gl} - Z_t\right) \right] = 0$$

$$y_{pl} = \frac{-b \pm \sqrt{b^2 - 4ac}}{2a}$$

d. Both tension and compression reinforcement yields along with timber in compression

This is also a common phase, with all the reinforcements as well as the timber in compression has yielded.

$$\left[f_{cu\_gl} b_{gl} \left(1 - \frac{\varepsilon_{el\_c\_gl}}{\varepsilon_c}\right) + \frac{f_{cu\_gl} b_{gl}}{2} - \left(\frac{f_{cu\_gl} b_{gl}}{2} \frac{(\varepsilon_c - \varepsilon_{el\_c\_gl})}{\varepsilon_c}\right) - \frac{\varepsilon_c b_{gl}}{2} E_{gl} \right] y_{pl}^2 +$$

$$\left[f_{c\_r} A_{rc} + b_{gl} \varepsilon_c E_{gl} - f_{t\_r} A_{rt} \right] y_{pl} +$$

$$\left[-\varepsilon_c \frac{b_{gl} h_{gl}^2}{2} E_{gl} \right] = 0$$

$$y_{pl} = \frac{-b \pm \sqrt{b^2 - 4ac}}{2a}$$

When the neutral axis is found out considering all the nonlinearities, the resisting moment can be found out using the following formula.

$$M_r = \sigma_{rc} A_{rc} (y_{pl} - Z_c) + f_c b_{gl} Z_p (y_{pl} - \frac{Z_p}{2}) + \frac{1}{2} f_c (y_{pl} - Z_p) b_{gl} \cdot \frac{2}{3} (y_{pl} - Z_p) +$$

$$\sigma_{rt} A_{rt} (h_{gl} - y_{pl} - Z_t) + \frac{1}{2} \varepsilon_t E_{gl} (h_{gl} - y_{pl}) b_{gl} \cdot \frac{2}{3} (h - y_{pl})$$

Where

$\sigma_{rc} = \varepsilon_{rc} . E_r$ till yield point of reinforcement and $\sigma_{rc} = f_{y\_c\_r}$ after yield point.

$\sigma_{rt} = \varepsilon_{rt} . E_{'r}$ till yield point of reinforcement and $\sigma_{rt} = f_{y\_t\_r}$ after yield point.

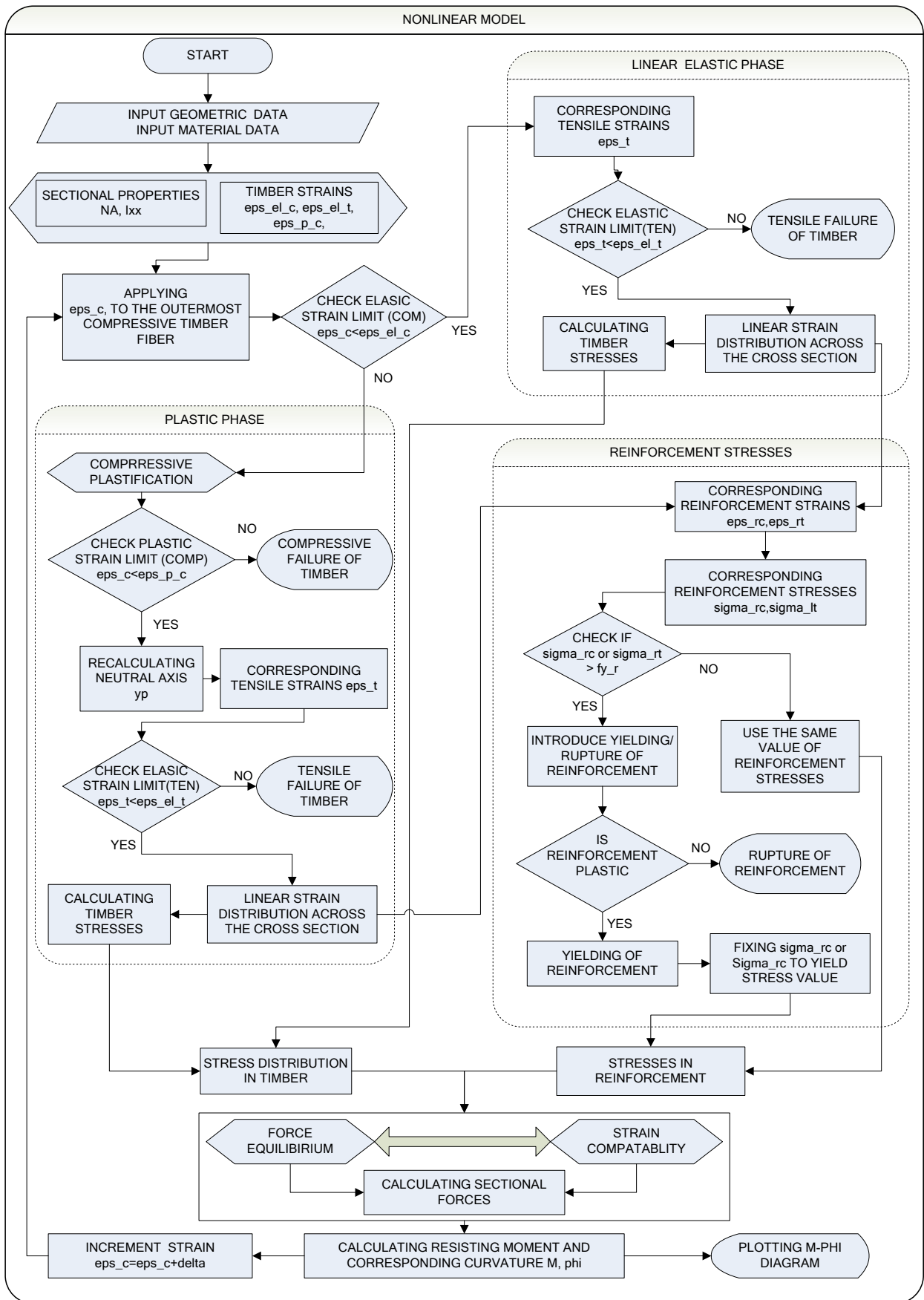The following flow chart shows the control flow in the case of the nonlinear model.

START

INPUT GEOMETRIC DATA
INPUT MATERIAL DATA

SECTIONAL PROPERTIES
NA, Ixx

TIMBER STRAINS
eps_el_c, eps_el_t,
eps_p_c,

APPLYING
eps_c, TO THE OUTERMOST
COMPRESSIVE TIMBER
FIBER

CHECK ELASIC
STRAIN LIMIT (COM)
eps_c<eps_el_c

YES

NO

LINEAR ELASTIC PHASE

CORRESPONDING
TENSILE STRAINS
eps_t

CHECK ELASIC
STRAIN LIMIT(TEN)
eps_t<eps_el_t

NO

TENSILE FAILURE
OF TIMBER

YES

CALCULATING
TIMBER
STRESSES

LINEAR STRAIN
DISTRIBUTION ACROSS
THE CROSS SECTION

PLASTIC PHASE

COMPRRESSIVE
PLASTIFICATION

CHECK PLASTIC
STRAIN LIMIT (COMP)
eps_c<eps_p_c

NO

COMPRESSIVE
FAILURE OF
TIMBER

YES

RECALCULATING
NEUTRAL AXIS
yp

CORRESPONDING
TENSILE STRAINS eps_t

CHECK ELASIC
STRAIN LIMIT(TEN)
eps_t<eps_el_t

NO

TENSILE
FAILURE OF
TIMBER

YES

CALCULATING
TIMBER
STRESSES

LINEAR STRAIN
DISTRIBUTION ACROSS
THE CROSS SECTION

REINFORCEMENT STRESSES

CORRESPONDING
REINFORCEMENT STRAINS
eps_rc,eps_rt

CORRESPONDING
REINFORCEMENT STRESSES
sigma_rc,sigma_lt

CHECK IF
sigma_rc or sigma_rt
> fy_r

NO

YES

INTRODUCE YIELDING/
RUPTURE OF
REINFORCEMENT

USE THE SAME
VALUE OF
REINFORCEMENT
STRESSES

IS
REINFORCEMENT
PLASTIC

NO

RUPTURE OF
REINFORCEMENT

YES

YIELDING OF
REINFORCEMENT

FIXING sigma_rc or
Sigma_rc TO YIELD
STRESS VALUE

STRESS DISTRIBUTION
IN TIMBER

STRESSES IN
REINFORCEMENT

FORCE
EQUILIBIRIUM

STRAIN
COMPATABLITY

CALCULATING SECTIONAL
FORCES

INCREMENT STRAIN
eps_c=eps_c+delta

CALCULATING RESISTING MOMENT AND
CORRESPONDING CURVATURE M, phi

PLOTTING M-PHI
DIAGRAM

Figure 4.8   Flow Chart- Nonlinear Model

Results

The nonlinear model was intended to predict the overall behaviour of the beam till failure. The effect of different parameters on the global behaviour of the beam was simulated by using the numerical model presented in the previous section. This section deals with the results of the nonlinear analysis.

a. Effect of introducing tensile reinforcement

Un-reinforced Glulam beams usually fail in tension. So reinforcements are introduced in the tension side to strengthen this part. This basically increases the tensile capacity of the beam which results in shifting of the failure mode to the compressive side.

Figure 4.9 illustrates a typical moment curvature relation for a beam reinforced at the tension side. It can be observed that the moment curvature relation is linear till the elastic limit, (point1) and afterwards is nonlinear due to compressive plastification till failure (point 2). This can be even clearly seen in the strain distribution diagram and the stress distribution diagram. It should be noted that the ultimate failure is still in tension, as the strain level in timber reaches limiting values ($\varepsilon_{el\_t\_r}$) in the tensile side far before it reaches the ultimate strain value ($\varepsilon_{pl\_c\_r}$) in compression. The depth of plastification can also be seen in the stress diagram.
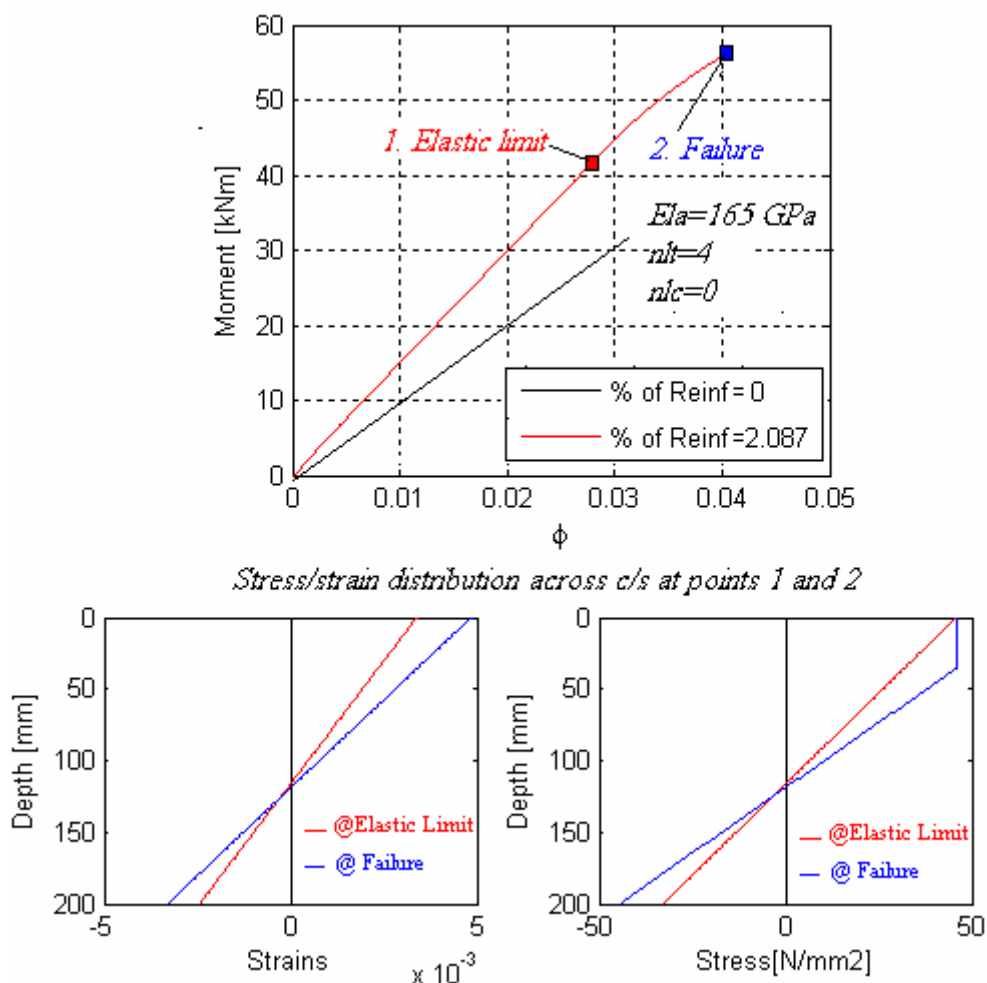
Figure 4.9   Behaviour of beam Reinforced at tension side (Ela=165Gpa)

The increase in moment capacity was seen to be around 85% and the beam stiffness increased by almost 50% with 2.087% of reinforcement of E-modulus 165GPa.

An analysis of the effect of increasing E modulus of the laminate was also done with the same reinforcement percentage as used before. This time the E-modulus of the beam was taken to be 300GPa. *Figure 4.10* shows the behaviour of the abovementioned beam. There is an obvious increase in strength and stiffness, but what is worth noticing is the corresponding increase in ductility which is the result of introduction of more plasticity in the compression side. Depth of plastification also increased correspondingly. But the failure was still brittle due to tensile failure of timber.
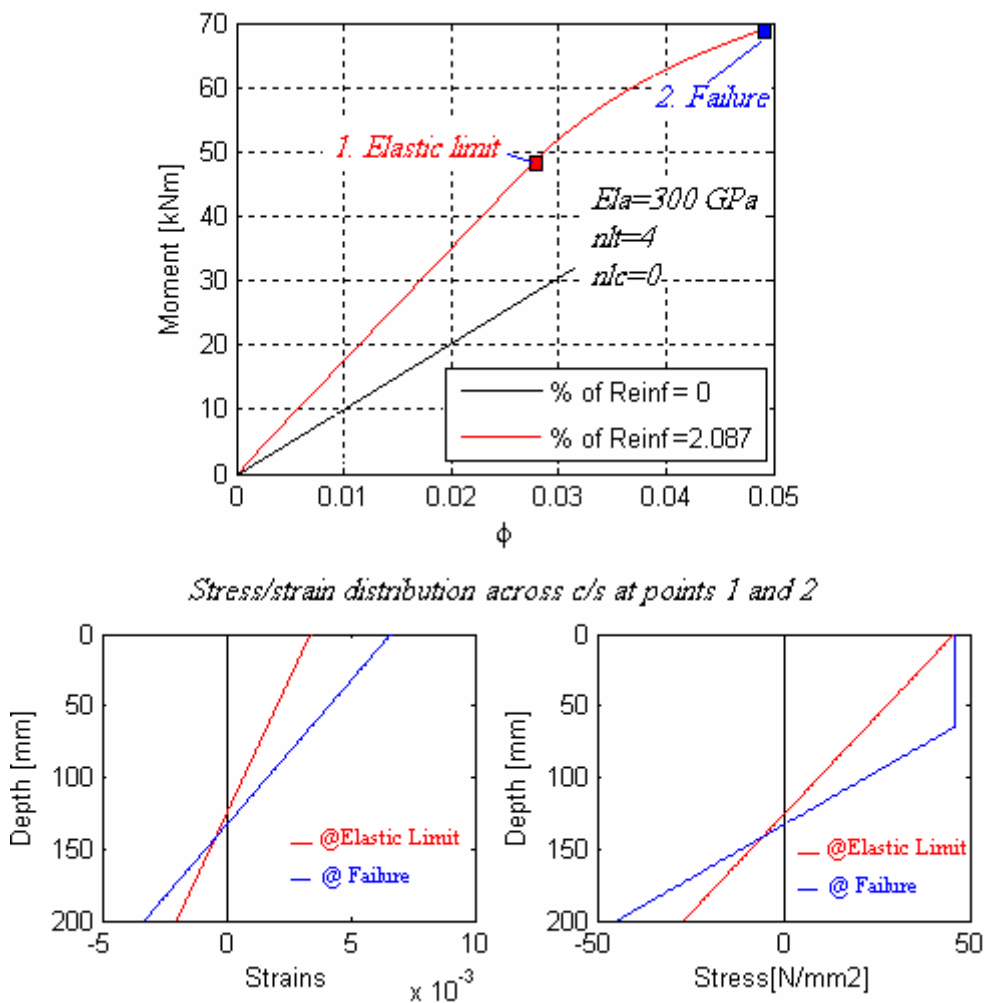
Figure 4.10   Behaviour of beam Reinforced at tension side (Ela=300Gpa)

It was quite interesting to know at what level of reinforcement at tension side, the beam will fail in pure compression. An analysis was done using the same configuration, using a laminate of E-modulus 300GPa. The reinforcement percentage at the tension side was increased till the beam fails in compression by the attaining the strain level equal to the ultimate plastic strain of timber. *Figure 4.11* illustrates the effect of increasing tensile reinforcement. It can be seen that the beam behaves linear elastic at very low tensile reinforcement levels, but plasticity comes into picture, as the reinforcement level goes up. But at this level, the failure is in tension as depicted

by the letter 't' in the diagram. But as the reinforcement level reaches 5.32% of the gross cross sectional area, pure compressive failure occurs. (Indicated by letter 'c')
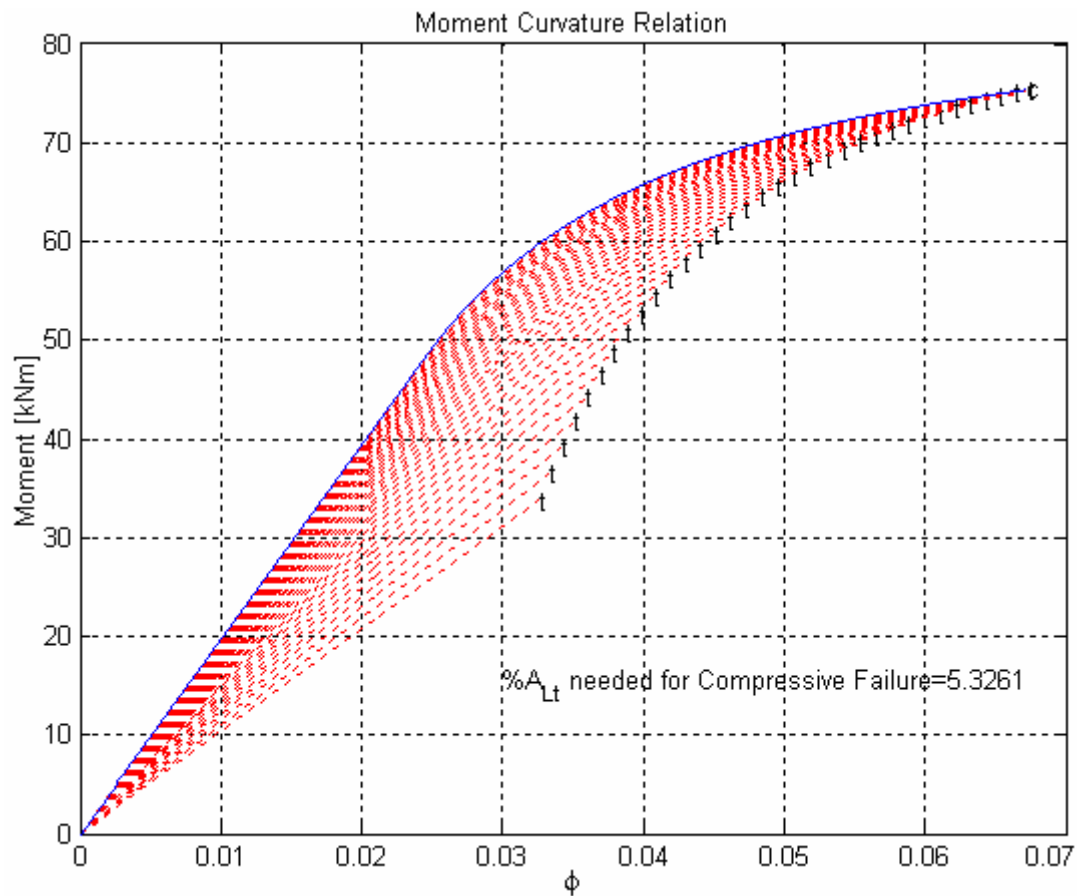

Figure 4.11 Effect of increasing tension reinforcement (Ela=300Gpa)

Figure 4.12 shows the increase in ultimate moment, stiffness and degree of plastification for each reinforcement levels compared to an un-reinforced beam. It can be seen that there is not much increase in the moment capacity as well as degree of plastification after a reinforcement level of 5%. This can be because the failure mode is in compressive zone. So the increased reinforcement will not have much effect, as timber is going to fail in compression at the same point, irrespective of the increased tensile reinforcement. But still there can be increase in the stiffness of the beam, as increasing reinforcement corresponds to incorporation of stiffer material to the cross section which is responsible for stiffness increase. We can even expect a decrease in the Φ value at failure after 5% of reinforcement, because the increased reinforcement in the tension side pulls down the neutral axis which results in a larger lever arm in the compression side.

The value stated here(5%) cannot be generalised for all beams, as the ultimate moment capacity, stiffness and degree of plastification depends on many parameters, such as e-modulus of timber and reinforcement, configuration of reinforcement etc. etc. So separate analysis has to be done for any other different beam configuration as well as while using other reinforcing material. But it should be kept in mind that the effect of shear failure is not included at this point of time(the beam will reach its shear capacity earlier for heavily reinforced beams).
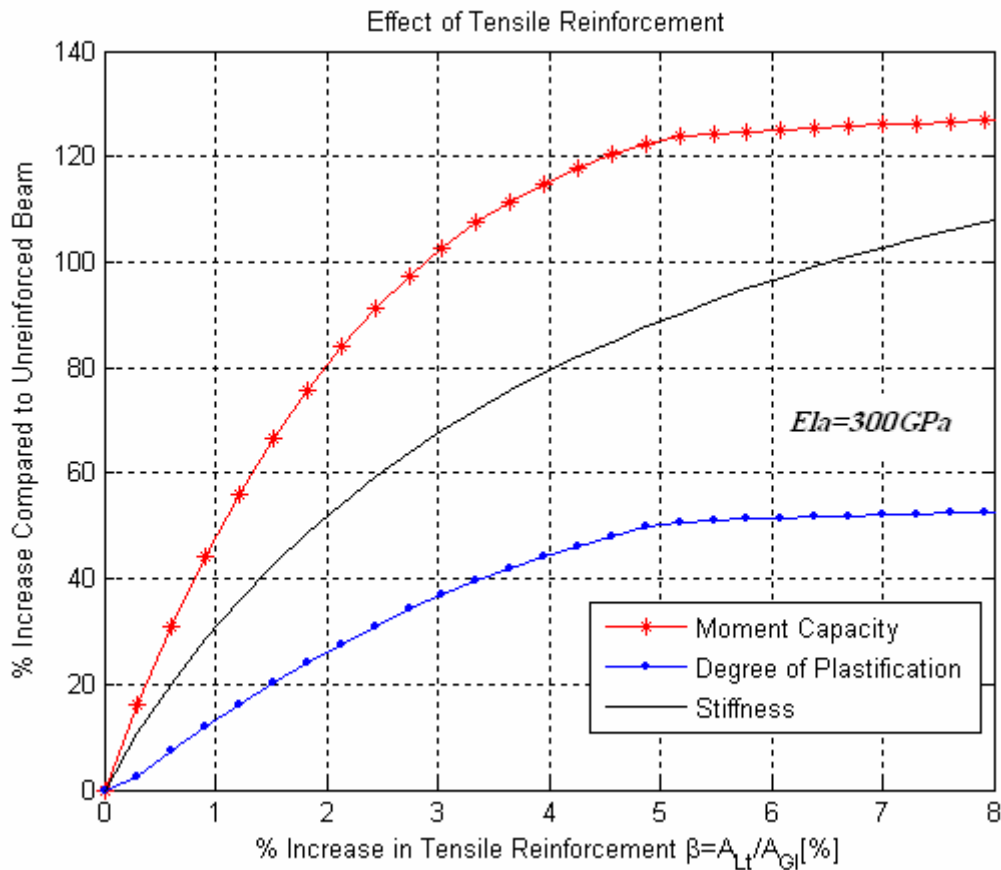
Figure 4.12 Effect of increasing tension reinforcement in ultimate moment capacity, stiffness and degree of plastification (E_{la}=300Gpa)

b. Effect of compressive reinforcement

The effect of introducing reinforcement in the compressive zone was also studied by using the non linear model. The addition of compressive reinforcement basically takes away the plastic behaviour of the beam. The stiffness increase is appreciable, but the failure is usually in tension.

The following figures (*Figure 4.13-Figure 4.17*) compare the responses of beams with varying amount of compressive reinforcement. Comparison was also made for different reinforcement percentages (from 1%- to 5% of gross cross section).

From *Figure 4.13* it can be noticed that the arrangement of the reinforcements in tension and compression sides affects the load bearing capacity, stiffness, and the failure modes of beams. The stiffness is almost the same, but the strength values vary a lot. The beam which is reinforced only in the tension side and beam which is reinforced lightly in the compression side shows some plastification before failure in tension. But a higher percentage of compressive reinforcements seem to reduce plasticity which in-turn result in a linear response and brittle failure.
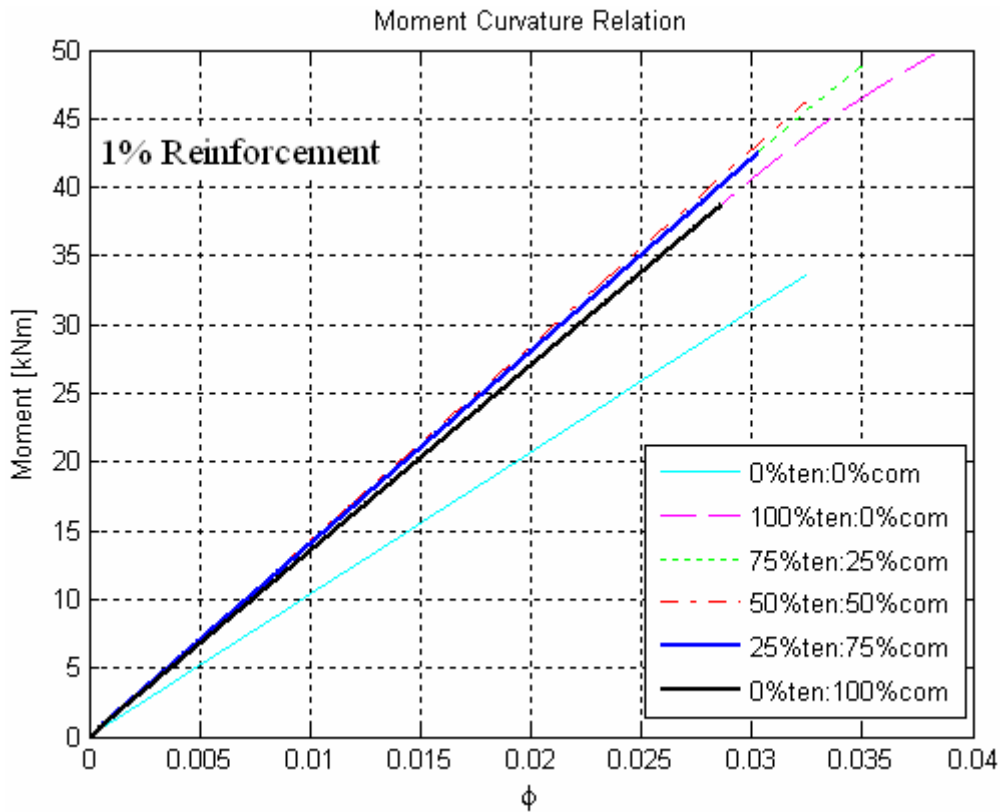
Figure 4.13 Response of different configurations reinforced with 1% of FRP
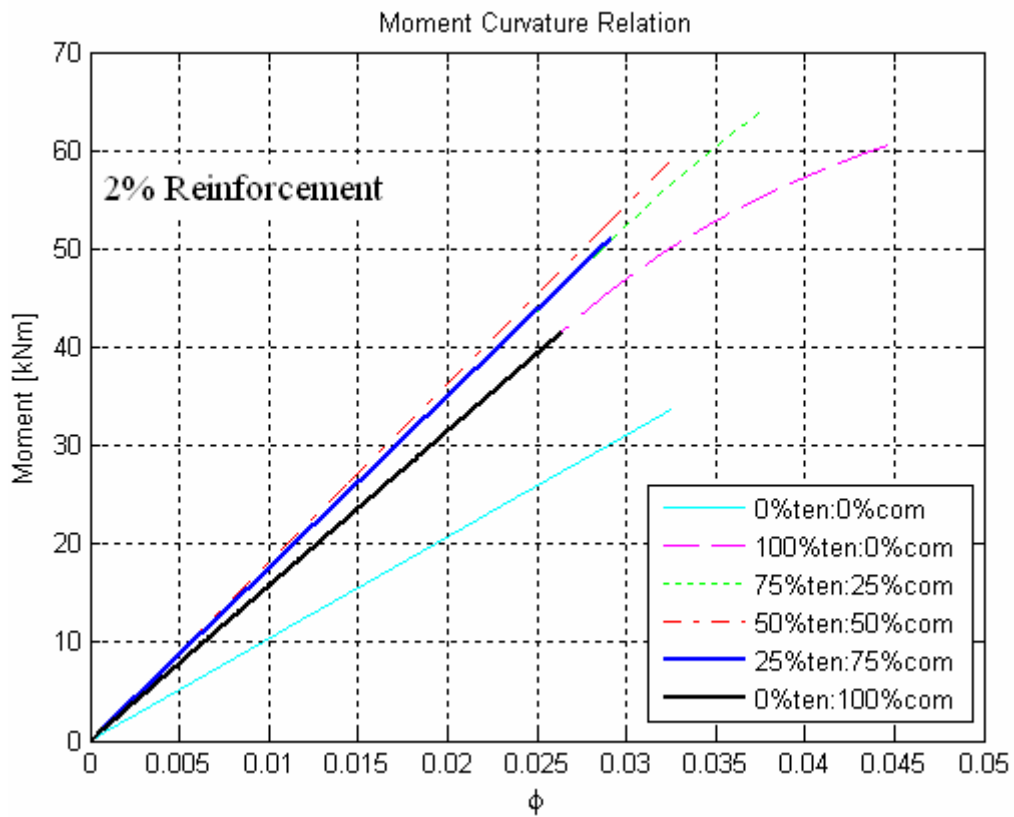
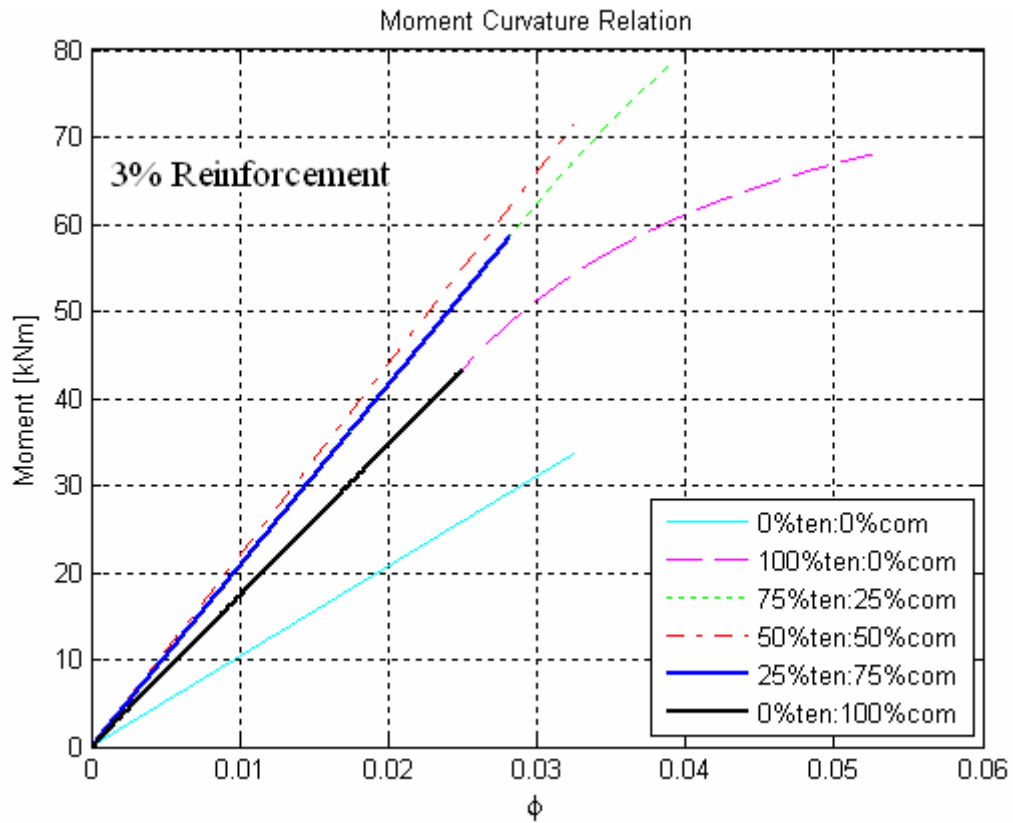*Figure 4.14   Response of different configurations reinforced with 2% of FRP*

Figure 4.15   Response of different configurations reinforced with 3% of FRP
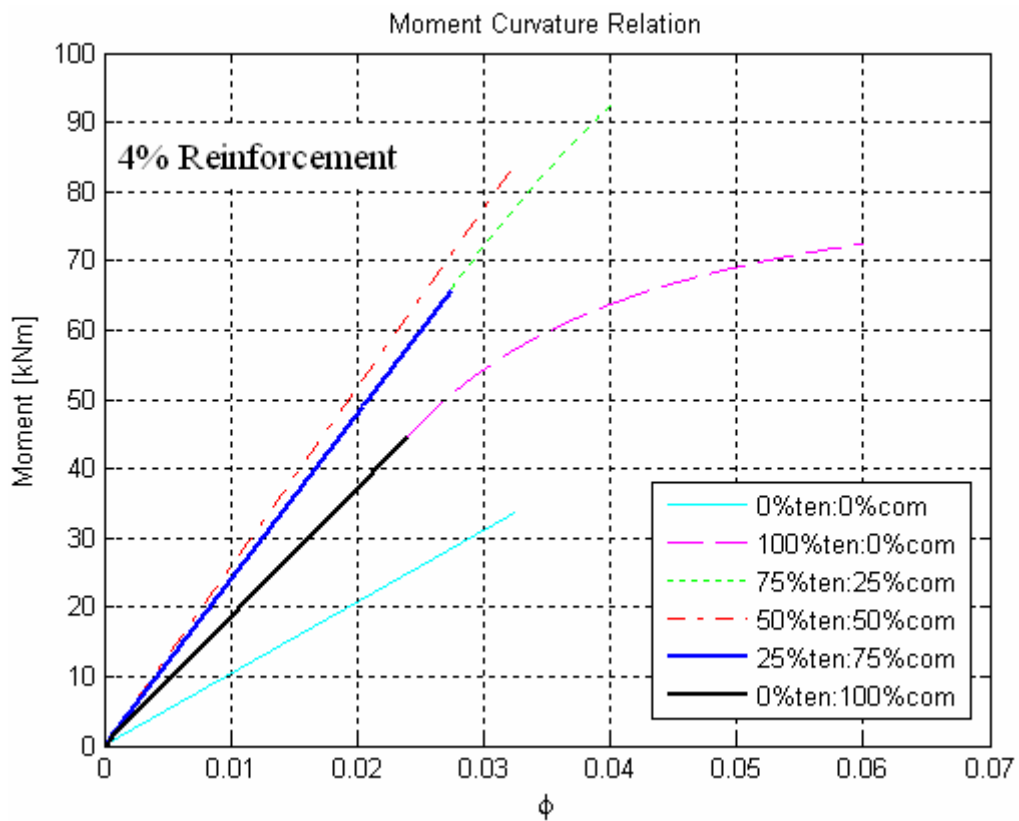

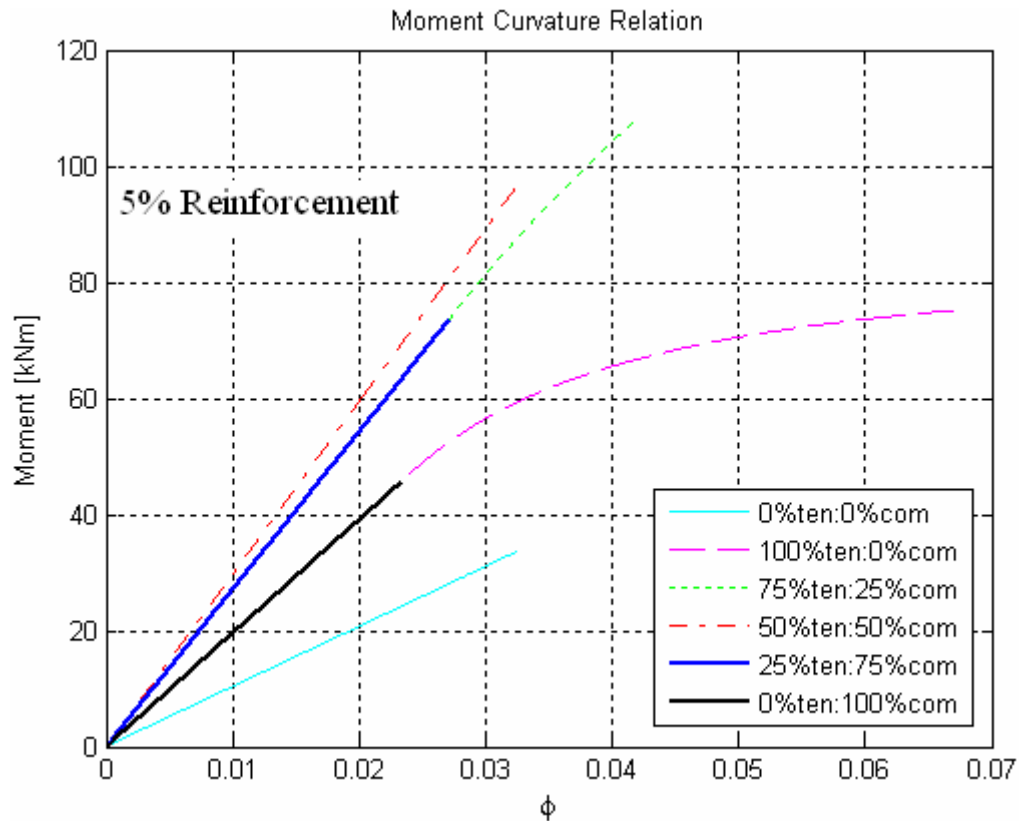*Figure 4.16   Response of different configurations reinforced with 4% of FRP*

Figure 4.17   Response of different configurations reinforced with 5% of FRP

Comparing the figures (*Figure 4.13-Figure 4.17*), it can be seen that the increase in reinforcement percentages also leads to responses which are not just extrapolation or responses which are not just a scaling of a particular configuration. If we compare *Figure 4.13* and *Figure 4.14*, the ultimate moment capacity of beam with 1% reinforcement is higher when all the reinforcement is provided in the tension zone, while for beam with 2% reinforcement, this happens when the reinforcement is distributed in the ratio 1:4 in the compression and tension respectively.

To have a further understanding of this phenomenon, the ultimate moment capacities and elastic stiffness of different configurations with different reinforcement ratios in the tension and compression zones were plotted (see *Figure 4.18* and *Figure 4.19*) for total reinforcement percentages ranging from 1% to 5%. Each curve corresponds to ultimate value of strength (or linear elastic stiffness in case of *Figure 4.18*) for beams with compressive reinforcement ratios varying from 0 to 100%. It can be seen that the stiffness as well as ultimate moment values are quite different even though the percentage of reinforcement is the same. But it should not give a wrong idea that the behaviour is just interpolation and extrapolation (respectively) or the failure modes are the same. Each configuration responded differently in terms of moment-curvature, as well as failure modes.
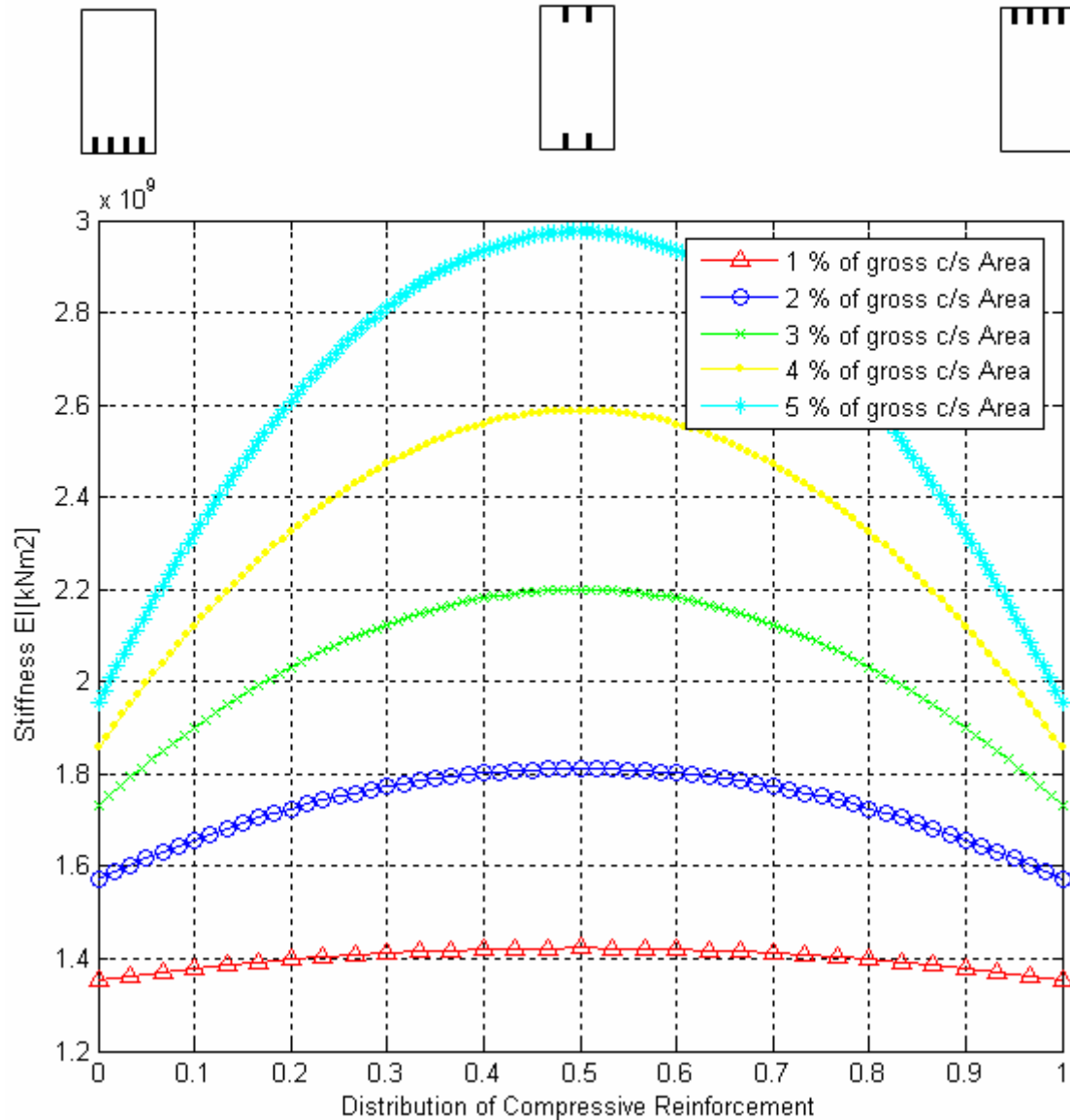
Figure 4.18 Stiffness values for different reinforcement distributions on tension and compression side (Ela=300Gpa)

It can be also noted from the graph that the stiffness distribution (see *Figure 4.18*) for different reinforcement configurations is symmetric for particular reinforcement ratio. But in case of ultimate moment, the graph is not symmetrical (see *Figure 4.19*), which is the result of difference in ultimate strength values in tension and compression. It can also be noted that with a reinforcement of E-modulus 300GPa, there is no point in increasing the reinforcement percentage above 2% as the beam is going to fail in shear which does not allow maximum usage of the cross section. But if we can provide some kind of shear reinforcement-a strut and tie model which can transfer the shear forces to the supports, we can further increase the reinforcement ratio without causing a shear failure. This can be done if we want a higher moment resistance or stiffness than that can be provided by a proper arrangement of 2% of CFRP
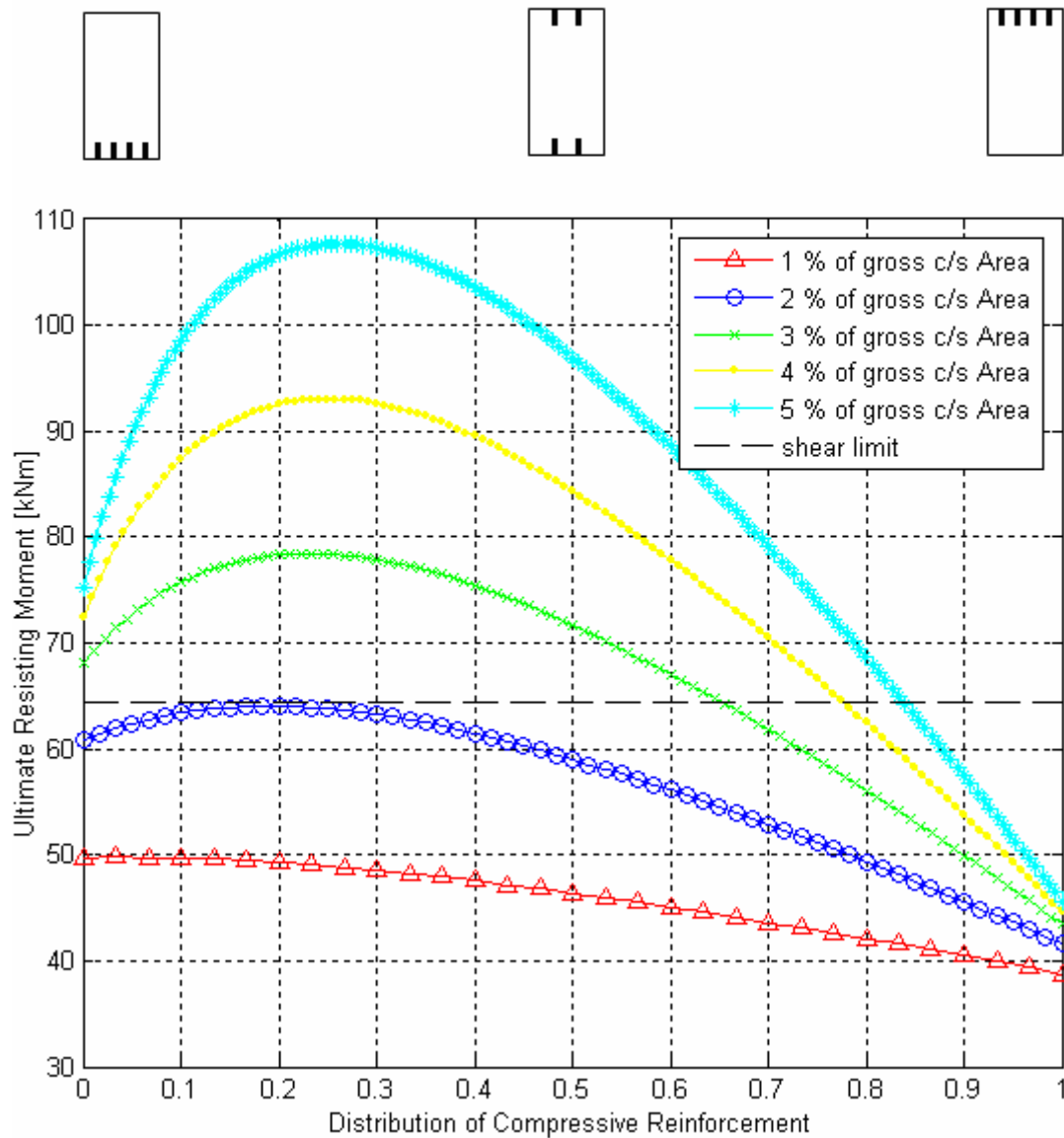
Figure 4.19 Ultimate revisiting moment values for different reinforcement distributions on tension and compression side (Ela=300Gpa)

c. Effect of Reinforcement Yielding

Yielding is a problem in metallic reinforcements. The effect of reinforcement yielding was also studied using the nonlinear model. *Figure 4.20* shows the effect of reinforcement yielding. The two curves represent two reinforcement types- one ductile and other brittle. It can be seen that the beam becomes more ductile even at low load levels while using metallic reinforcements. The global stiffness of the beam is reduced at the onset of the steel yielding. The steel no more takes any stresses, which eventually results in lesser moment capacity.

The yielding of the steel is quite advantageous as it induces more ductility into the global behaviour. This reduces the chance of un-warned brittle failure which otherwise can lead to disasters due to inadequate evacuation time.
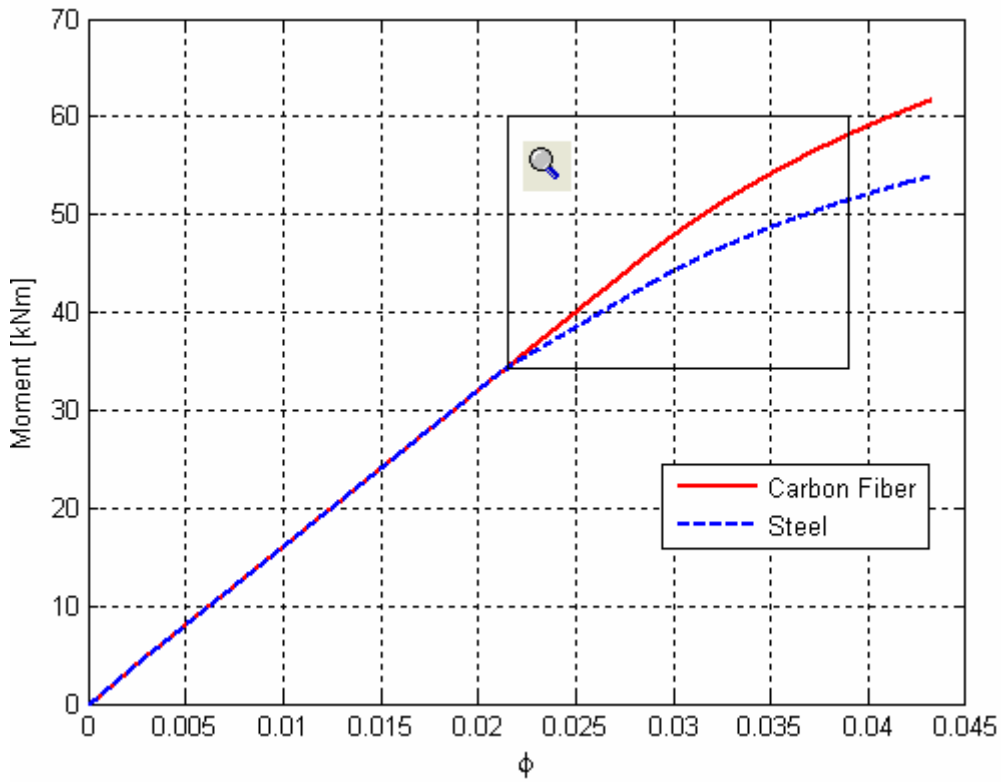
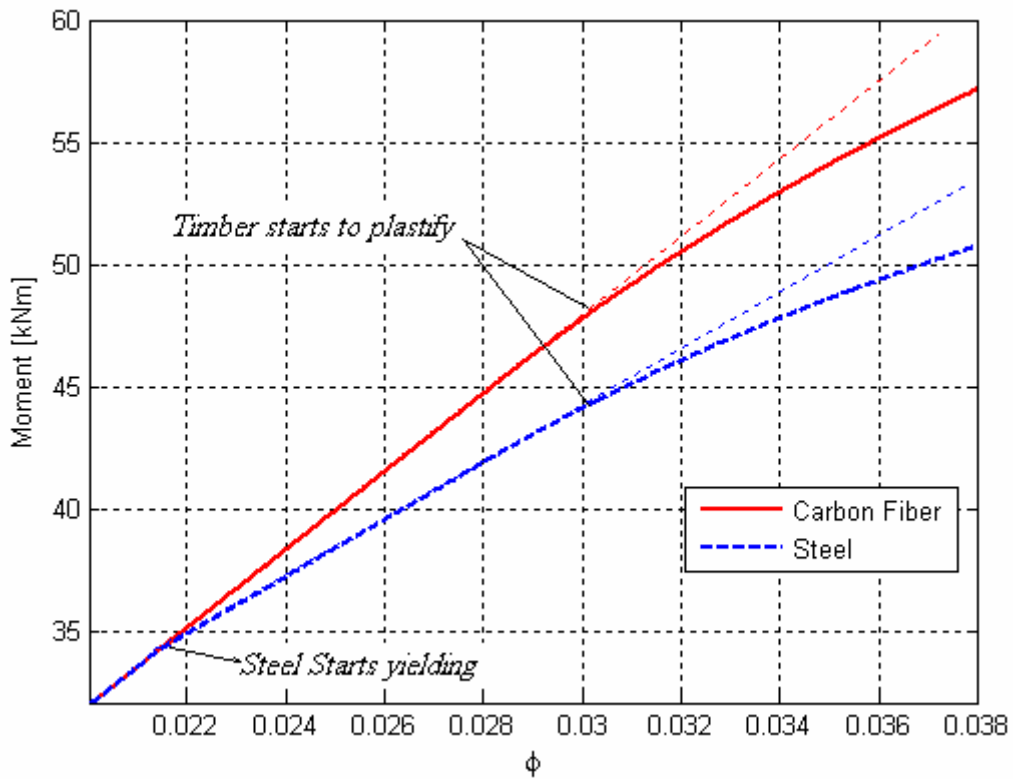*Figure 4.20 Effect of yielding of reinforcement (Ela=210Gpa)*

Figure 4.21 A more zoomed view of Figure 4.20

4.4 FE Model

The main postulate of finite element analysis (FEA) is that complex domains can be discretized and represented by an assembly of simpler finite sized elements. This enables description of the global problem through a system of differential equations that account for inter-element compatibility and boundary conditions requirements. FEA can be used to model a large array of physical situations and processes including problems in the domains of continuum mechanics, heat and mass transfer and fluid flow. The main advantage in the context of modern engineering is that the finite element models can be used simulate real life situations which if done in more conventional ways- with experiments and observations- would take quite lot of tests, time, and money. FE models can even be used to extrapolate beyond the range of test data- for example, in case of long term effects like creep, relaxation etc.; prediction can be done for a point of time in far future. But it should be kept in mind that modelling of a phenomenon taking all parameters involved into consideration would be cumbersome and practically difficult to achieve. FEA and other numerical analysis techniques can therefore never be a total replacement for experimental observations. They are a powerful adjunct that has to be allied with experimental observation and material characterization.

Description of the FE model

In the context of modelling the reinforced timber beams, the main focus was to get an idea of the interstitial stresses in the interfaces. The finite element model was created using the commercial software I-Deas. It should be noted that the model created here is not exactly the same as that were used in testing or non linear modelling. The idea was to study the effect of interstitial stresses with a simple working model, to ensure that the shear stresses created in the glue line does not exceed the limiting value so that there will be no de-lamination under loading.

A two-dimensional finite element model was developed to predict the shear s distributions along the length of an adhesively bonded joint. The model used linear material properties for both timber and reinforcements. Plane stress elements were used in all the analysis. This reduces the number of nodes which is advantageous in terms of computing power.

Geometry and Materials

For the sake of simplicity and saving computing power, symmetry of the beam was considered in selecting the geometry for modelling. The modelled beam had a cross section of 115mm x 180mm and was 4m long. Only half of the beam section was modelled as shown in *Figure 4.22*. The laminate was 115mm wide and 1.4mm thick and the thickness of the adhesive was taken as 1mm.
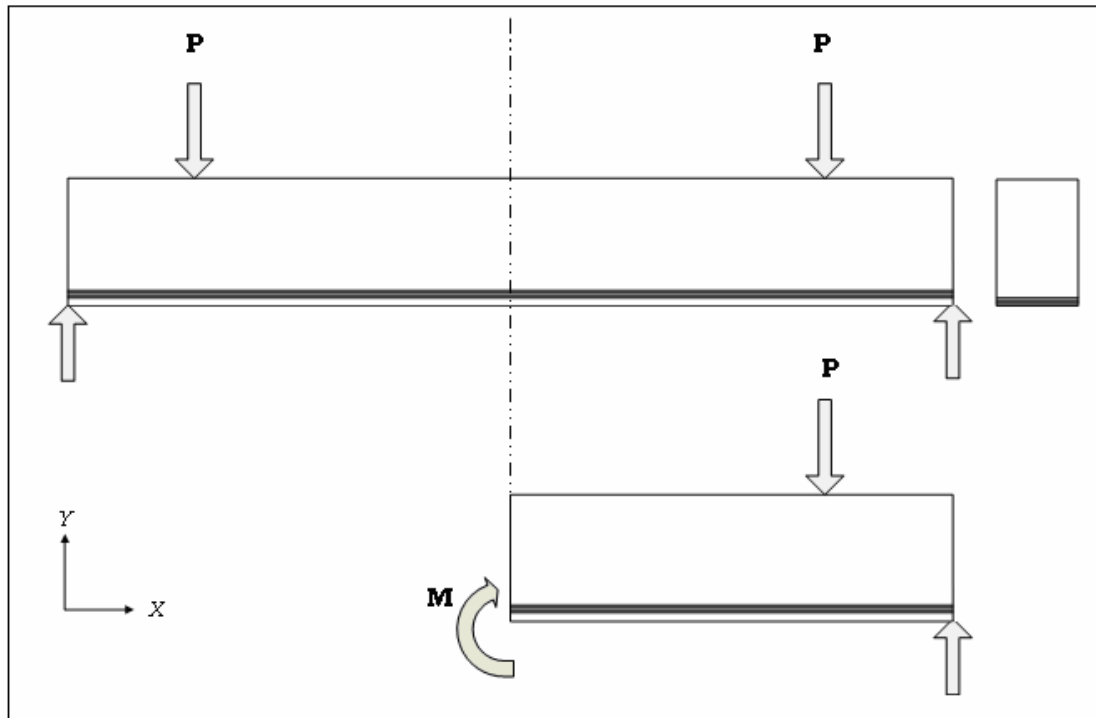
Figure 4.22 Loads and boundary conditions

The material properties used in the analysis are shown in the table given below (*Table 4.2*)

Table 4.2 Material Properties

Material	E-modulus	Shear Modulus	Poisons Ratio
Glulam	*13.5 GPa*	*850 MPa*	*0.28*
CFRP	*300 GPa*	*3750 Mpa*	*0.33*
Adhesive	*3.8GPa*	*500 MPa*	*0.39*

Boundary conditions and loads

The boundary conditions were accordingly chosen which would give the same effect of a full scale beams. The model was simply supported at one end. At the other end, a moment was added in the place of the removed half section. This was done in a simpler way taking the advantage of the height of the beam. The boundary condition in the mid-span of the beam was simulated just by locking all displacements in the x directions. The effect of the moment was automatically created because of the fact that the mid section is allowed to move only in the y direction and no rotation is possible as all the nodes in the mid-plane are fixed in the x direction.
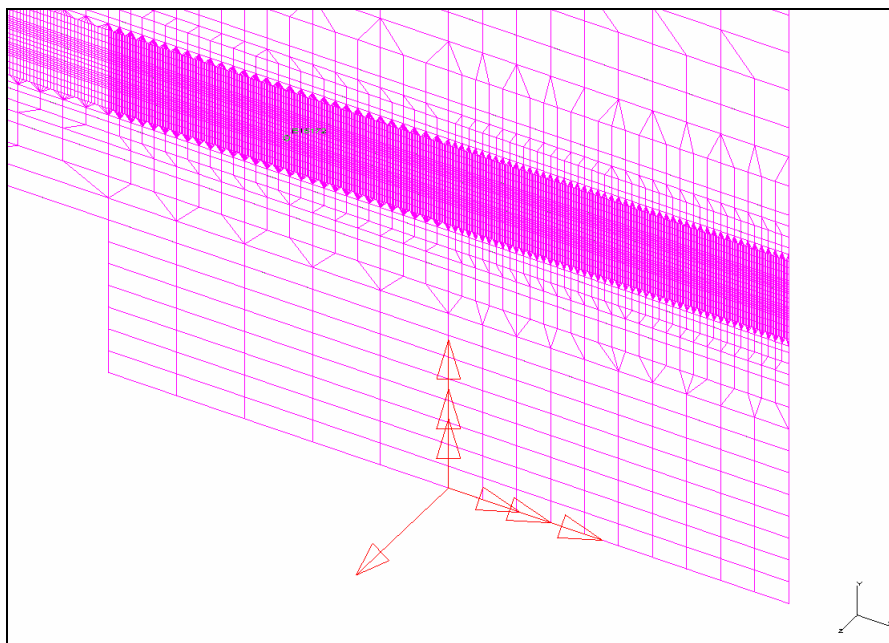
Figure 4.23 shows the boundary condition applied to the model. It can be seen that the displacement in the x direction is locked. But displacements in the y direction are

allowed, resulting in the creation of a moment analogous to that created by the full scale beam.
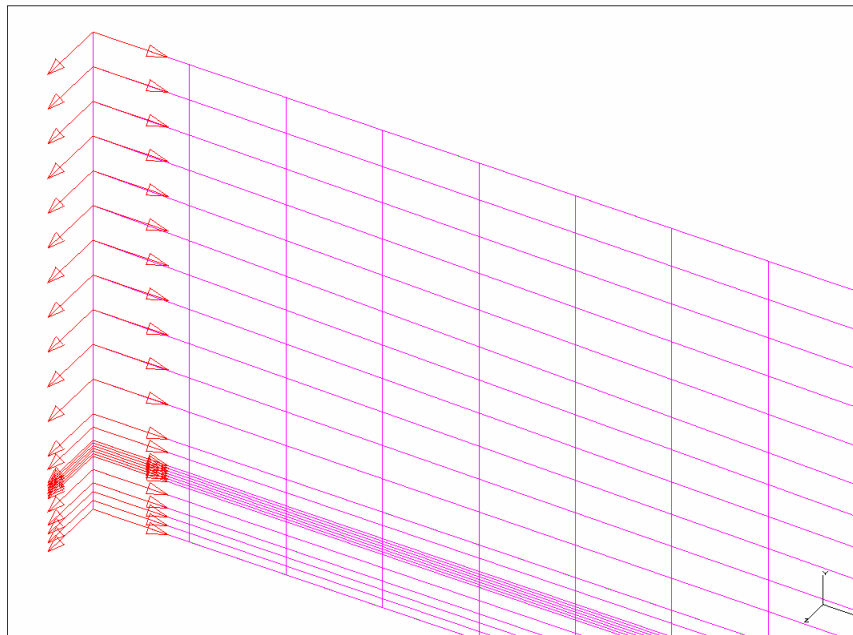

Figure 4.23 Boundary condition at the mid-span

A plate support was provided at the support analogous to the bearing plate in reality. The plate support was then simply supported at its centre by providing a hinge joint (*Figure 4.24*). Special type of contact elements were used to model the support. It should be noted that the displacements in all the three directions are locked. Rotation is allowed only about the z axis. This results in a support case analogous to a pinned joint.

Figure 4.24 Boundary condition at the support

The load application was done in a four point bending arrangement. The loads were applied directly to 3 number of nodes in order to simulate the effect of the bearing plate.
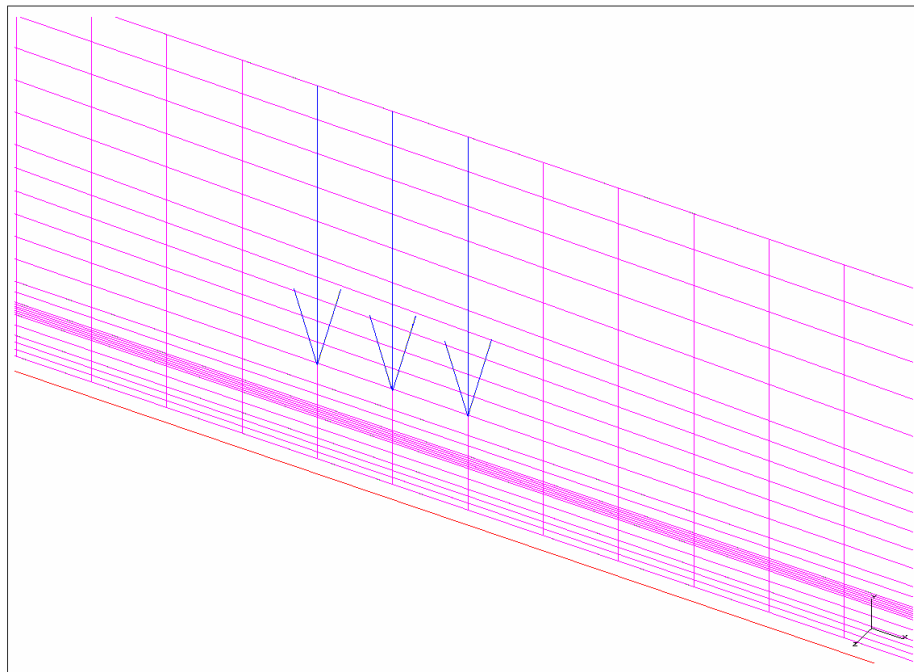
Figure 4.25 Loads

Meshing

Meshing was done in such a way to catch the shear forces generated from along the glue line. As it is obvious that the shear force near support will be maximum, a finer meshing (2mm x 1mm) was done near to supports. A very fine meshing was used for the adhesive, in order to see the shear stress development clearly.
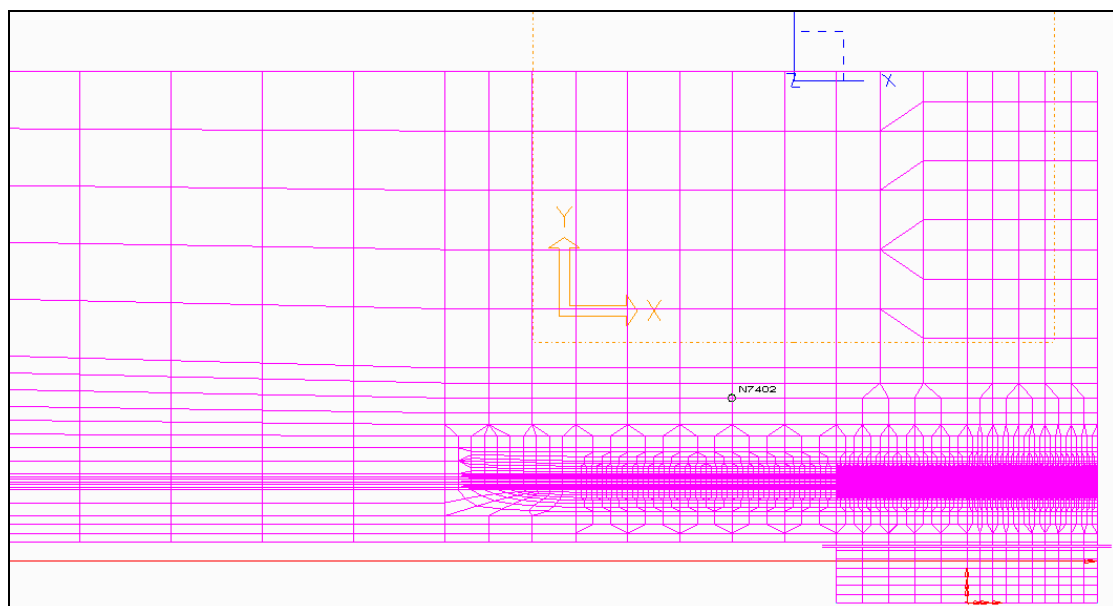
Figure 4.26 Meshing near to supports

The FE analysis used plain stress elements as the beam was considered to have plaate like behaviour, with all out of plane properties and loading remains constant . The following section provides the basic theory behind usage of plane stress elements.

Plane State of Stress

In general, the state of stress at a point in a body can be characterized by six independent normal and shear stress components. However due to the complexity of analyzing problems in three dimensions, engineers often reduce the analysis to a single plane by assuming a state of plane stress. A class of common engineering problems involving stresses in a thin plate or on the free surface of a structural element, such as the surfaces of thin-walled pressure vessels under external or internal pressure, the free surfaces of shafts in torsion and beams under transverse load, have one principal stress that is much smaller than the other two. By assuming that this small principal stress is zero, the three-dimensional stress state can be reduced to two dimensions. Since the remaining two principal stresses lie in a plane, these simplified 2D problems are called plane stress problems.

Plane stress is defined to be a state of stress in which the normal stress, and the shear stresses directed perpendicular to the x-y plane are assumed to be zero.

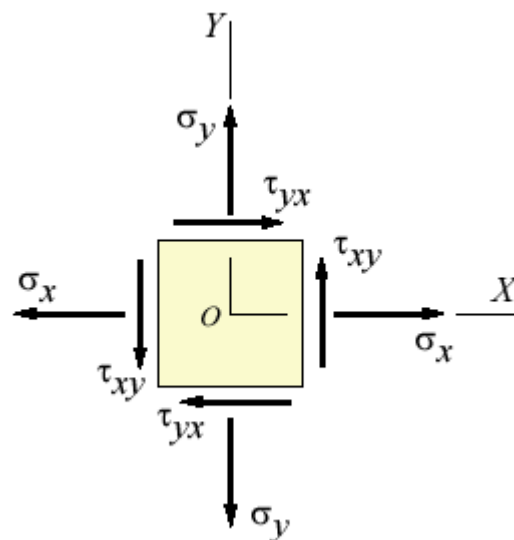 Figure 4.27 shows this state of stress.

Figure 4.27 Plane stress state ($\tau_{xy} = \tau_{yx}$ for static equilibrium)

For isotropic materials assuming,

$$\sigma_z = \tau_{xz} = \tau_{yz} = 0$$

$$\gamma_{xz} = \gamma_{yz} = 0$$

$$\{\sigma\} = [D]\{\varepsilon\}$$

Where D is the stress/strain matrix or constitutive matrix and is given by

$$[D] = \frac{E}{(1-v^2)}\begin{bmatrix} 1 & v & 0 \\ v & 1 & 0 \\ 0 & 0 & \frac{1-v}{2} \end{bmatrix}$$

Where E is the modulus of Elasticity and v is the poisons ratio.

The strains in the plane stress are then calculated by

$$\{\varepsilon\} = [C]\{\sigma\}$$

Where $C = D^{-1}$

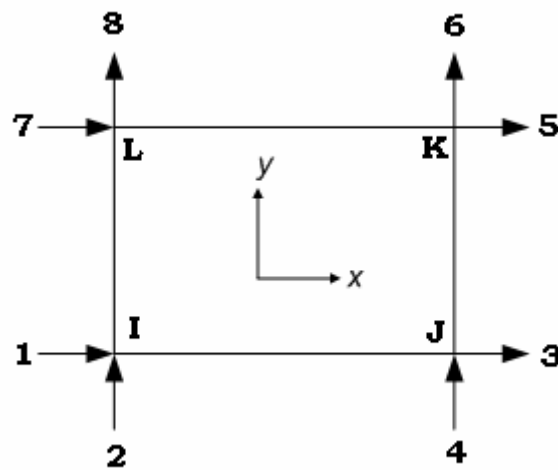*Figure 4.28* shows the two dimensional 4-node plane stress element.

Figure 4.28 Four Node Plane Stress Element with conventional nomenclature

Model verifications

The model verification was done by hand calculations of the reaction forces as well as the deformation. A suitable mesh size was thus chosen which gave satisfactorily consistent results**.**

Analysis

The analysis was done with the solver module in I-deas. The output information needed was specified in advance in order to eliminate unwanted results as well as save time and computing power. The main focus of our study was the interstitial stresses in the glue line.

Results

The XY shear along the glue line was plotted for different load levels. *Figure 4.29* shows the distribution of shear stresses along the glue line for different load level. It could be noted that the shear stresses are not high enough to produce failure of the

adhesive in shear. The maximum shear stress is developed at the support, with a peak exactly above the point of support reaction.
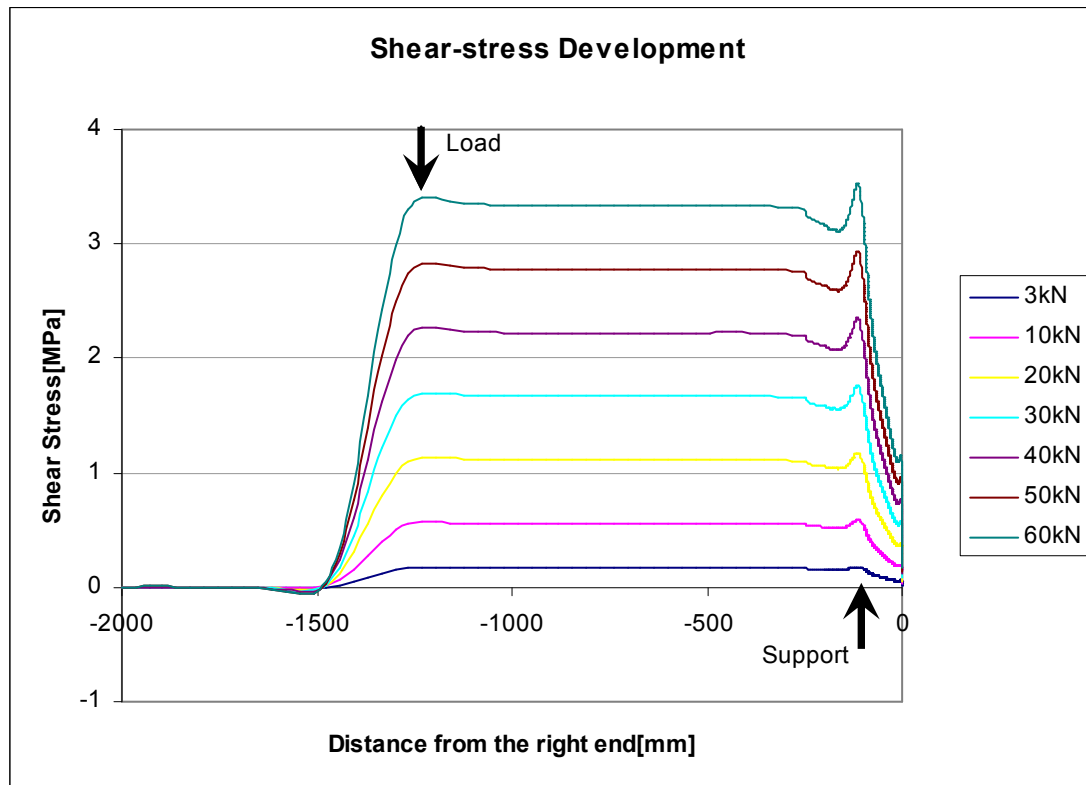

Figure 4.29 Shear stress development along Glue-line at different load levels

The maximum shear stress developed at a load level of 60kN is 3.563kN. But the value is well below the allowable limit of 15- 30 MPa for adhesive and 7 Mpa for timber.

Figure 4.30 shows the normal stress distribution in the interface between the laminate and the adhesive. It should be noted that the normal stresses are compressive in nature from the end of the beam till support and it changes from zero to maximum and then back to zero. This change in the normal stress explains the peaks in the shear stress diagram near to the support.

This simulation is done with simply supported boundary condition. But fixity at the support, due to moment resistant connections as well as continuous spans, can induce additional normal stresses in the glue-line. This situation should be studied well before implementation as the combined effect can cause up-normal peaks in the shear stress in the adhesive.
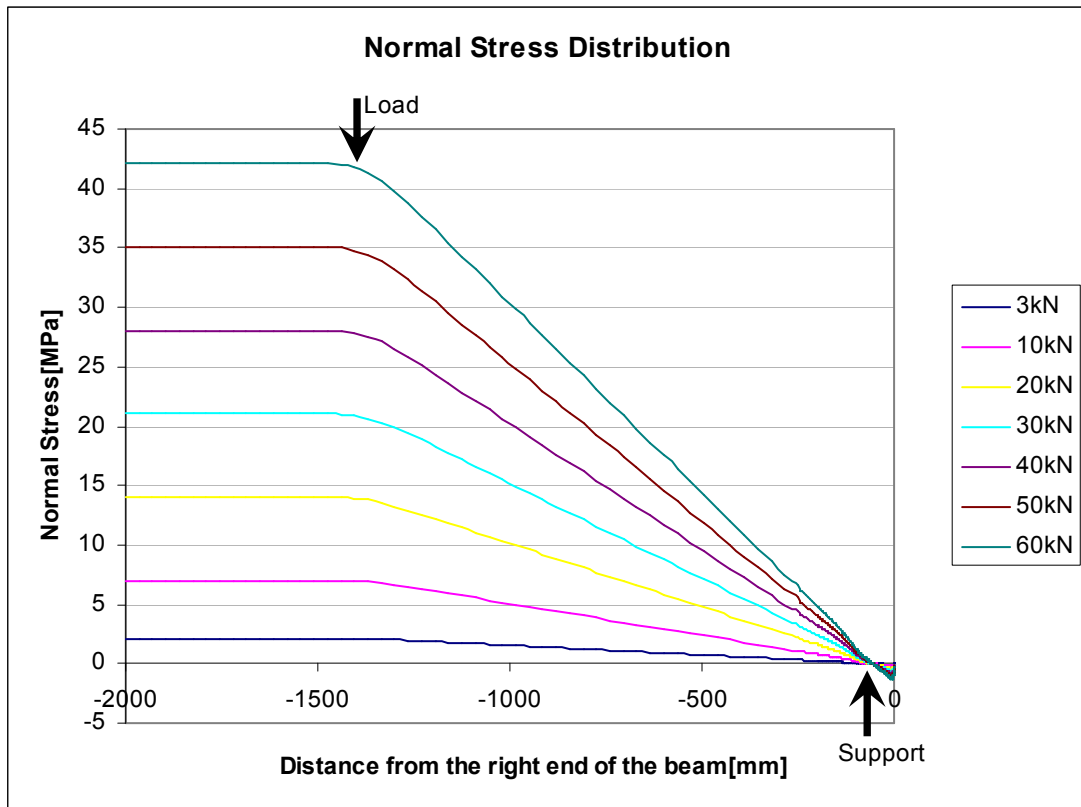
*Figure 4.30 Normal stress development at different load levels*

5 EXPERIMENTS

5.1 Test Configurations

On the basis of modelling, five configurations were chosen for testing. (see *Figure 5.1*).All the beams were tested till failure under monotonic loading in a four point bending configuration with loads applied at one third span. A total of 9 beams including two un-reinforced ones were fabricated and tested until failure. Two plain glulam beams were tested to establish a control set of data. 4 beams were reinforced with steel and another 3 beams were reinforced with CFRP.

Figure 5.1 shows the different schemes of reinforcements. Configuration (a) was for reference. Configuration (b) which was reinforced only in the tension side was intended to study the effect of compressive plastification. Configuration (c) and configuration (d) was aimed to bring forth the effect of a symmetric reinforcing arrangement in tension and compression zone, using two different reinforcing materials. Configuration (d) was intended to see the effect of light compression reinforcement (33%).
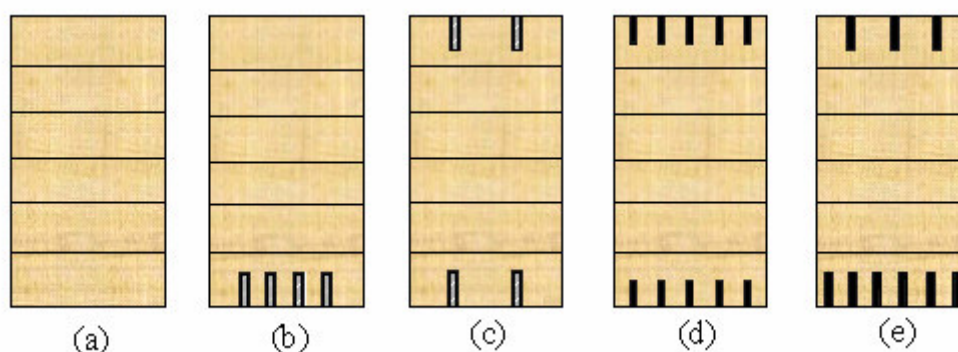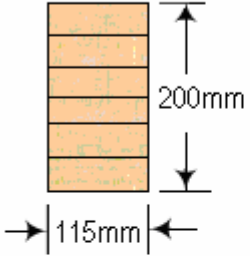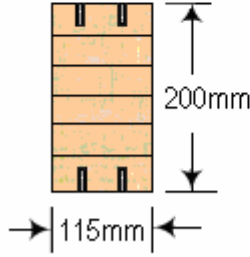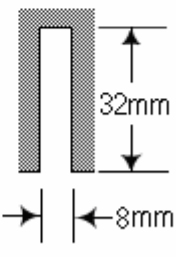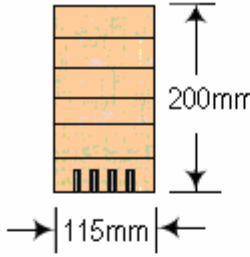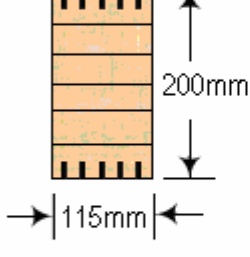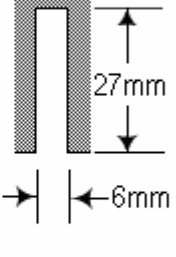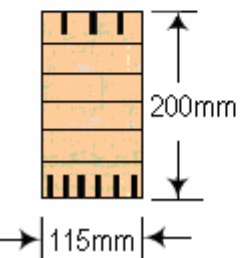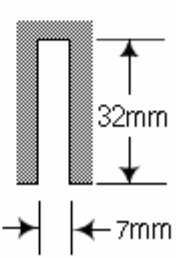

Figure 5.1 Experimental specimens (a) Reference Beam (b)Beam with Steel reinforcement on tension side (c)Beam with Steel reinforcement distributed equally on compression and tension sides (d) Beam with CFRP reinforcement distributed equally in tension and compression (e)Beam with CFRP reinforcement on both tension and compression in the ratio 1:2.

Efforts have also been made to study the effect of two basic types of reinforcing systems- (i) yielding reinforcements as well as (ii) brittle reinforcements. The effects of reinforcement yielding, as well as brittle nature of reinforcements results in quite different global response as well as failure modes. Efforts have been made to study different failure modes also, by controlling the amount of reinforcement based on the numerical modelling results. For example, the shear failure mode was deliberately induced by introducing higher reinforcement ratios in the beam.

Table 5.1 shows the different scheme of reinforcements and overall geometries.

Table 5.1 Configurations used in Experiments

Geometry		Reinforcement	Adhesive	No of beams tested	Beam Nomenclature
Model	Slot				
200mm, 115mm		No Reinforcement	-	2	Beam-1
					Beam-2
200mm, 115mm	32mm, 8mm	Steel E=210GPa 4x(4mm x 30mm) 2% of Gross c/s 50% ten 50% com	Sikadur-30	2	Beam-3
					Beam-5
200mm, 115mm	32mm, 8mm	Steel E=210GPa 4x(4mm x 30mm) 2% of Gross c/s 100% ten 0% com	Sikadur-330	2	Beam-4
					Beam-6
200mm, 115mm	27mm, 6mm	CFRP Sika CarboDur H E=300GPa 10x(1.4mm x 25mm) 1.5% of Gross c/s 50% ten 50% com	Sikadur-330	1	Beam-7
200mm, 115mm	32mm, 7mm	CFRP Sika CarboDur S E=165GPa 9x(1.4mm x 30mm) 2.8% of Gross c/s 66.6% ten 33.3% com	Sikadur-330	2	Beam-9
					Beam-10
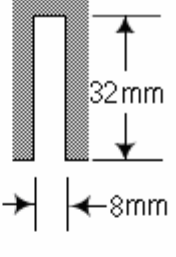
Specimens and Numbering System

The beams are identified as Beam1- Beam7 and Beam 9- Beam 10. Beams 1 and 2 are the control beams (un-reinforced, Type (a) as in *Figure 5.1*). Beams 3 and 5 are reinforced with steel only at the tension side (Type (b) as in *Figure 5.1*). Beams 4 and 6 are also reinforced with steel, but distributed equally in tension and compression (Type (c) as in *Figure 5.1*). Beam 7 is reinforced with CFRP (E-modulus=300GPa), distributed equally on tension and compression side (Type (d) as in *Figure 5.1*) Beam 9 and 10 are reinforced using CFRP (E-modulus=165GPa), distributed in the ratio 1:2 in tension and compression (Type (e) as in *Figure 5.1*).

5.2 Beam Fabrication

The timber specimens were provided by Moelven Töreboda AB, Sweden. The beams were prepared from stress graded lumber (Class 2). The reinforcing of the beams was done at Chalmers University of Technology. The process of beam fabrication is explained in the following sections.

The beams were fabricated under factory condition at Moelven Töreboda AB. The slots for placing reinforcements were made at the factory as per dimensions provided in *Table 5.1*. The slots were cleaned thoroughly to ensure dust free bonding surface. *Figure 5.2* shows the slotted test specimens.


Figure 5.2 Test Specimens- Before reinforcing

a. ***Surface Preparation for reinforcements***

The surfaces of the reinforcements were cleaned thoroughly in order to avoid the presence of dirt and grease which can cause ineffective bonding. The steel plates were sand blasted to remove rust and also to make the surface rough. The reinforcements are then treated with acetone which removed the grease. Steel plates are then treated with primer which acts as a base for the adhesive and also prevents further rusting of iron till it is placed in the beam (see *Figure 5.3*). The carbon fiber reinforcements were cut into halves longitudinally in order to obtain correct dimensions. The Sika CarboDur H is typically 60mm wide, and the Sika CarboDur S is 50mm wide. So after cutting, the widths were reduced to 30mm and 25mm respectively. The carbon fiber laminates showed slight bowing after cutting because the cutting process released some residual stresses which got incorporated in the laminate during

manufacturing process (see *Figure 5.4*). Cutting of Sika CarboDur S was done by a special arrangement of cutting tool which made a small crack at one end and this crack was propagated in a controlled way to the other end of the beam along the fiber direction. But for Sika CarboDur H, which was stiffer and harder, cutting was done using the conventional Band Saw.

Figure 5.3 Surface preparation- Primer application for steel reinforcements
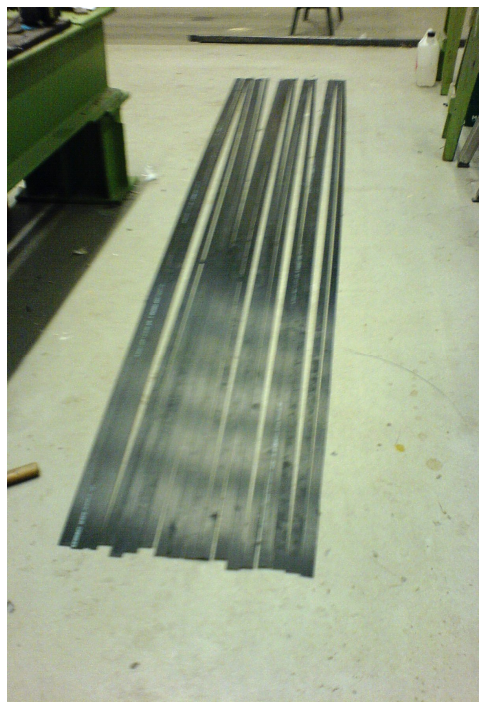
Figure 5.4 CFRP Specimens- After slicing

b.   *Preparation of Adhesive*

The two component adhesives were from Sika, the details of which can be seen in *Table 3.4* and *Table 3.5*. The components A and B are mixed in the ratio prescribed by the manufacturer. The component A is basically an epoxy resin, and Component B is a hardener, which on mixing will start reactions which are responsible for hardening. The components were first weigh batched using precise electronic weighing machine and then mixed thoroughly to form a homogeneous paste. Care has

been taken to assure that the gluing process is done within the initial setting time of the adhesives. *Figure 5.5* shows the weigh batching of the adhesive components.

Figure 5.5 Preparation of Adhesives- Weigh batching of components

c.   *Adhesive Application*

The application of the adhesive was done in a typical way. The slots for the reinforcements were filled 3/4th full with adhesive mixture using nozzle arrangement and spatula. Care has been taken to avoid any air entrapment. Two types of adhesive were used for the steel test, Sikadur 330 and Sikadur 30; both of them having epoxy as a principal component. The sikadur-30 was stiffer and less viscous, but sikadur-330 was viscous and easy to work with. *Figure 5.6* shows the application process of the adhesive. It should be noted that the viscosity of the adhesive plays a very important role in the workability which in-turn affects the overall quality of the process. Lower viscosity is more advisable when working with smaller groove widths. But higher viscosity will result in lesser shrinkage on curing due to the presence of particulate matter within the adhesive.

Figure 5.6 Application of Adhesive

d. Reinforcement placement

Spacers are glued to the reinforcements before placement in order to maintain straightness and also to ensure adequate adhesive cover between the reinforcement and the timber. These reinforcements are then pressed into the slots manually. The reinforcement displaces the adhesive which comes out through the cover between the reinforcement and timber. Additional spacers were provided wherever required (see *Figure 5.7*).

Figure 5.7 Placing additional spacers to ensure straightness and even adhesive cover

e. Curing

The reinforced Glulam beam was then left for curing for 5 days before testing. Small weights were placed on top of the reinforcements in order to ensure the reinforcements are held at place. *Figure 5.8* shows a specimen with all the reinforcements at place, and finished.
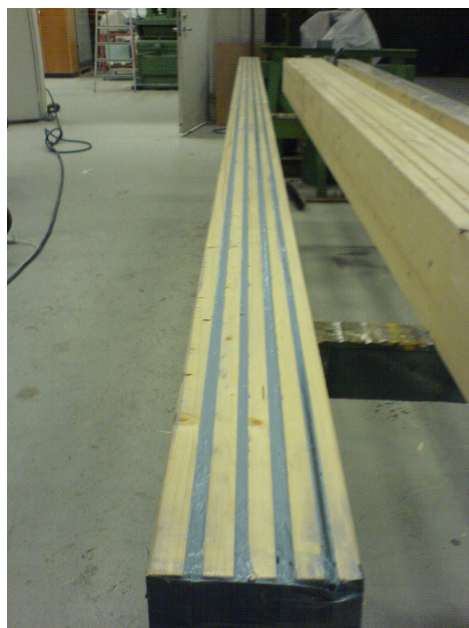

Figure 5.8 Finished specimen

5.3 Testing

Testing was done using the instrument setup at Chalmers University of Technology, Department of Structural Engineering. The beams were tested in four point bending configuration (explained in section 5.3.1). BS EN 408: 1995 specifies test methods for determining mechanical properties of structural timber and glued laminated timber. The information recorded during tests comprised of beam deflections at the mid-span and at 600mm from the support as well as strain values at different locations across the height.

5.3.1 Four Point Bending Configuration.

Four point bending configuration corresponds to a load-support arrangement where two transverse vertical loads are applied to a simply supported horizontal beam such that a constant bending moment is obtained in between the two inner load locations. A conventional four point bending arrangement was used in our tests, where the upper loading cells thrusts the beam down against the static roller supports. This test is basically deflection based test and it facilitates extension of test beyond linear elastic range. Deflection based test allows strain increment even after linear elastic range and further in the cracked stage too. This helps us to follow the post linear behaviour as well as cracked behaviour. *Figure 5.9* represents a typical four point bending configuration. In our experiments the load was applied at one third of the unsupported length (i.e. a= L/3). The dimensions and details of the tested specimen are explained in the following section.
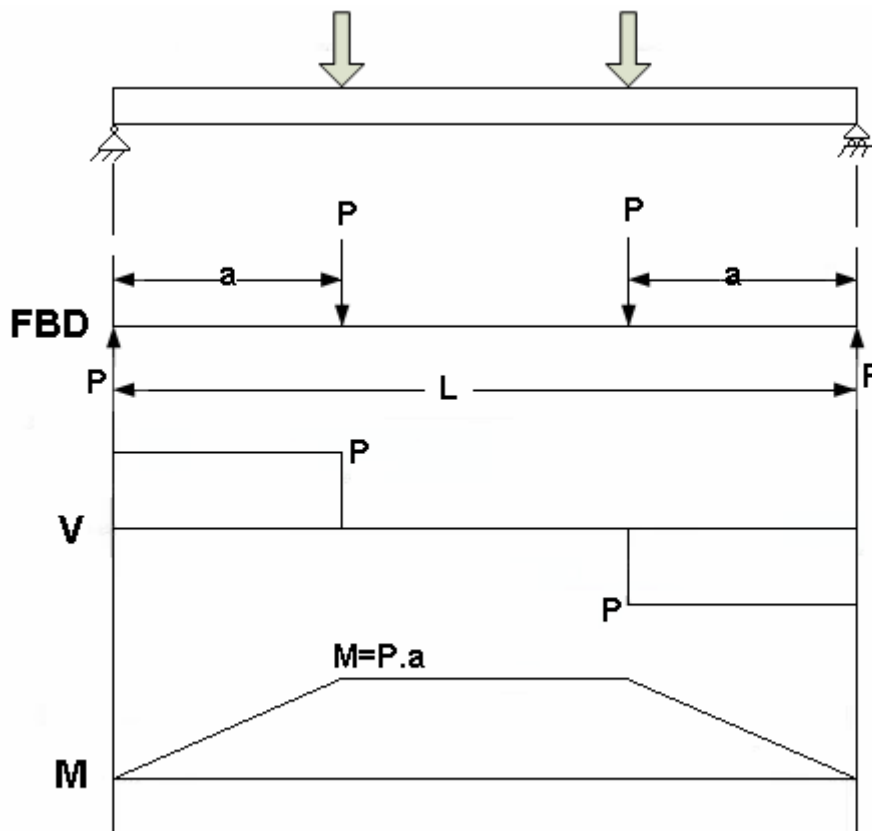
Figure 5.9 Four point bending configuration- Free Body Diagram, Shear Force Diagram and Bending Moment Diagram

Specimen Details

The specimens used for our tests were 4000mm long, 115mm wide and 200mm deep. The clear distance between the supports was fixed to be 18 times the beam depth. Accordingly, the members were tested over a clear span of 3600mm with load applied at one third of the clear span (*Figure 5.10*). This was done to have a pure bending failure avoiding shear stresses in the maximum moment area. Lateral support system was provided in order to prevent lateral distortions. The tension edge was randomly chosen, with little preference to the ones with lesser defects in the critical zone.

5.3.2 Instrumentation and Data Acquisition

The instrumentation consisted of a bending test machine configured to give a four point bending arrangement for the proposed span-depth ratio (see *Figure 5.10*) and associated data collection equipments. The beam was simply supported on roller bearings. The load was applied at 1.2 m from each support. Roller bearings were used at the load application points also, to ensure pure vertical loading even in case of differential deformations (for example in case of failure of a knot away from mid-span) at these loading points, and also to provide moment free loading.

Equipment Details

The loading was done using two loading cells (SENSORIC) which are having a maximum capacity of 200kN each, powered by 250kN hydraulic jacks (LARZEP). A precision measurement logger (Schlmberger 3530 orion) along with precise amplification arrangement (HBM MGC) was used to record strain data at every second. Two LVDTs (Linear Variable Differential Transducers) were used - one at the mid-span (RDP LDC 3000A ±75mm) and one at 600mm from right support (HBM W50TS ±50mm) - in order to measure the corresponding deflections. Strain gauges were attached along the height of the beam at the mid-span, the details of which can be seen in the following section. The functional mechanical parts of the test setup can be seen in the figure given below (*Figure 5.10*)
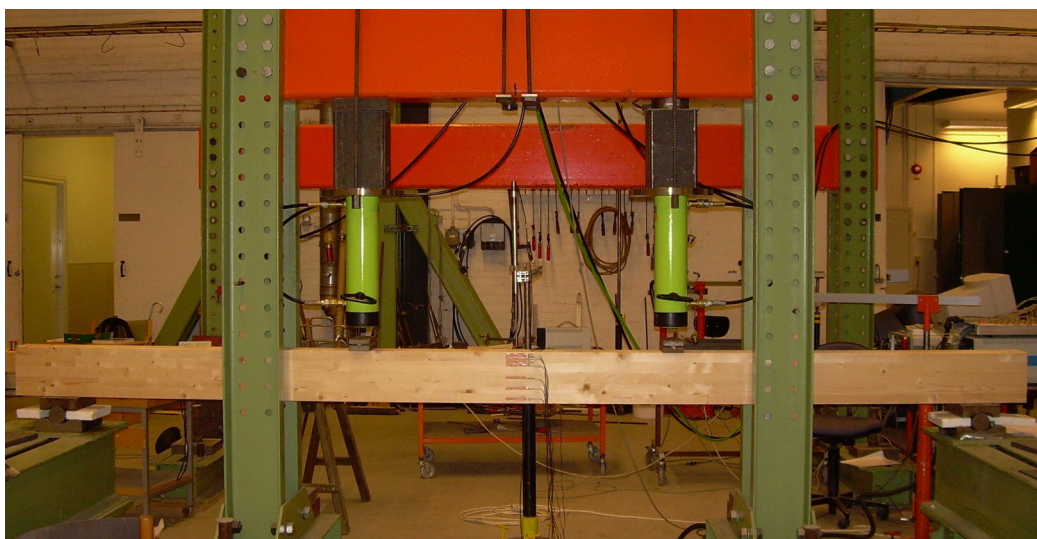

Figure 5.10 Experimental Setup- Four Point Bending Configuration.

Strain Gauge Configurations

A total of 10 strain-gauges (TML FLA6-11, 60mm long) were attached to the beam, one each on the top and bottom and 8 more along the height at mid-span in order to measure the strain distribution across the cross section. This was necessary to catch the degree of plastification of the timber and shift in neutral axis due to compressive plastification as well as yielding of steel. The distribution of the strain gauges across the cross section can be seen in *Figure 5.11*. This strain gauge configuration was used only for one beam from each beam-pair of same configuration, where as the other beam had strain gauges only on the top and bottom faces. The strain gauges were fixed on cleaned surface with special type of glue for strain gauges. Care has been taken to avoid air entrapment while gluing the strain gauges. These strain gauges were then connected to the measuring device by means of small wires.
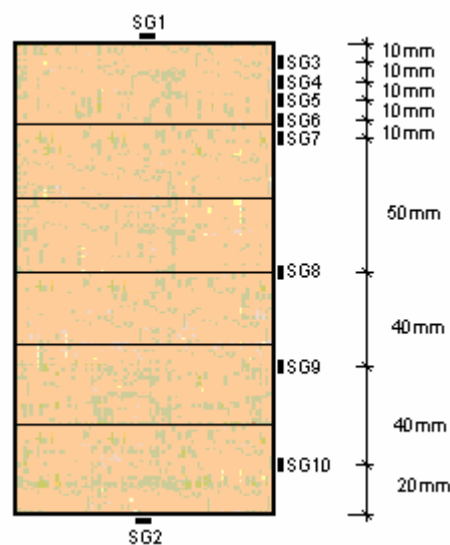
Figure 5.11 Strain gauge arrangement across cross section.
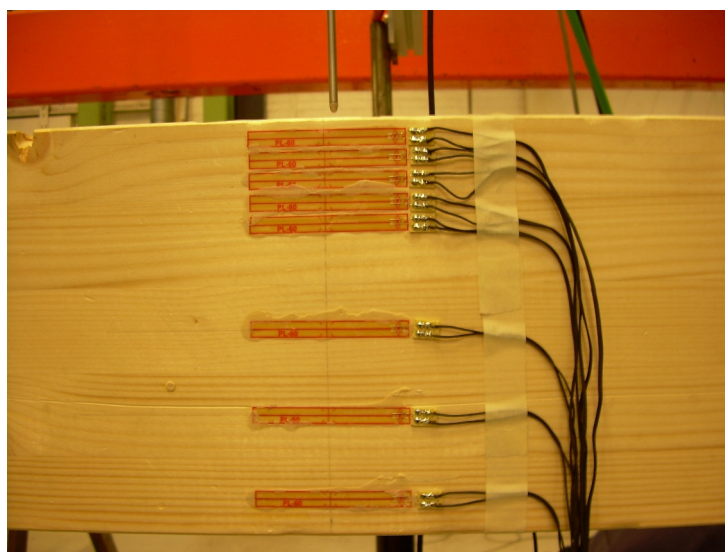
Figure 5.12 Strain gauges fixed on the lateral face of the beam

Figure 5.12 shows a beam with strain gauges fixed on its lateral face (there are two more strain gauges on the top and bottom, which are not visible in this view)

5.3.3 Test Procedure

Loading was done at a rate of 0.001mm per second. The loadings were keenly followed in order to identify key events which led to failure. Strains and deformation data were collected at every second. A load deformation graph was plotted using an XY recorder (GRAPHTEC WX3000) to visually realise the different phases (linear elastic, plastic, cracked and so on) during testing. The beams were first tested until failure. Further strains were induced in order to study the post cracked behaviour. The strain data from the strain gauges, the deformation data from the LVDTs, and the corresponding load data from the loading cell were collected and stored in excel format.

5.4 Results

This section deals with the results from the different tests done. The results are plotted as load deformation graphs as well as strain distribution diagrams across the height of the beam.

Behaviour and Failure descriptions

This description is classified on the basis of configurations. Detailed description of each beam can be found in the corresponding sections. Careful study of each beam is very important as the number of test specimens were less, which otherwise can lead to misinterpretations as there is very low statistical control.

5.4.1 Reference Beams

Two control specimens were tested to failure to provide a basis for comparing the flexural strengthening effect of steel and CFRP. All the control specimens failed in tension as expected; no evidence of compressive failure was noticed. The failure initiated at a knot or finger-joint location, and propagated. The control specimens experienced a sudden brittle failure upon reach of tensile capacity of the fibers in tension side. The following figures (*Figure 5.15* to *Figure 5.18*) show the failure modes as well as behaviour of the control specimens. The control specimens varied significantly in measured strength properties due to imperfections in the wood

Beam 1

The load deformation was quite linear till failure which was abrupt at a load level of 20.578kN and deformation at mid-span was 57.87mm (see *Figure 5.13*). The strain distribution shows no shift in the neutral axis (see *Figure 5.14*).

Beam1 failed in tension. The crack was initiated near to a knot in the tension side (see *Figure 5.16*), not very far from the mid-span. Afterwards the crack propagated longitudinally in the fibre direction (see *Figure 5.15*). There was no sign of compressive plastification.
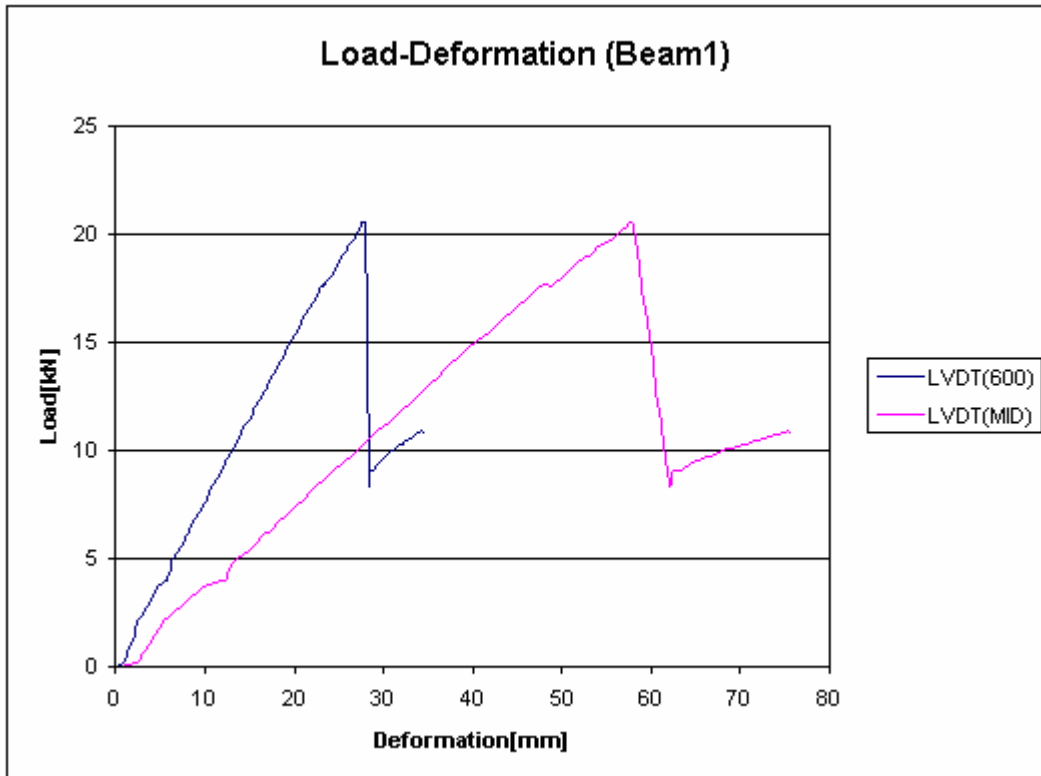
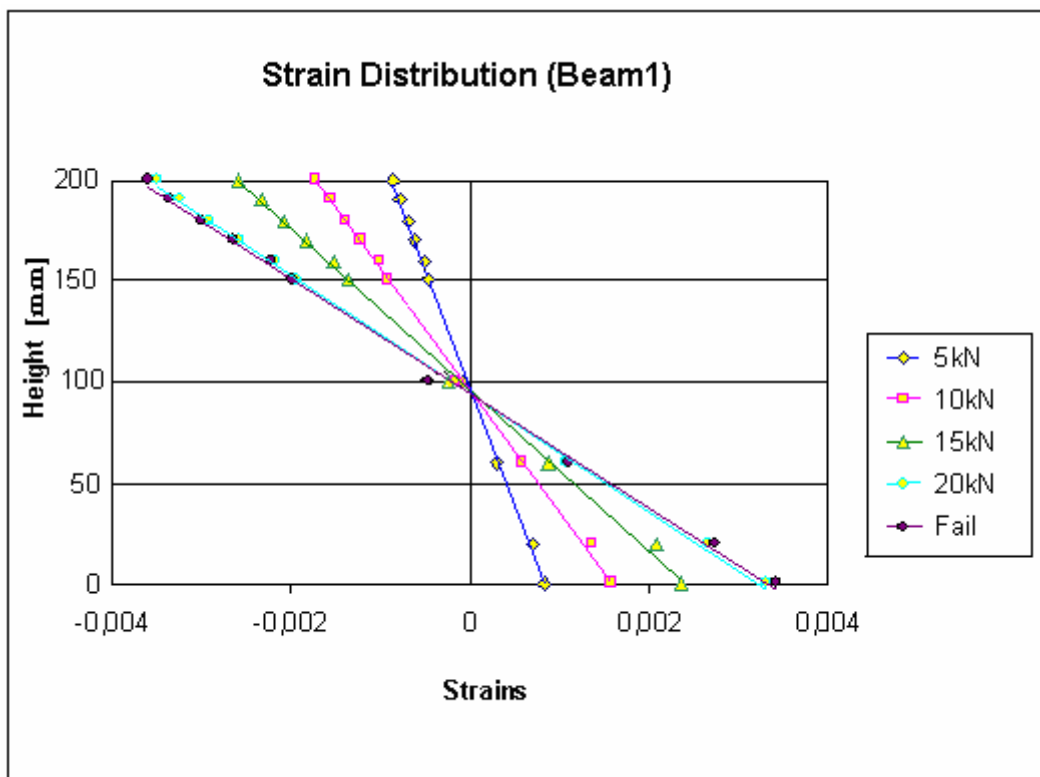*Figure 5.13 Load Deformation graph for Reference Beam (Beam 1)*

Figure 5.14 Strain distribution across height for different load levels (Beam1)

Figure 5.15 Beam 1 – Tensile failure

Figure 5.16 Beam 1 Knot on tension side which initiated tension failure

Beam 2

Beam 2 also behaved the same as Beam 1. The response was linear till failure. The failure was initiated at a knot in the tension-side (see *Figure 5.20*), resulted in a brittle failure which almost destroyed the whole cross section (see *Figure 5.21*)
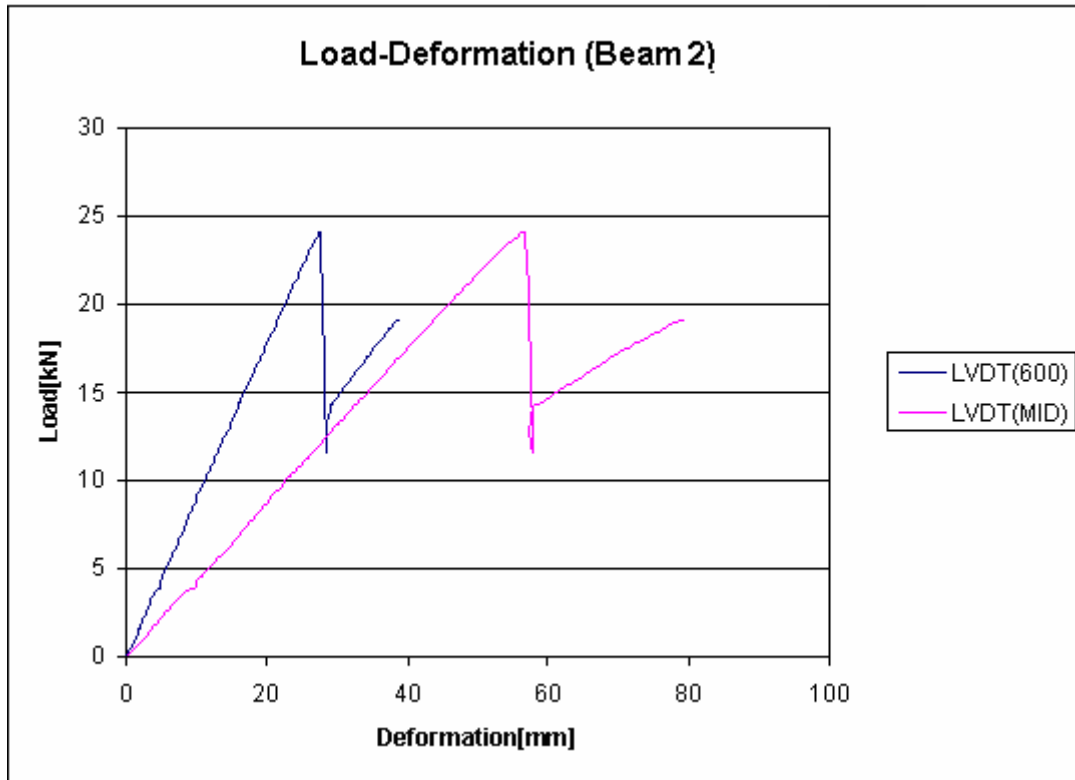
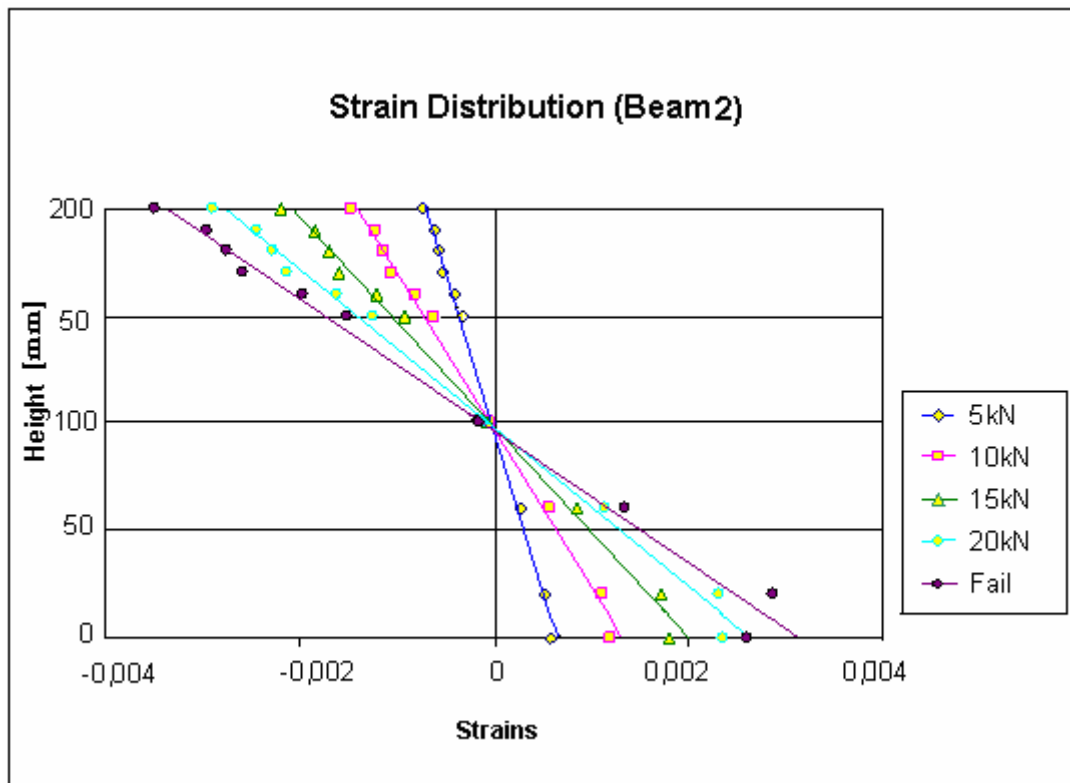*Figure 5.17 Load Deformation graph for Reference Beam (Beam 2)*

Figure 5.18 Strain distribution across height for different load levels (Beam2)

Figure 5.19 Beam 2 – Tensile failure

Figure 5.20 Knot on tension side which initiated tension failure (Beam 2)

Figure 5.21 Failure (Beam 2)

Looking at the load deformation graph, it could be found that the behaviour was quite linear till failure. This beam showed a slight higher load resistance ie. 24.11kN with a mid-span deflection of 56.696mm (see *Figure 5.17*) compares to Beam 1. The strain distribution across cross section was quite linear till failure and there was no shift in the neutral axis which means no compressive plastification (see *Figure 5.18*).

5.4.2 Steel Reinforced beams

Two reinforcement configurations with steel were used in the tests (see *Table 5.1*). The beams ultimately failed by rupture of fibers in tension zone. But the interesting phenomenon was the yielding of steel which happened much earlier than the tensile failure or compressive crushing of the timber. This was due to the fact that the difference in stiffness properties of steel induced more stresses in the steel (stiffer material attracts more stresses). So the steel reached its yield point well before the timber. It can also be explained in terms of induced strains. The steel which is almost 20 times stiffer than timber allows lesser strains before it yields, where as the ultimate yield strain of timber has values much greater than ultimate yield strain of steel. This induces additional ductility in the beams and results in larger deformations. The two beams tested were having same reinforcement ratios for easier comparisons.

### i)   *Steel Beams Reinforced both in tension and compression (Beams 3 and 5)*

The behaviour of the two beams was quite similar, even though the ultimate values of strength varied a little bit. Non linear behaviour was observed in both the beams due the combined effect of compressive plastification as well as yielding of steel (see *Figure 5.22* and *Figure 5.27*). The straight part of the curve just after the liner elastic part corresponds to the yielding of steel, and the nonlinear part after that corresponds to the combined effect of steel yielding and compressive plastification. It was quite interesting to see that the steel reinforcement followed the deformations quite well

without having any de-bonding until failure. This shows the effectiveness of the configuration, bonding capacity of the adhesive as well as good workmanship.

Beam 3

Beam 3 was reinforced with 2 steel plates each on tension and compression sides. The behaviour was quite ductile compared to the un-reinforced ones (see *Figure 5.22*). This was due to the compressive plastification as well as the yielding of the steel. The beam overall deformation went up to 92.863mm at an ultimate load level of 48.133kN. *Figure 5.24* and *Figure 5.25* shows the failure modes.

This beam had the adhesive Sikadur-30, bonding the steel plates to the timber. It should be noted that there was no failure in the adhesive till failure of the timber. Even at failure, it could be seen that the bond between the timber and the wood was intact, the de-bonding (which had occurred due to post failure loading) was in timber rather than in the adhesive or the interface between the adhesive and timber(and adhesive and steel too). This shows the effectiveness of the adhesive. This had helped the steel to follow the global deformation, and be quite effective as a reinforcing element. The low stiffness value of the timber induced more stresses to the steel which ultimately led to its yielding. This can be noticed in *Figure 5.22* by a sharp bend in the load deformation graph at a load level of 22kN. It could be noticed from the strain-gauge readings at the bottom of the beam that the strain levels were in the range of 0.0013 in extreme tension fiber.
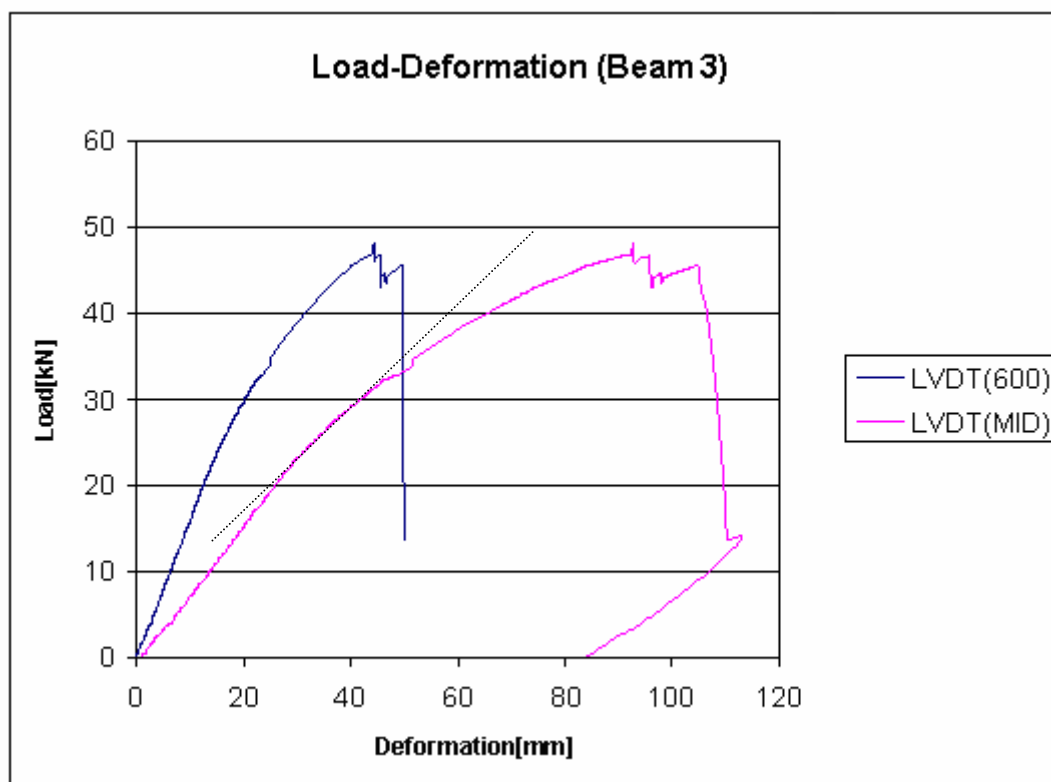
Figure 5.22 Load Deformation graph for Steel Reinforced Beam (Beam 3)

The strain diagram (see *Figure 5.23*) was expected to have some shift in the neutral axis due to non-linearity in the timber and steel, but it seems that the neutral axis stays

more or less unchanged which can be because of the inter-cancelling effect of the two nonlinearities. Compression wrinkles could be seen in the top face of face of the beam.
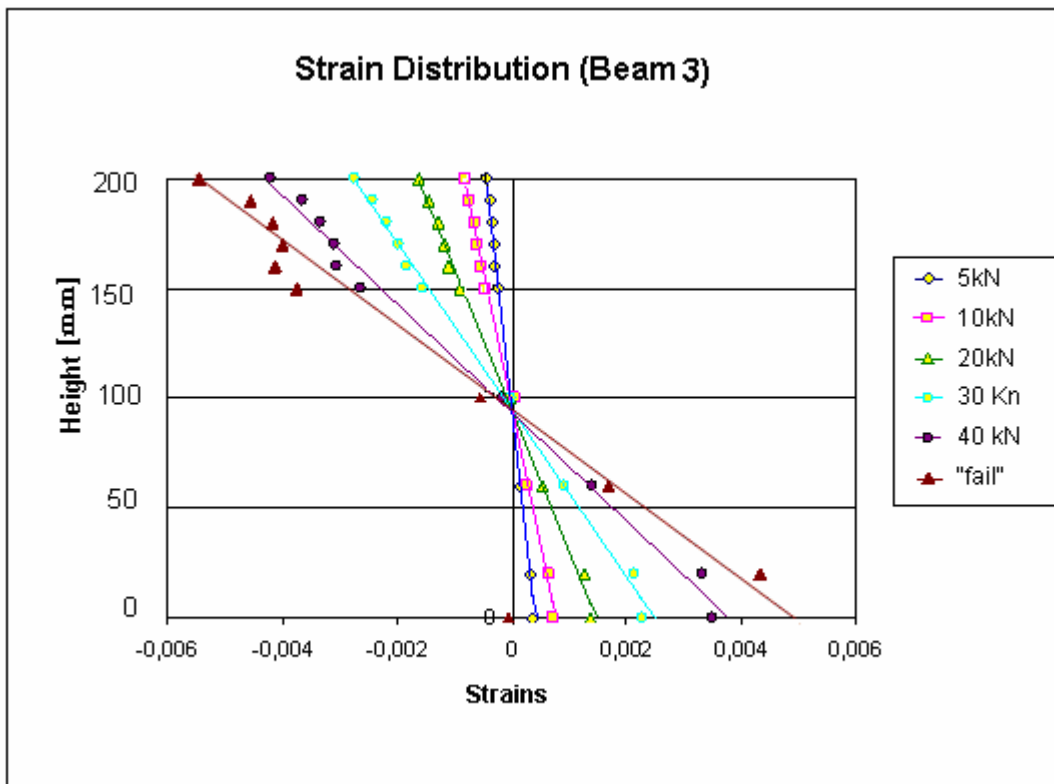

Figure 5.23 Strain distribution Across height for different load levels (Beam 3)

Figure 5.24 Failure (Beam 3)

Figure 5.25 Failure (Beam 3)

The failure was initiated by a knot in the tension side (see *Figure 5.26*), which resulted in increased deformations which ultimately caused the adjacent timber fail due to reach of tensile strain limit.

Figure 5.26 Cause for Failure, knot at the bottom

Beam5

The response of Beam 5 was quite similar to that of Beam 3 except for the fact that the load values were not as high as beam 3. This was supposed to be because of the presence of a knot and a finger joint very near to the maximum bending zone (see *Figure 5.31*).
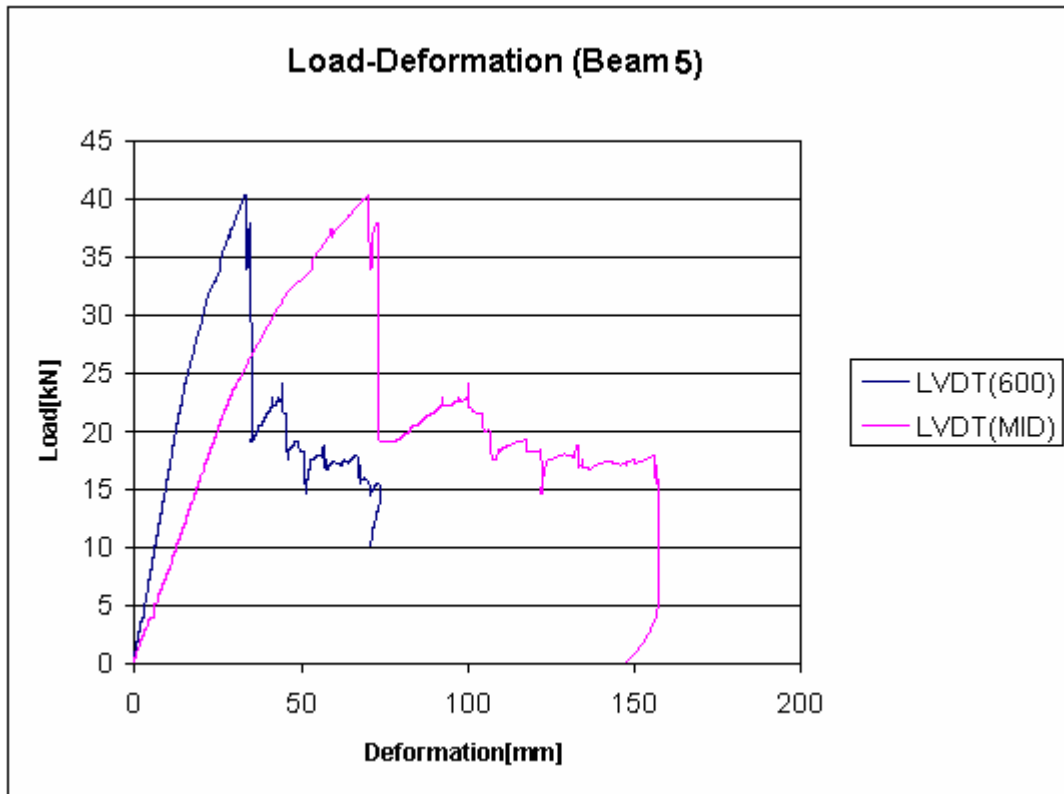
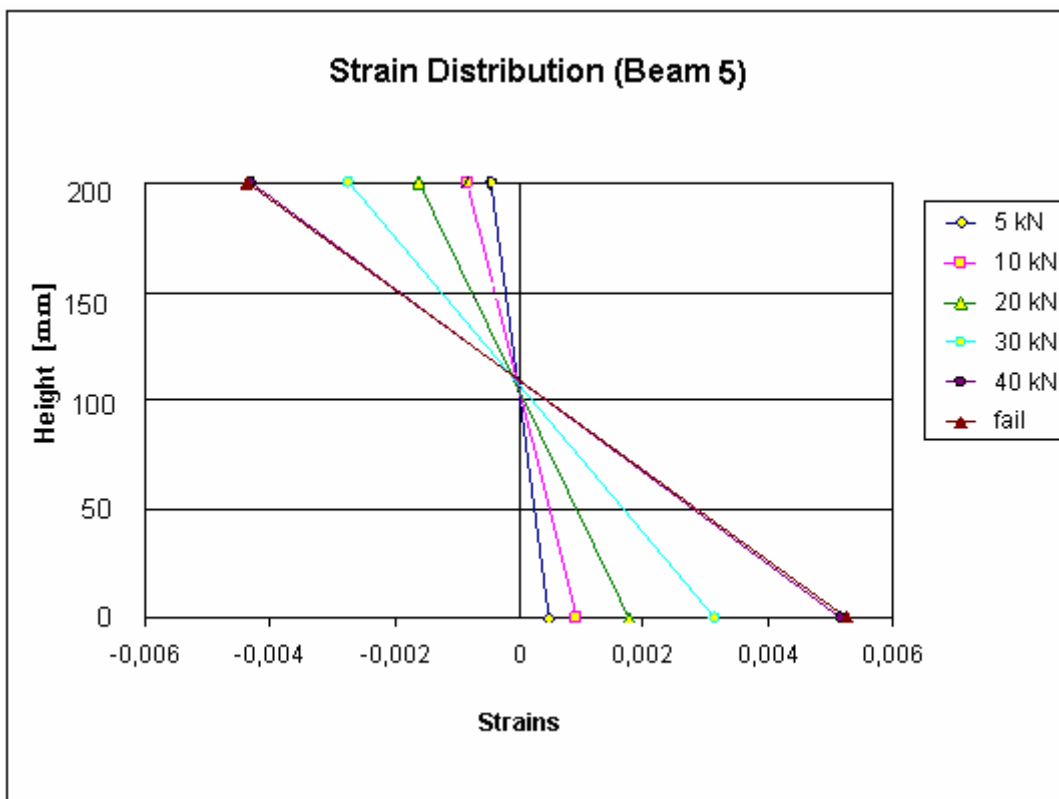*Figure 5.27 Load Deformation graph for Steel Reinforced Beam (Beam 5)*

Figure 5.28 Strain distribution Across height for different load levels (Beam 5)

Figure 5.29 Failure (Beam 5)

The overall behaviour showed nonlinearity, but the ultimate failure was tensile and brittle, as can be see in *Figure 5.29* and *Figure 5.30*. The adhesive used was Sikadur 30(same as in beam 3) which performed very well in holding the reinforcement in place. The load level could reach up to 40.378kN with an overall deflection of 70.287mm. The lower deflection value does not correspond to the increased stiffness, but was due to the premature failure due to defects/discontinuity in the critical zone.

Figure 5.30 Failure(Beam 5)
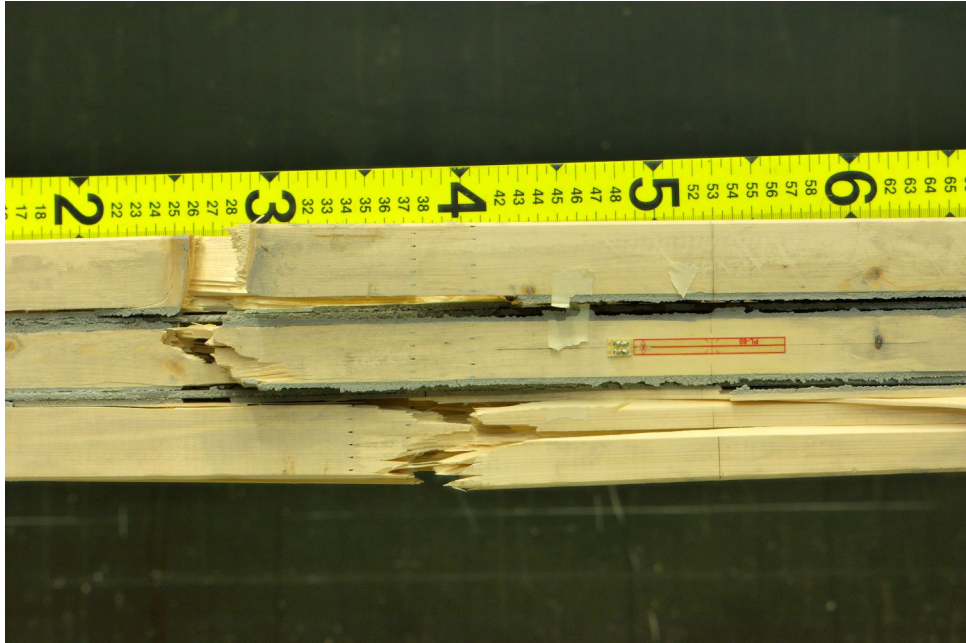
Figure 5.31 Crack at knot which eventually led to finger-joint failure

Observing the strain distribution diagram (*Figure 5.27*), it can be seen that the neutral axis shifts up after a load level of 30kN. This is due to the effect of compressive plastification as well as reinforcement yielding. It could be noted that there were compression wrinkles near to the load application point.

ii) Steel beams Reinforced only on the tension side (Beam 4 and Beam 6)

These beams were reinforced by 4 steel plates in the tension side only. The behaviour was ductile with compressive plastification of the wood and steel yielding. The beams ultimately failed in tension, but it could be noticed that the deformation levels were quite high compared to the previous beams. The adhesive (Sikadur 330) worked very well in the two beams, with no de-bonding till failure.

Beam 4

Beam 4 failed in tension at a knot in the tension side (see *Figure 5.35*), which eventually resulted in the failure in the finger joint very near to the load application point (see *Figure 5.34* and *Figure 5.36*). Compressive plastification was very visible in the compressive zone, with distinct crushing of timber (see *Figure 5.34* and *Figure 5.37*). The crack propagated in the fiber direction after the failure of the finger joint. The combined effect of timber plastification and the reinforcement yielding has induces very good ductility in the overall behaviour. The effect of plastification can also be seen from the curvature of the beam and the reinforcements even after the removal of loads.

Figure 5.32 Load Deformation graph for Steel Reinforced Beam (Beam 4)

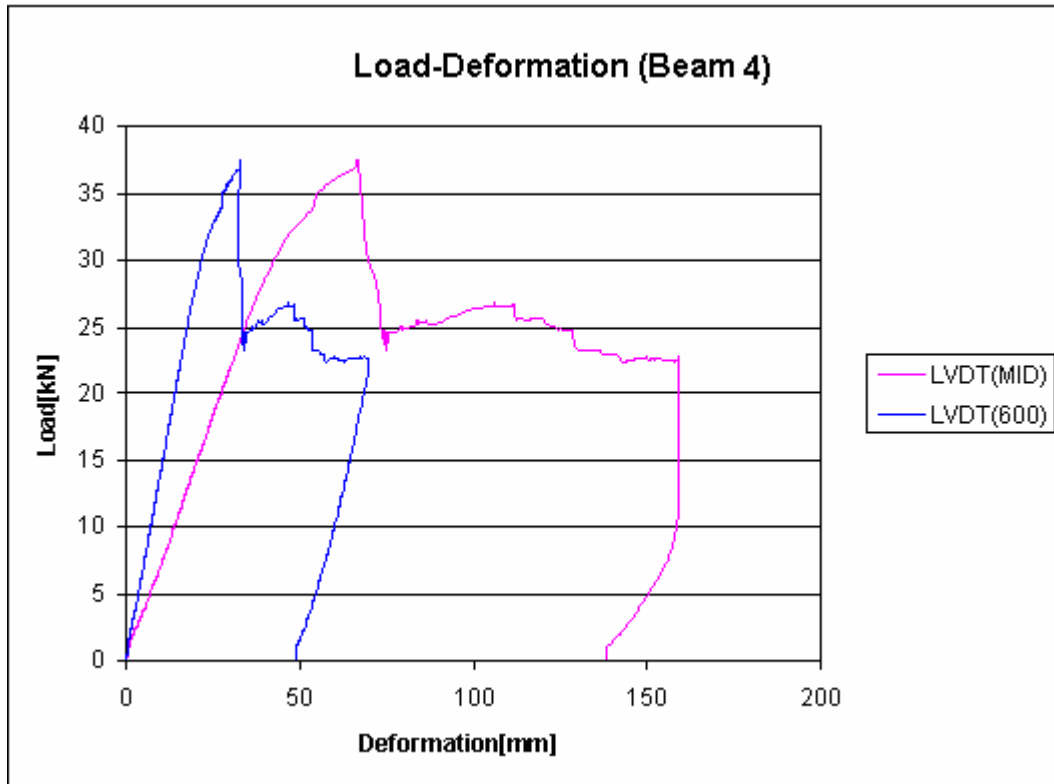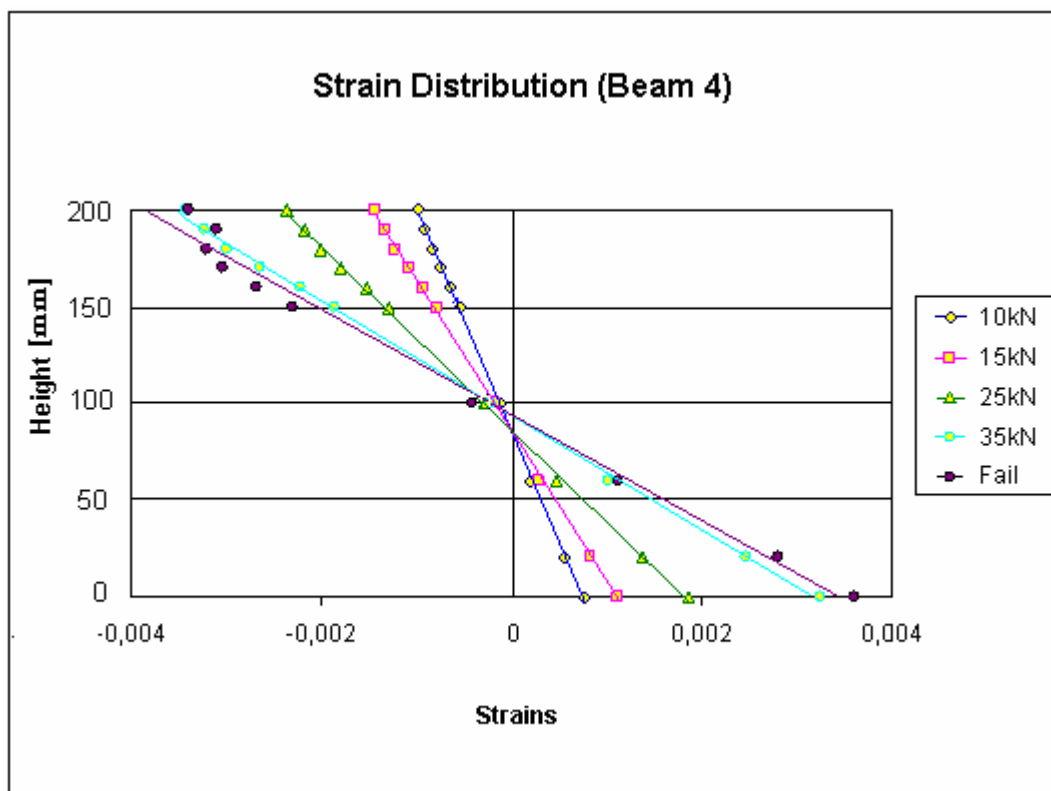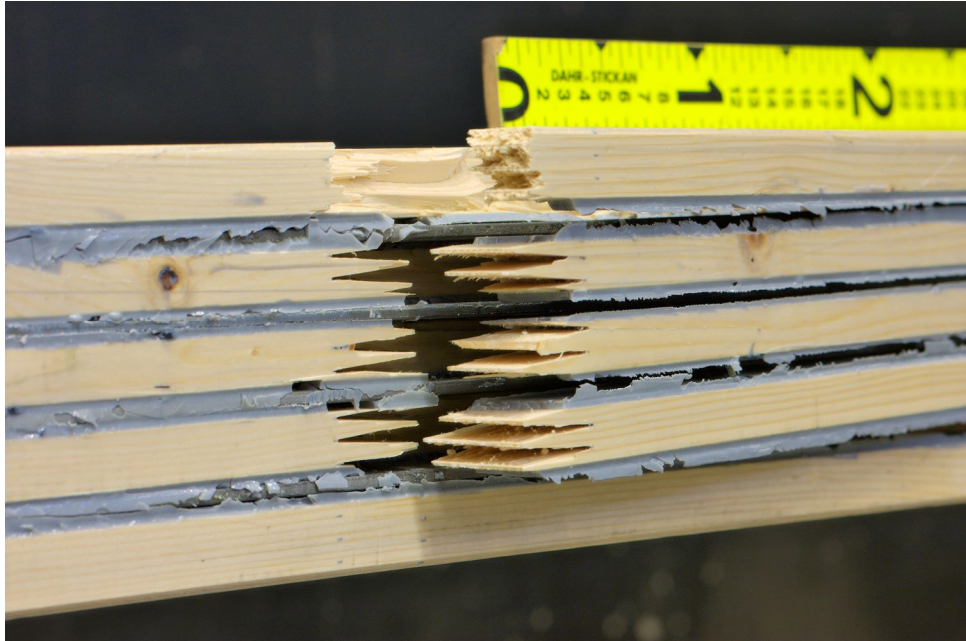*Figure 5.33 Strain distribution Across height for different load levels (Beam 4)*

Figure 5.34 Failure(Beam 4)

Figure 5.35 Crack initiation at knot

Figure 5.36 Finger-joint failure which resulted in de-lamination of the reinforcement

It could be noted that there is some de-bonding between the steel and timber, which was a post failure phenomenon which was caused by the sudden transfer (linking) of forces at the failure of the finger joint.

The loads reached 37.511kN before failure and the corresponding mid-span deflection was 66.48mm (see *Figure 5.32*). Keenly observing the strain diagram (*Figure 5.33*) it can be seen that the neutral axis shifts up as s result of yielding of steel.

Figure 5.37 Compressive plastification (crushing of timber)

Beam 6

Beam 6 also failed ultimately in tension after some plastic behaviour in the post-elastic phase. The load level reached till 33.032kN with a corresponding deflection of 76.06mm in the mid span. The failure was initiated by a knot in the tension side.

The failure was initiated at a node in the tension zone (see *Figure 5.41*). a calear plastic behaviour was seen in the compressive zone. In *Figure 5.41* and *Figure 5.42* the crushing of the timber in the compressive zone can be seen clearly. The depth of plastification was almost 45mm measured directly from the beam.
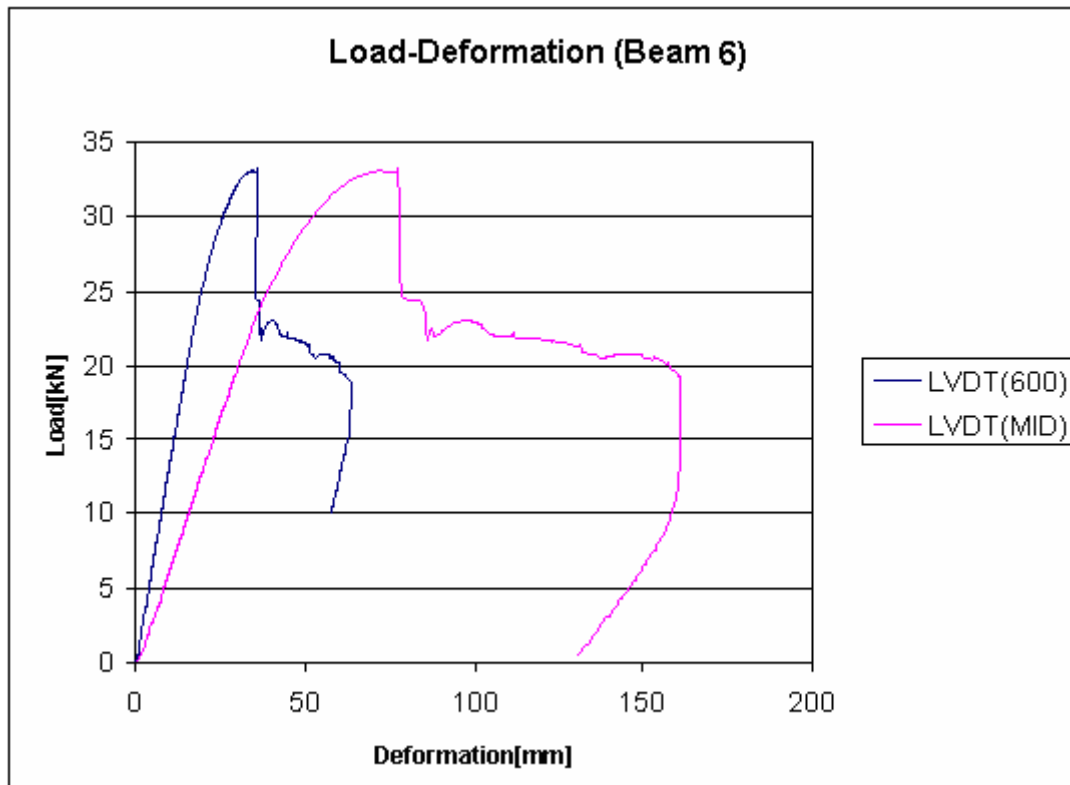
Figure 5.38 Load Deformation graph for Steel Reinforced Beam (Beam 6)

Looking at the strain distribution diagram also we can see the shift in the neutral axis, which is the effect of the compressive plastification. The adhesive action was also satisfactory; there was no failure in adhesive till the global failure of the beam.
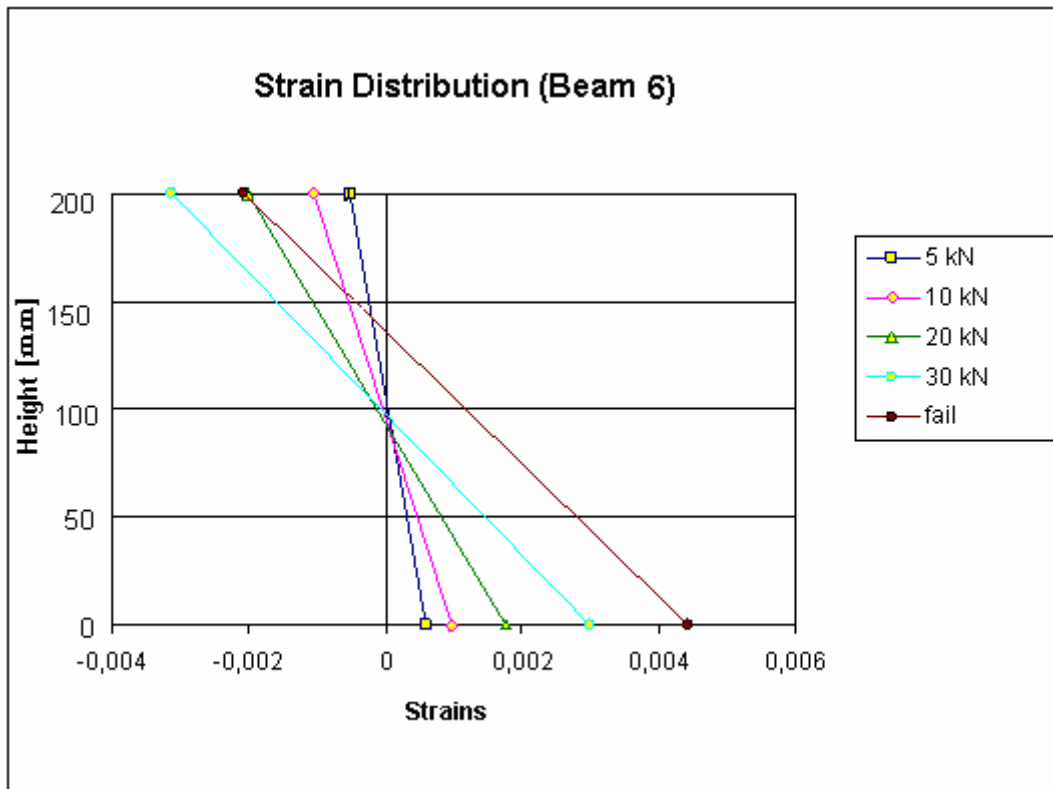
Figure 5.39 Strain distribution Across height for different load levels (Beam 6)

Figure 5.40 Failure (Beam 6)

Figure 5.41 Crack initiation at knot

Figure 5.42 Plastification in the compressive zone

5.4.3 Beams Reinforced with CFRP

Beams were reinforced with two types of CFRPs (see *Table 5.1*). Sikadur 30 was used as adhesive in all configurations with CFRP. The beams showed considerable increase in strength and stiffness properties. The failure was controlled by the configuration

and also the amount of reinforcement. The details of the failure-modes are explained in the following sections

iii) Beam reinforced with High stiffness CFRP (300GPa) Beam 7

This beam was reinforced by high stiffness CFRP reinforcement. This had 2% of reinforcement distributed equally in tension and compression. The load level went up to 41.841kN with a corresponding deformation of 83.487mm. We did not expect much plastic behaviour of this beam (because of symmetric reinforcement arrangement), but it was seen that the behaviour becomes plastic when the load level increases.

On close observation, it could be seen that there are wrinkles in the compressive zone. Also the reinforcement in the compressive zone was crushed (see *Figure 5.48*). The ultimate failure was in tension which was initiated at a crack near to load application point (see *Figure 5.45* and *Figure 5.46*). This crack has resulted in failure in the nearby finger- joint. This caused the entire forced to be linked to the laminates suddenly, which caused the laminates to fail at the tension (see *Figure 5.45*).
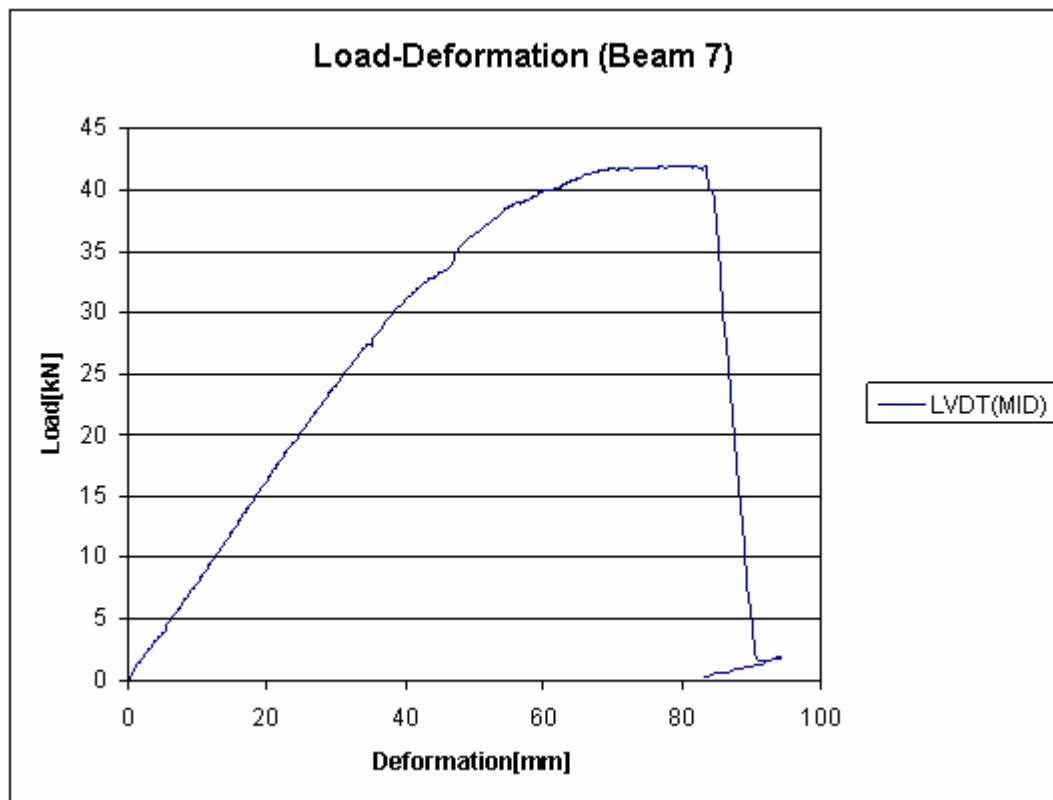

Figure 5.43 Load Deformation graph for Steel Reinforced Beam (Beam 7)
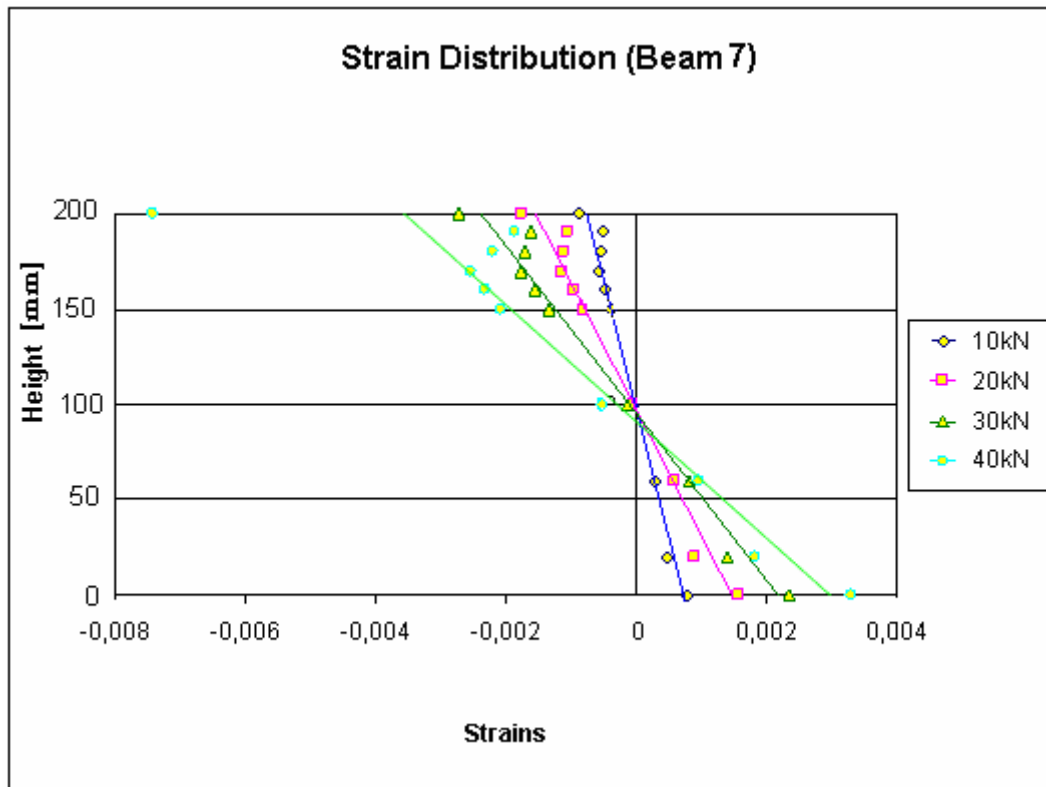
Figure 5.44 Strain distribution Across height for different load levels (Beam 7)

Figure 5.45 Failure (Beam 7)

It can be noted that individual fibers in the laminate came out from the matrix after the tensile failure (see *Figure 5.46*). The compressive failure of the reinforcement looks like buckling of individual fibers, which caused the de-bonding in the matrix, and local crushing.

Figure 5.46 Crack initiation at knot

Figure 5.47 Rupture of the laminate at the finger-joint location

The beam is almost fully cracked with no more load carrying capacity, i.e. no post crack loading was possible. (See *Figure 5.43*). The strain diagram was quite different from the other beams with strain gauges very near to compressive reinforcements reading lesser strains than expected (*Figure 5.44*). We could not find a satisfactory explanation for this behaviour. But at 40kN, it was seen that the strains in one of top strain-gauge (strainguage1) is quite high, and we assume that this reading was not acceptable (and we disregarded it), may be due to some error in measurement, or some local phenomenon (like spalling of timber slices).

Figure 5.48 Compression failure, crushing of Timber fibers as well as CFRP

iv) Beam reinforced with Lower stiffness CFRP (165GPa)

These beams were reinforced with High Strength (but Lower stiffness) CFRP, Sika CarboDur S, heavily reinforced (2.8% reinforcement) with 1:2 distribution among tension and compression. Both the beams showed very good stiffness increase. The ultimate failure was in shear, which was a consequence of the higher reinforcement ratio in the cross section. The higher reinforcement ratio in the cross section prevented failure in tension as well as compression, and the failure mode switched to shear.

The shear failure in beams was sudden or abrupt. The crack was initiated near to the supports and propagated towards the mid-span. The failure was observed just above the reinforcements. No de-bonding was observed.

Beam 9

Beam 9 failed in tension at load levels of 45.489kN with a corresponding mid-span deflection of 66.34mm. The failure was initiated by the onset of the shear stresses in the close vicinity of shear limit, causing a brittle failure (see *Figure 5.52*and *Figure 5.53*). The load response was linear till around 32kN, but the slope decreases a little after that (see *Figure 5.49*) this can be due to the effect of 'controlled plastification in the compression side (see *Figure 5.50* and *Figure 5.51*) as the reinforcement in the compression side influences free plastification. The reinforcement in the compression side seems to be crushed too. The strain distribution was linear across cross section till failure, and no significant change in the neutral axis was observed.
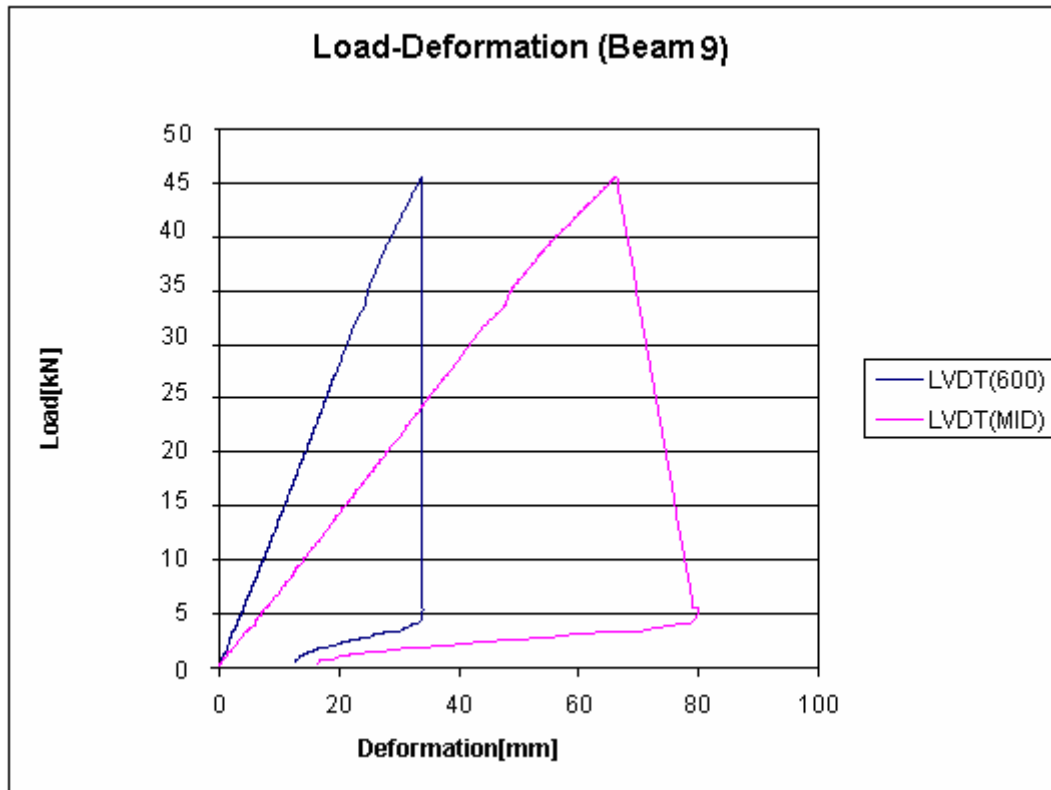
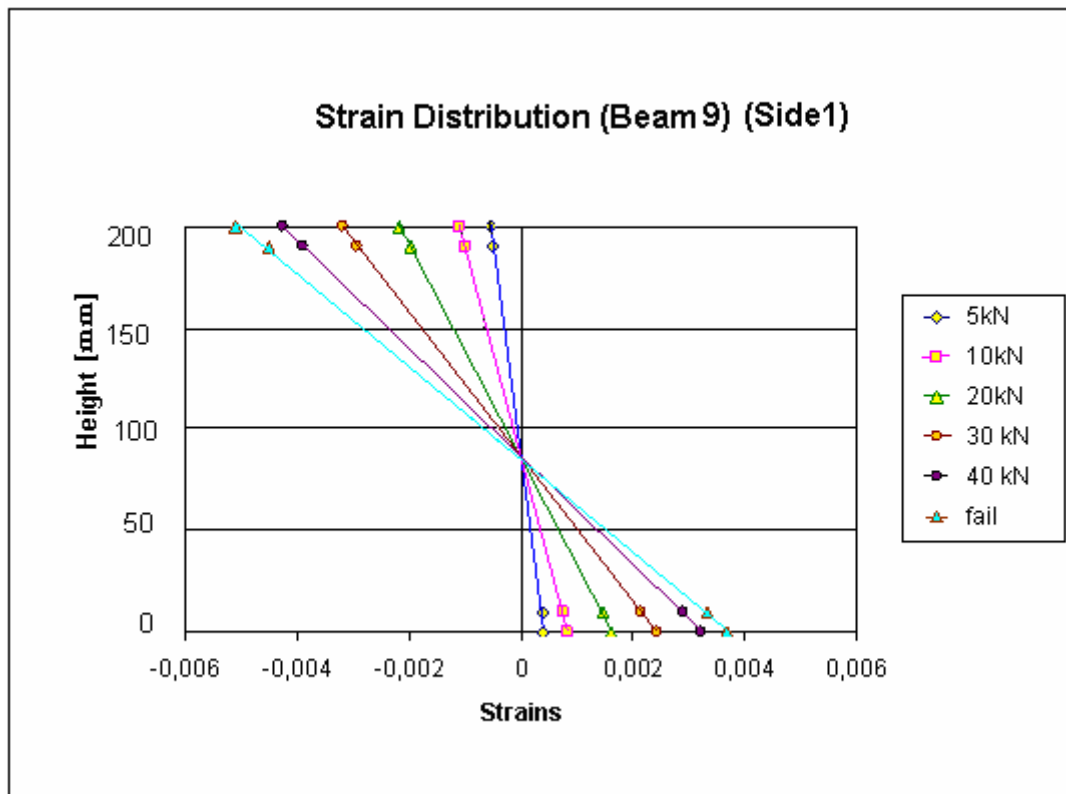*Figure 5.49 Load Deformation graph for CFRP Reinforced Beam (Beam 9)*

Figure 5.50 Strain distribution Across height for different load levels (Beam 9)
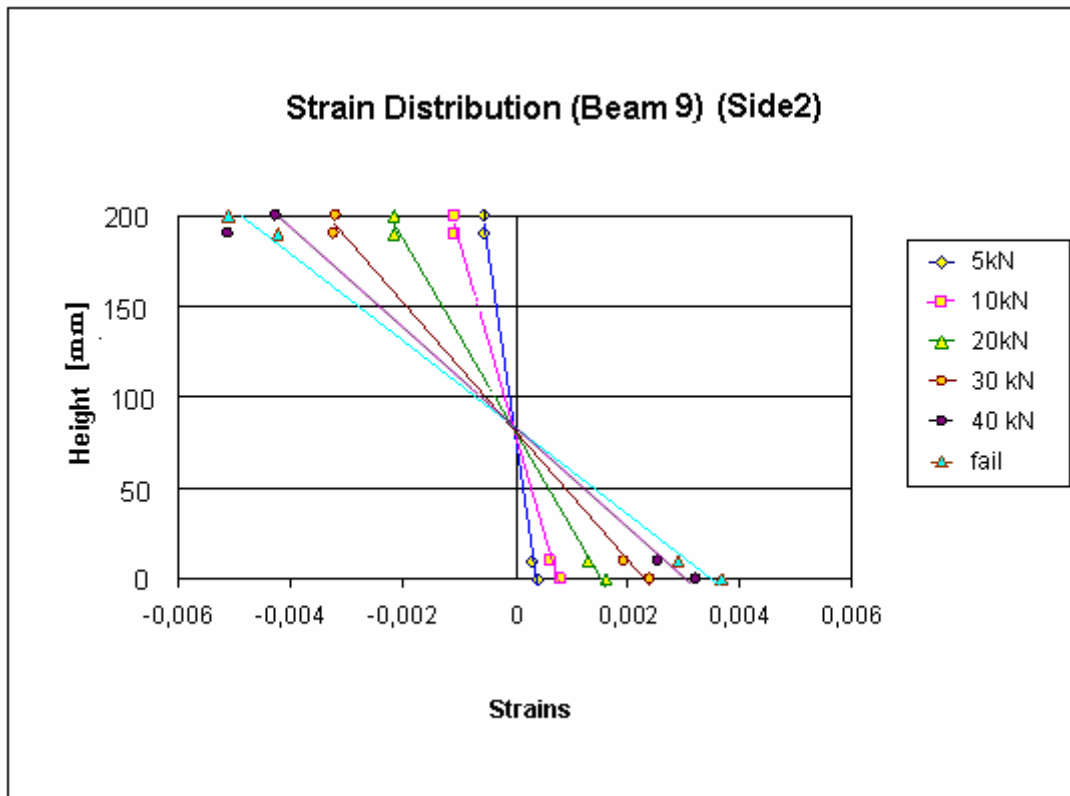
Figure 5.51 Strain distribution Across height for different load levels (Beam 9)

Figure 5.52 Failure (Beam 9)

Figure 5.53 Shear failure near supports (Beam 9)

Beam 10

Beam 10 also had the same behaviour as beam 9, except for the fact that there was some splitting failure in the compressive zone just below the reinforcement (see *Figure 5.56*). This would have probably originated from a knot at this level. This occurred near to a load level of 42kN, after which the load dropped. The load could be again increased a little bit which resulted in generation more splitting cracks in the compressive area. But the decisive failure mode was in shear, with abrupt propagation of crack in the fiber direction at a load level of 39.06kN. The splitting in the compressive zone has prevented the beam from reaching higher load levels.

Some compression failure in the timber was also seen near to the load application point, which caused the timber fibers to buckle (see *Figure 5.58*).
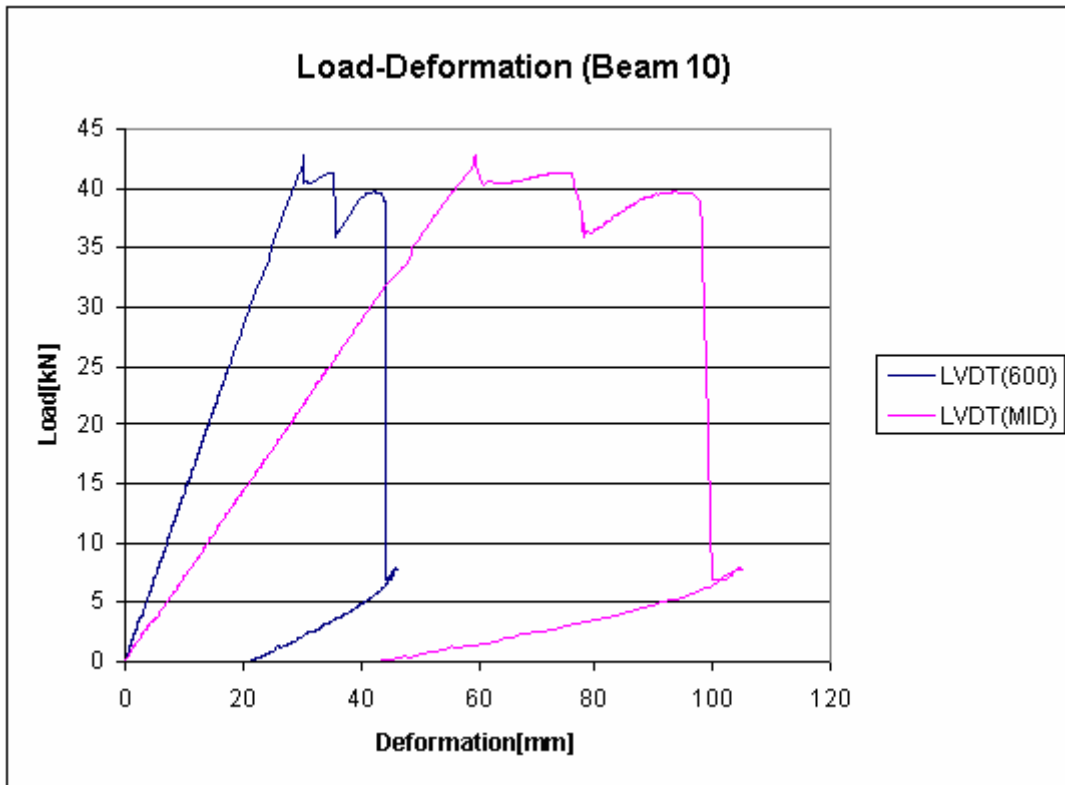
Figure 5.54 Load Deformation graph for Steel Reinforced Beam (Beam 9)
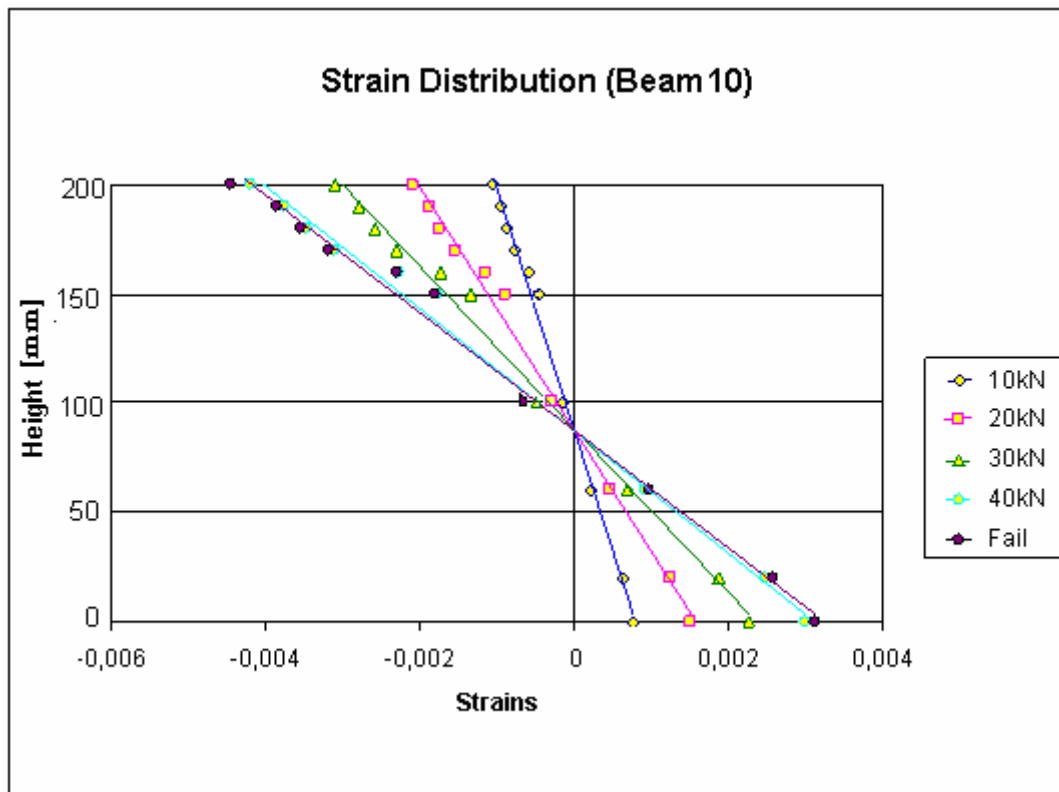
Figure 5.55 Strain distribution Across height for different load levels (Beam 9)

Figure 5.56 Failure (Beam 10) Split Crack in the compressive zone

There was no sign of de-lamination in the glue line. The adhesive acted perfectly in transferring the load to the reinforcement. The strain distribution across the cross section (see *Figure 5.55*) was linear and the neutral axis remains does not move so much as the load increases in spite of compressive plastification.

The shear failure restricts the beam from achieving higher loading levels for heavily reinforced beams. But if we can provide necessary to take care of the shear forces, the load carrying capacity can be increased further, by adding more reinforcement.

Figure 5.57 Failure(Beam 10) Shear Failure near to support

Figure 5.58 Compressive crushing in timber as well as laminate

5.4.4 Assessment of Stiffness

Stiffness of a piece of lumber, or a log, can be measured by placing it in a suitable static bending test apparatus, recording the deflection as load is applied, and calculating the modulus of elasticity (MOE or E), which is a measure of stiffness or resistance to deflection. Although this "static bending" MOE can be measured without testing the piece to failure, it is slow and involves expensive equipment that is not very portable. Consequently researchers have been exploring the use of the "dynamic" MOE, which is well correlated with the static MOE. Dynamic MOE is obtained by measuring the velocity of an acoustic wave through the material and is expressed by the following formula

$E = 4.f^2.l^2.\rho$

Where,

E_d dynamic modulus of elasticity [Pa]

ρ density of the material [kg/m^3)]

f   fundamental Eigen-frequency [Hz]

l   length if the test specimen [m]

In practice, the density of many materials is relatively constant; hence the velocity of the acoustic wave can be used as a direct indicator of the dynamic MOE, a measure of the material's stiffness. In our calculations the density of timber was taken to be 400kg/m^3

We have assessed the stiffness of the beams both by acoustic method and by static bensing. But the static bending results are calculated from the experimental tests of the reinforced beams. The details of the calculations are given in APPENDIX 3.

The following table shows the results of the stiffness calculations.

	E-Modulus Acoustic test	E-Modulus Bending Tests
Beam1	10089	8200
Beam2	-	9490
Beam3	-	8380
Beam4	-	10500
Beam5	10584	9051
Beam6	9308	8900
Beam7	11017	9110
Beam9	10193	9255
Beam10	10608	9299

Table 5.2 E-Modulus Values

5.5 Comparison and Discussion

Most of the reinforced specimens ultimately failed in flexural tension, as the test specimens were not so heavily reinforced on the tension side in order to induce a pure compressive failure. Shear failure was also seen in a couple of beams. The yielding of steel reinforcements resulted in a more ductile global behaviour of the steel reinforced beams. Beams reinforced only on tension side (and also beams which are reinforced lightly in compressive side) showed compressive plastification with progressive collapse of fibers in compression side enabling a more gradual ductile failure. Several members displayed visible plastic hinge behaviour in the compression zone. The following sections give a more focussed discussion on the different aspects.

Effect of Reinforcement

For comparison purposes, a moment- curvature relationship was plotted for each configuration (one beam each from each configuration are plotted). It could be seen that all interventions resulted in considerable increase in moment capacity as well as stiffness, when compared to the un-reinforced beam.
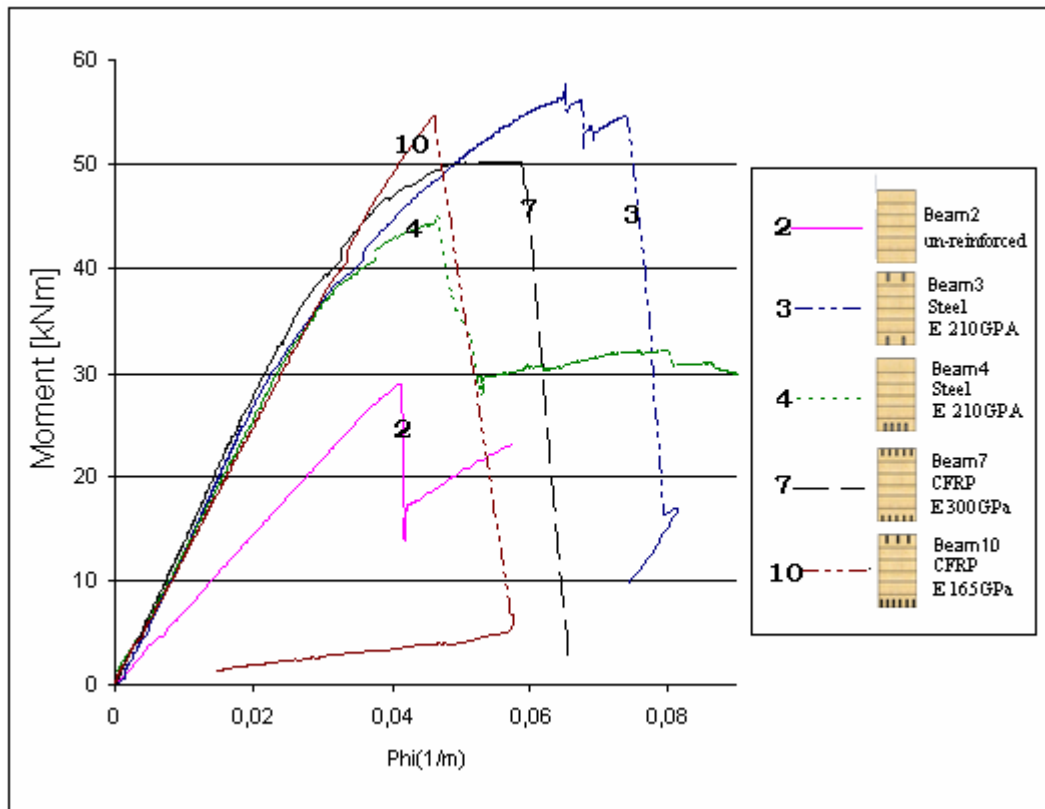
Figure 5.59 Moment-Phi Diagram
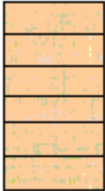
a) Effect on Global Stiffness

The main observation was that the stiffness increase was very much according to the amount as well as stiffness of the reinforcement introduced. It could be noted that the maximum increase in stiffness was for Beam 7(109%), which was reinforced by CFRP of stiffness 300GPa, 1.5% of gross cross section. It can be seen that the stiffness is retained till a higher load level in the case of CFRP reinforced beams (see *Beam 7* and *Beam 10* in *Figure 5.59*). But in steel reinforced beams, there is considerable reduction in stiffness even at low load levels which is the effect of the yielding of steel (see *Beam 7* and *Beam 10* in *Figure 5.59*).

b) Effect on Ultimate moment Capacity

The moment capacity was controlled by the failure mode, presence of imperfections in the vulnerable zones, distribution of reinforcement in the tensile as well as compressive zone etc. The increase in Ultimate Moment capacity was between 57% and 95.8%. The maximum moment capacity increase was seen in Beam 3 which was reinforced with steel (only in the tension zone, 2% of gross cross section). But this does not for certain indicate the effectiveness of the reinforcement, as the failure is controlled mainly by the defects in the timber.

Table 5.3 shows the Ultimate load carrying capacity (P_{ult}), ultimate moment resistance (M_{ult}), and stiffness values of the beams tested along with their .

Table 5.3. Ultimate values of Load carrying capacity, Ultimate moment capacity, Stiffness and the corresponding increase in percentage.

Geometry	Reinforcement	Beam Nomen-clature	P_{ult} kN	δ mm	Mult kN.m	Incre-ment %	EI N.mm2	Incre-ment %
	No Reinforcement	Beam-1	20,58	57,83	24,69		6,12E+11	
		Beam-2	24,11	56,83	28,93		7,06E+11	
		Average	22,34	58,23	26,81	0	6,59E+11	0
	Steel E=210GPa 4x(4mm x 30mm) 2% of Gross c/s 50% ten 50% com	Beam-3	47,71	92,86	52,25		1,34E+12	
		Beam-5	40,38	70,28	48,45		1,39E+12	
		Average	47,54	81,57	50,35	87.8	1,36+E12	107
	Steel E=210GPa 4x(4mm x 30mm) 2% of Gross c/s 100% ten 0% com	Beam-4	37,11	66,48	44,25		1,26E+12	
		Beam-6	33,3	77,34	39,96		1,12E+12	
		Average	35,21	71,96	42,11	57	1,19E+12	80.57
	CFRP Sika CarboDur H E=300GPa 10x(1.4mm x 25mm) 1.5% of Gross c/s 50% ten 50% com	Beam7	41,84	83,77	50,21		1,38E+12	
		Average	41,84	83,77	46,16	72,21	1,38E+12	109
	CFRP Sika CarboDur S E=165GPa 9x(1.4mm x 30mm) 2.8% of Gross c/s 66.6% ten 33.3% com	Beam-9	45,24	65,79	54.52		1,23E+12	
		Beam-10	42,02	59,61	50.45		1,24E+12	
		Average	43,64	65,74	52.49	95,78	1,24E+12	87.4
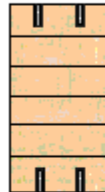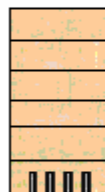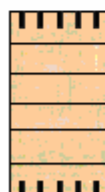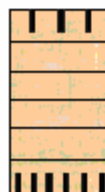
* Pult=Ultimate load[kN], δ=deflection at centre[mm], Mult= Ultimate moment resistance[kNm], EI=Stiffness[Nmm2]

c) Effect on Variability of results

The experiments show that the introduction of reinforcements in the cross section reduces the variability in results. This is clearly shown in *Figure 5.60*. The un-reinforced sections (Beam 1 and Beam 2) vary a lot in their stiffness (almost 15 %) as well as ultimate load carrying capacity (about 17 %). But when it comes to reinforced sections, the variability is diminishing, as the reinforcements takes over and are now responsible for the key properties. Beams 9 and 10, which are reinforced with CFRP (165GPa), show excellent similarity in their properties. This can be due to the increased effect of CFRP reinforcements, which basically are produced under high quality control, and possess less variation in its properties. The same case can be seen in the case of Beams 3&5, which are reinforced with steel in both tension and compression. But in case of Beam 4 and Beam 6, reinforced only in tension side, the compressive behaviour of timber is decisive, which is the reason for the variation in behaviour.
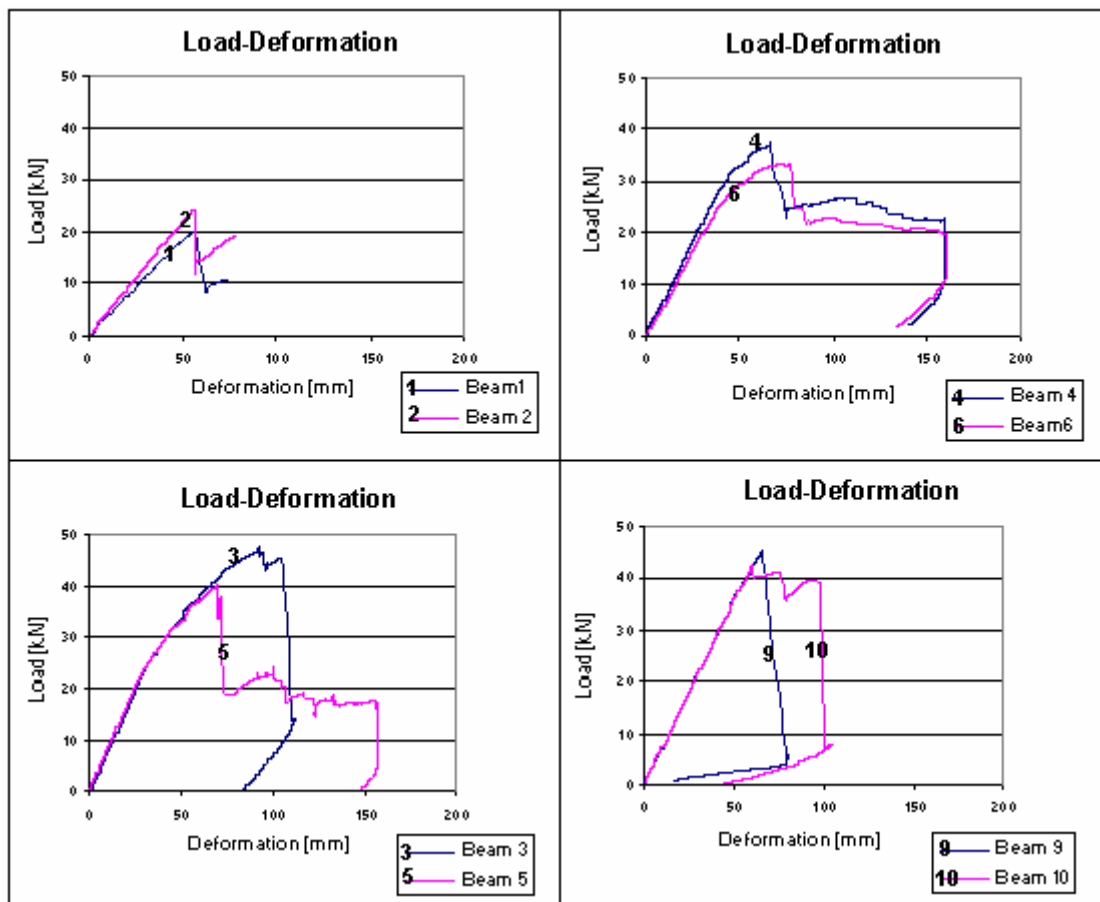
Figure 5.60 Variability of results for different reinforcement schemes.Beam 1&2-unreinforced, Beam 4&6- steel reinforced equally on tension and compression, Beams 3&5-steel reinforced at tension side only, Beam 9&10 CFRP reinforced(E 165GPa)in the ratio 1:2 in compression and tension.

d) Effect on overall ductility of the beam

All the reinforcing schemes had a positive effect on the overall ductility of the beams. The ductility is introduced in two ways, a) due to the use of yielding reinforcement b)

controlling the reinforcement percentage in the compressive zone so that the compressive failure is induced in the timber. This can be clearly observed in *Figure 5.61*. Beam 3 and beam 4 which are reinforced with steel attains ductility due to yielding of steel reinforcements. An interaction between the effect of steel yielding and timber plastification is also proposed. Beam 9 which was reinforced by high stiffness CFRP, did not show much ductile behaviour as the beam failed in shear before the onset of plasticity in timber.

Usually ductility is produced by a ductile reinforcement or a reinforcement arrangement which allows plastification of compressive timber. An exception for this phenomenon was beam7 which was reinforced with CFRP (non-yielding) equally distributed in the tension as well as compressive zones. But still a clear ductile behaviour is seen in the post elastic phase, which was a result of the lesser compressive strength of the CFRP used (Sika Carbodur H, unidirectional fiber arrangement results in fiber buckling under compressive loads), which in turn induced compressive failure of timber.
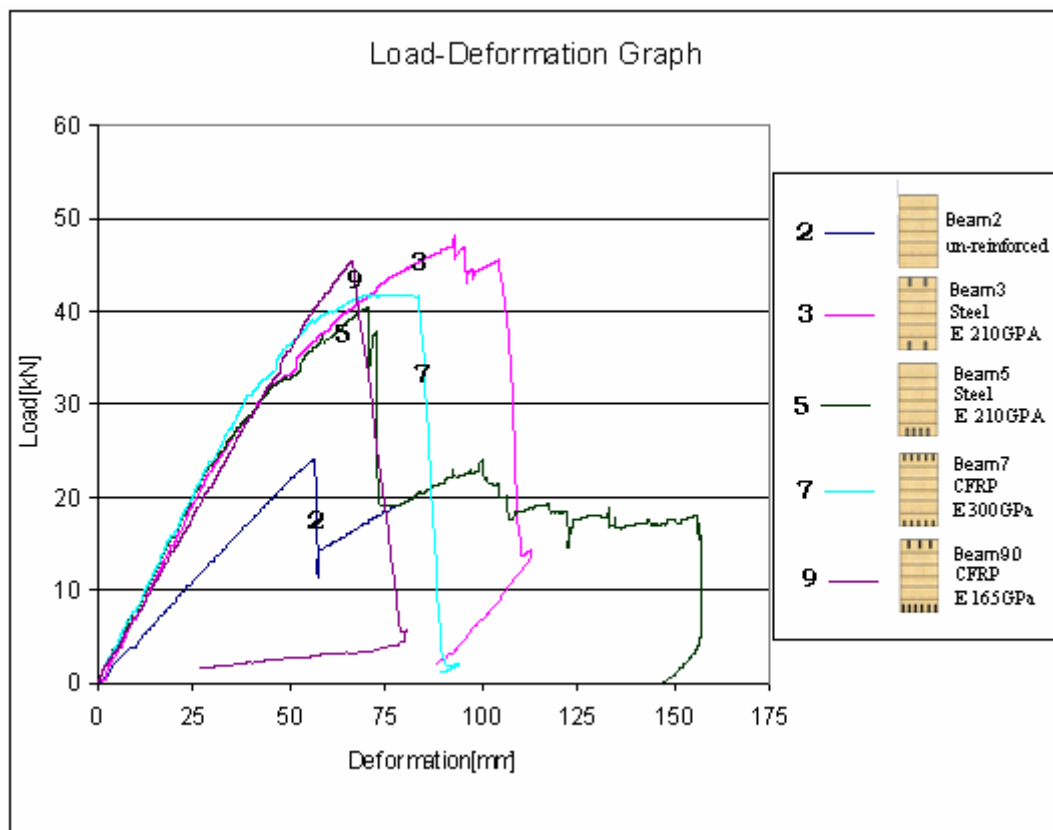
Figure 5.61 Overall Ductility of beams

e) Effect on failure modes

The ultimate failure was in tension for almost all beams when the timber reached its tensile limit, except for heavily reinforced sections where the failure was in shear. But the events leading to failure were very much affected by the type, amount and arrangement of the reinforcements. Reinforcing influences the plastic behaviour of the beam, which otherwise is not so predominant due to the low tensile strength of the timber. So the un-reinforced beam usually fails in tension before there is any

substantial plastification of the compressive zone. But reinforcing the tensile zone shifts the failure mode to the compressive zone which in effect will introduce more plasticity in the beams. But in principle, if we reinforce the section equally on tension and compression, there should not be any plastification in the timber, and the failure mode should be brittle. But in our tests, it could be seen that Beam 7, reinforced equally on tension and compression with CFRP(E=300GPa), had a very nice plastic behaviour.

Comparing with the un-reinforced sections, the reinforced ones failed at much higher loads and allowed larger deformations before the onset of cracks. It should be noted that the failure modes can be controlled by carefully planning the reinforcement arrangement as well as choosing appropriate material.

Effect of Different Adhesives

Failure modes and experimental data showed excellent bond properties between wood and the reinforcing materials, with timber properties mainly responsible for critical events leading to failure. This means that the adhesive were quite successful in transferring the loads to the reinforcements. But the degree of effectiveness of the adhesives (for comparison purposes) could not be realised within the scope of this project as it needed more sophisticated strain-gauge setup as well as more focussed study on adhesive properties. But in general, the effectiveness of both the adhesives was very good in short term loading as there existed no single case of adhesive failure. The long term behaviour is a matter of further studies.

The properties of the adhesive before setting are very important with regard workability. The initial setting time as well as the viscosity of the adhesive mixture (before setting) affects workability a lot. A less viscous adhesive (more particulate matter inside the adhesive as additive) is advantageous in terms of shrinkage on curing, but poses difficulties in while working with narrow slits for reinforcements. More viscous adhesive is rather easier for placement in the slits, but have shrinkage problems while curing.

Effect of placement of reinforcements

a) Comparison based on symmetry of reinforcements

It was observed from the nonlinear model that the symmetry of the reinforcement (about the centre line of the glulam section) is favourable in terms of stiffness when compared to a beam which lacks symmetry in terms of reinforcements. This was verified by the two reinforcement arrangements realised by Beams 3&5 and Beams 4&6. The symmetric reinforcement arrangement results in a more brittle failure as it does not allow much compressive plastification. It should be noted that he nonlinearity that is seen in beam 5 is due to yielding of reinforcement.

But it should be kept in mind that symmetric arrangement of reinforcement is not the optimum one with regard to ultimate moment resistance. From our studies using the nonlinear model, a reinforcement arrangement which has 25-30% compression reinforcement is ideal with regard to ultimate moment resistance.
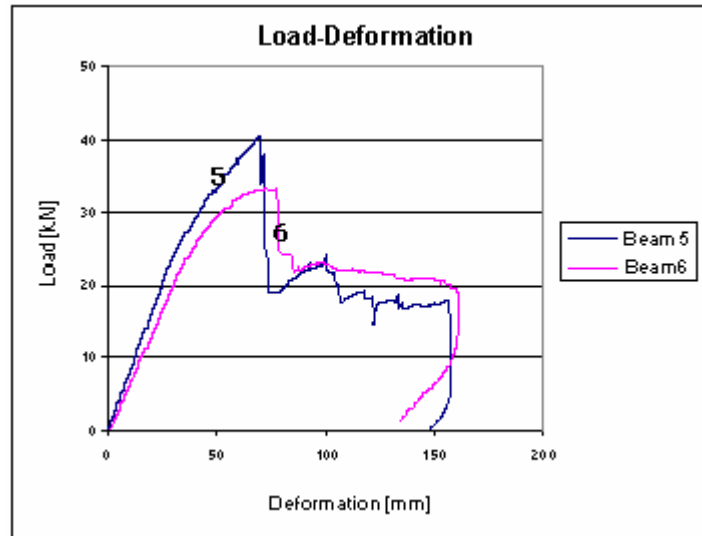
Figure 5.62 Symmetric vs. Un-symmetric reinforcements(Beam5 -Symmetric, Beam6-Un-symmetric)

The following two sections intends to have a more focussed view the special behavioural aspects of symmetric and non symmetric reinforcement arrangements

a. Symmetrically placed Reinforcements

Beams 3 and 5 had symmetrically placed steel reinforcements (2% Gross c/s, E=210GPa) while Beam7 had symmetrically placed CFRP reinforcements (1.5%. Gross c/s, E=300GPa). It can be seen from *Figure 5.63* that the elastic stiffness imparted by both the reinforcement schemes are almost the same. But the steel reinforced beams (Beam 5 in figure) become more flexible at load levels of 26kN due to yielding of steel. But Beam 7 retains stiffness till 34kN and then starts failing in compression along with crushing of timber as well as CFRP laminate.
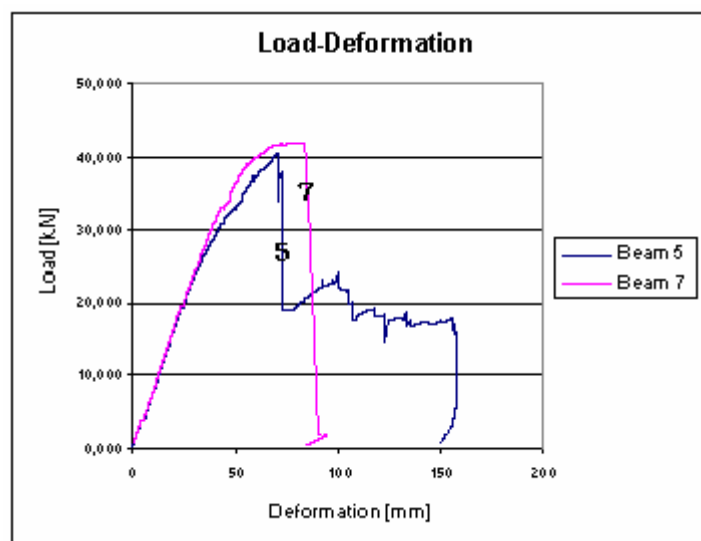
Figure 5.63 Load-deformation for symmetrically reinforced beams (Beam 5-Symmetric steel, Beam7- Symmetric CFRP)

b. Asymmetrically placed reinforcements

The main purpose of asymmetry in reinforcement arrangement was to introduce plasticity, taking the advantage of plastic behaviour of timber in compression. This was realised effectively in beam 4& 6 and (even though the overall nonlinearity was the result of combination of reinforcement yielding as well as timber plastification). But in the case of beam 9, the effect had been much diminished as the shear failure occurred before the plastification of timber in the compression side.
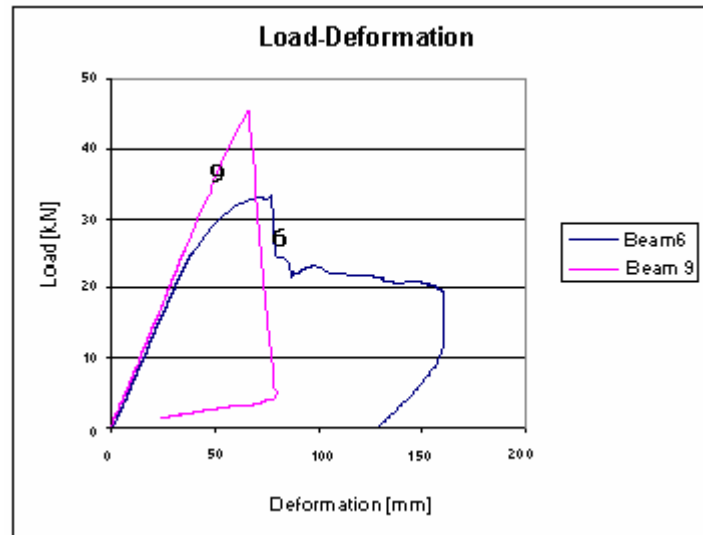
Figure 5.64 Load-deformation for beams with asymmetric reinforcements(Beam 6-steel asymmetric, Beam9- CFRP asymmetric)

b) Beams reinforced on compression side vs. beams which are not.

a. Effect of tensile reinforcement

Tensile reinforcement is basically provided as a supplementary material in the cross section that can take the tensile forces. The increase in moment capacity and stiffness are obvious, but the interesting part is the introduction of ductility in the global behaviour. This can be seen clearly in *Figure 5.65*.

The introduction of tensile reinforcement enhances the tensile capacity, and prevents the fibers from failing in tension. This results in further load carrying capacity. On further load increase, the fibers in the outermost compressive zone starts failing due to crushing, this results in the global plastic behaviour. tis is because of he fact that the timber plastification allows much ductility and is not abrupt compared to tensile failure.
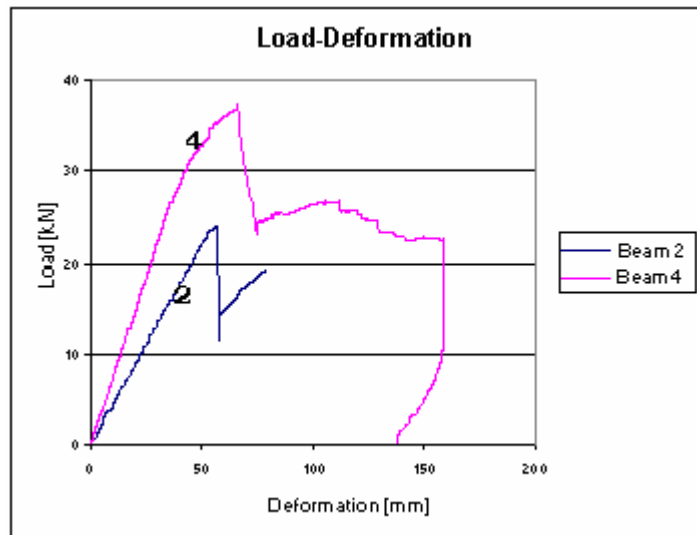
Figure 5.65 Effect of tensile reinforcement.(Beam2- Unreinforced, Beam4-Reinforced in tension side)

b. *Effect of introducing compressive reinforcement*

The addition of compressive reinforcement is advantageous in terms of elastic stiffness of the beam. But the addition of compressive reinforcement increases the stiffness of the compression zone and prevents the timber from failing in compression. Therefore the global behaviour of beams reinforced in the compression side will be more linear and the failure will be brittle. This can be seen in *Figure 5.66.* Beam 4 which is reinforced with steel only in compression side is compared with Beam 9 which is reinforced in tension as well as compression sides. This was done because the e modulus of the reinforcing materials are comparable *($E_{steel}=210GPa$ and $E_{frp}=165GPa$)*. But it should be kept in mind that the nonlinearity in case of Beam 4 is the combined effect of steel yielding and timber plastification.

But in principle, the ultimate moment resistance of a beam having 25-30% reinforcement in the tension side will be higher than beams with no compressive reinforcement even if the percentage of reinforcement in the cross section is the same.
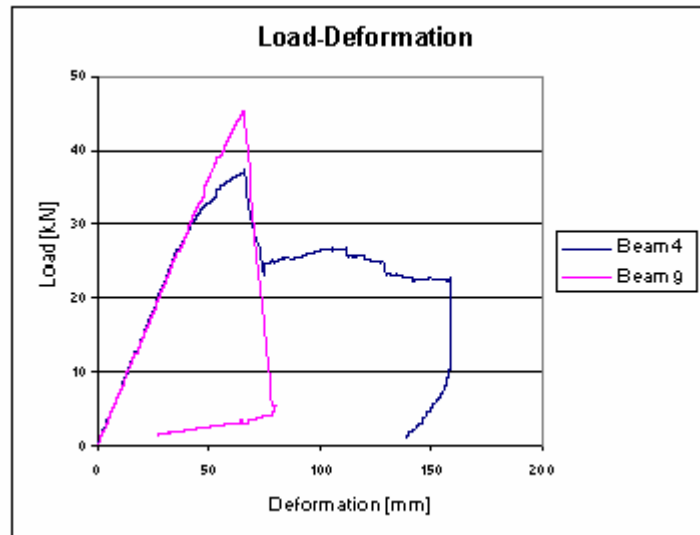
Figure 5.66 Introducing compression reinforcement(Beam 4- Steel reinforcement(E=210GPa) in only tension side, Beam 9- CFRP(E=165GPa) Reinforcement in both tension and compression.)

The following figure (*Figure 5.67*) intends to compare differences between beams reinforced only in the tension side and beams which are reinforced in the tension as well as compression side. All the beams compared are having the same reinforcement ratio and same reinforcement type. Only the arrangement is different. It can be seen that the beams which are reinforced only in the tension side is more ductile and has lower load bearing capacity compared to their compressive reinforced counterparts.
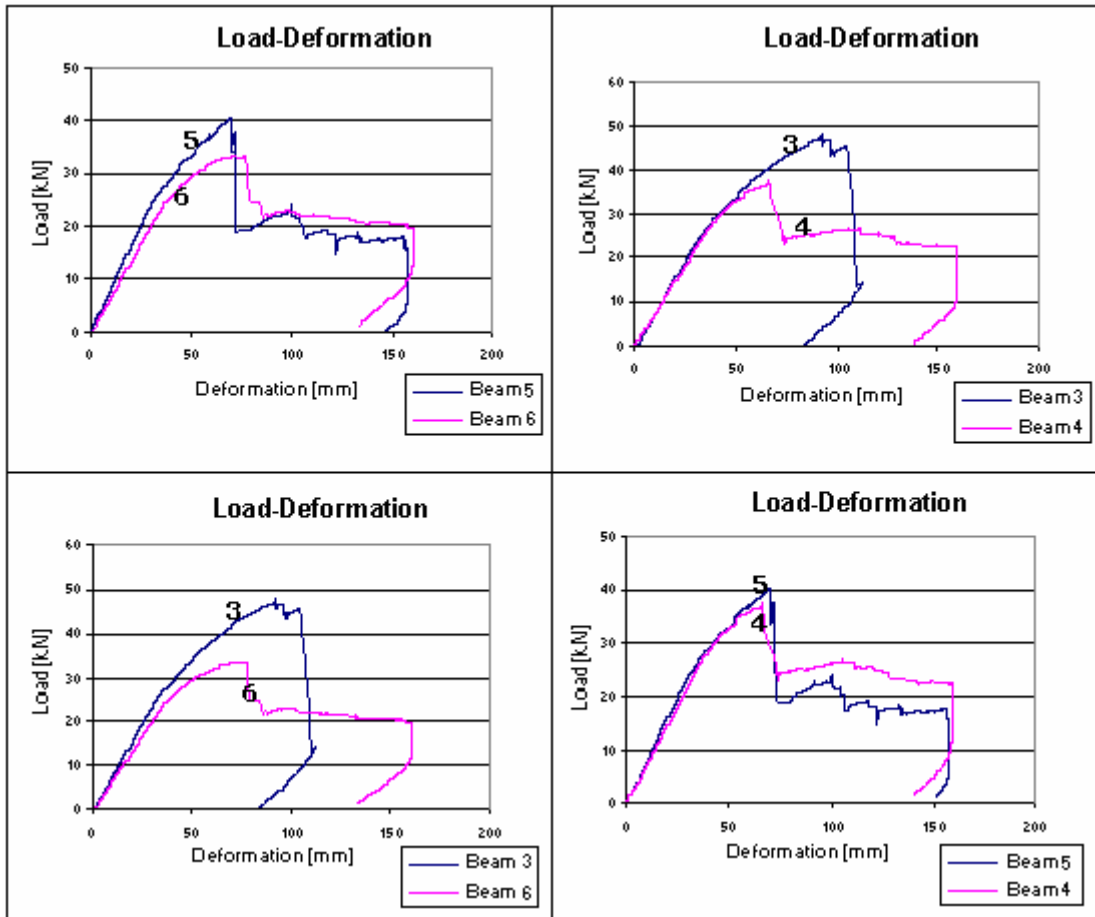
Figure 5.67 Beams reinforced on compression side vs. beams which are not.

Effect of Material used for reinforcing

In this thesis we dealt with 3 different materials for reinforcement, i.e. steel, CFRP (165GPa) and CFRP (300GPa). The reinforcing material has a very important role in the overall behaviour of the beam. The increase in stiffness as well as moment capacity is a factor of the stiffness as well as the amount of the reinforcing material. *Figure 5.68* shows the effect of different reinforcing materials on the global behaviour of the beam. The areas of reinforcements are not the same, but the comparison can give a feel of the effect of material used on the global behaviour.

It can be seen that the steel yields before the timber reaches its tensile/compressive limits. This occurs because the steel which is much stiffer than the timber will attract much more stresses and will reach its yields point. This increases the ductility of the beam which can be considered advantageous considering safety and warning in the case of a failing structure, but prove disadvantageous in terms of larger deflections.

But CFRP reinforced sections are much stiffer as CFRP does not have ductility. But care should be taken in using CFRP in the compressive zone as unidirectional fibers can buckle and loose all its strength when loaded in compression (as in case of Beam7). Earlier identification of such failure mode is advantageous as the designer can go for alternative material to be used in such highly compressive zone.
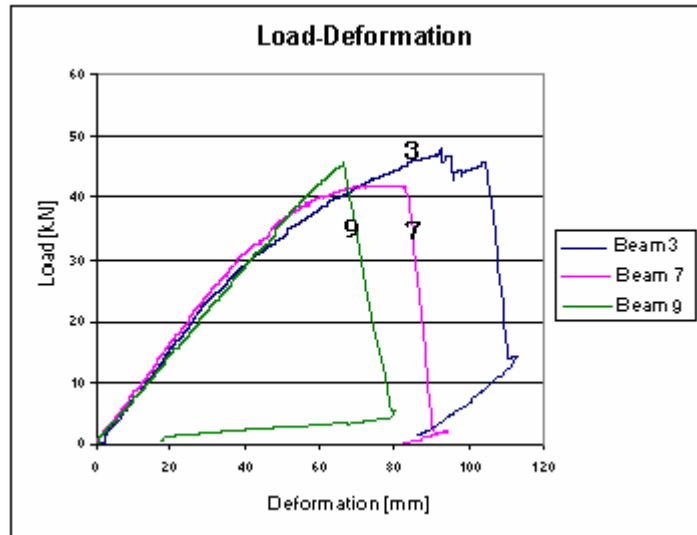
Figure 5.68 Effect of CFRP vs. Effect of steel (Yielding vs. Non-yielding)(Beam3-Steel (E=210 GPa)reinforced both tension and compression, Beam 7-CFRP(E=300Gpa) reinforced on both tension and compession, Beam9 CFRP(E=165GPa) reinforced in both tension and compression)

Effect of amount of reinforcement

The amount of reinforcement is also an important factor in the global behaviour of the beam. Reinforcement ratios are determined by the stiffness/ strength requirements of the beam. But the following points has to be noted

Lower reinforcement ratios can cause early yielding of steel as the higher stresses in bending has to be born by the small cross sectional area of the reinforcement.

The increase in stiffness is obvious as increasing area of reinforcement basically means introducing stiffer material to the cross section. But when the reinforcement percentage goes higher, the failure mode shifts from the normal bending failure to shear failure. This is because of the fact that the increased percentage of reinforcement makes the beam stiffer, and as a result, the timber fibers never reach their ultimate strain value. But due to load increase, the shear stresses increases and reaches its limiting value which eventually results in shear failure. The same phenomena can be expected while using reinforcements with very high stiffness.

 It should be noted that the shear failure is brittle and the crack growth is in the fiber direction, which makes it more dangerous. This could be seen in beams 9 and 10, which were reinforced by 2.8% of CFRP.

So if the loading requires more reinforcement to be incorporated in the cross section, provision should be made for shear reinforcing.

The figure shown below (*Figure 5.69*) is a comparison between beam 7 and Beam 9 which are reinforced with CFRP 2% and 2.8% respectively. Beam 7 started failing in the compression zone (buckling of fibers) which induced more deformations which caused the tensile strains in the timber to reach the limiting value and the beam failed in tension. But in the case of beam 9, the higher reinforcement percentage did not

allow much deformation which means lesser timber strains. But due to load increase, shear stresses built up and reached the limiting value and failure occurred.
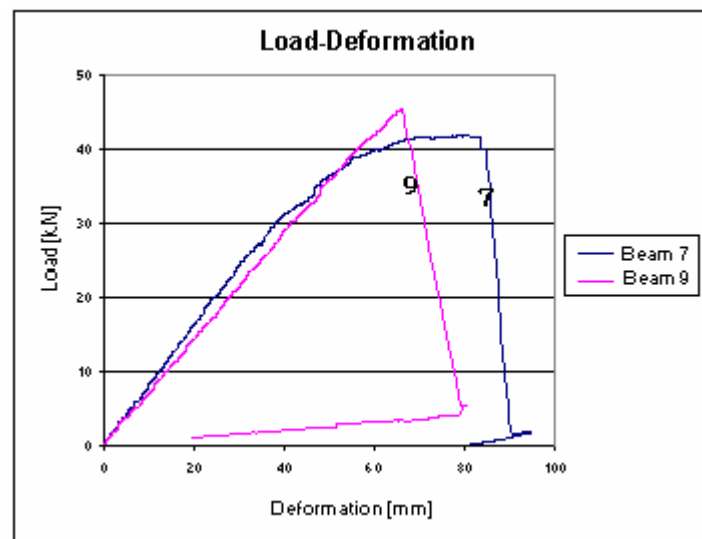
Figure 5.69 Effect of amount of reinforcement(Beam 7-2% CFRP(E=300GPa), Beam9-2.8%CFRP(E=165GPa))

Comparison of the experimental results with the Non-linear model

By comparing the results from the experiments with the non linear results it could be seen that the model predicts the behaviour quite well. The model could very well predict the linear elastic phase and also the global non linear behaviour due to the onset of plasticity in timber as well as in steel.

The validation of the model was done by curve-fitting. The E-modulus calculated based on the deformations (as given in appendix) were used for the timber. Minor adjustments in this E-modulus were needed for fitting the curve as its calculation was based on dimensions in the drawing, whereas in actual practice, the grove dimensions had slight variations. The actual values used for curve fitting is given in Appendix 4.

The deviations due to local failures due to small knots or other imperfections were not included in the model.

a) Un-reinforced beam

Figure shows the global behaviour of the un-reinforced beam. It could be seen that the model predicts the behaviour in a very good manner. The behaviour was linear as predicted by the model, and the ultimate strength was also predicted with good accuracy.
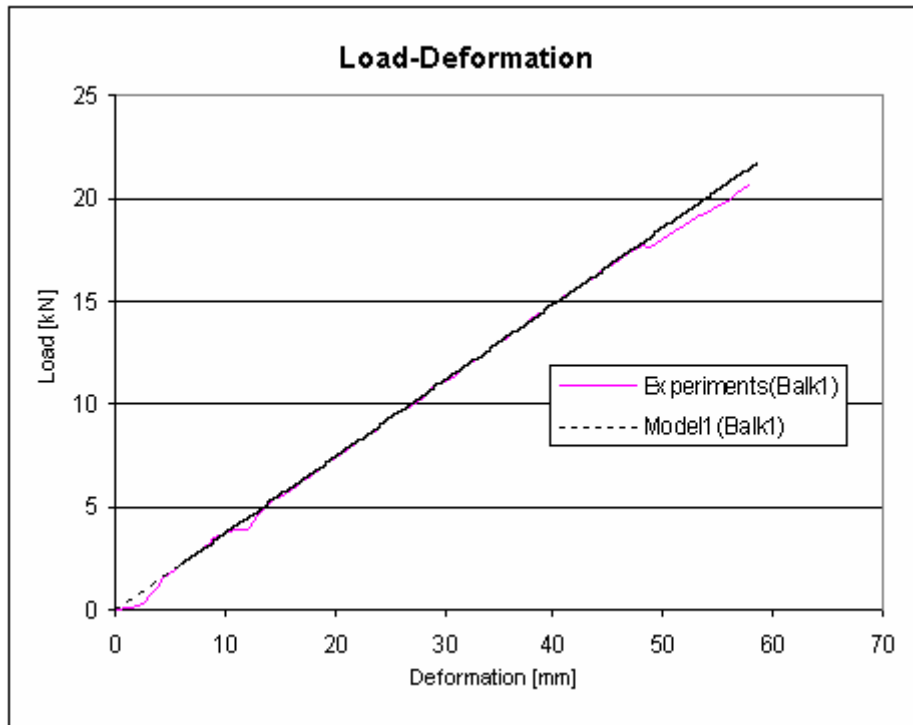
Figure 5.70 Comparison with model (Beam1)

b) Beam reinforced only on tension side with steel

It could be seen that the nonlinearity is predominantly originating from timber compression rather than steel yielding. This could be seen by observing the control flow while running the non linear model.
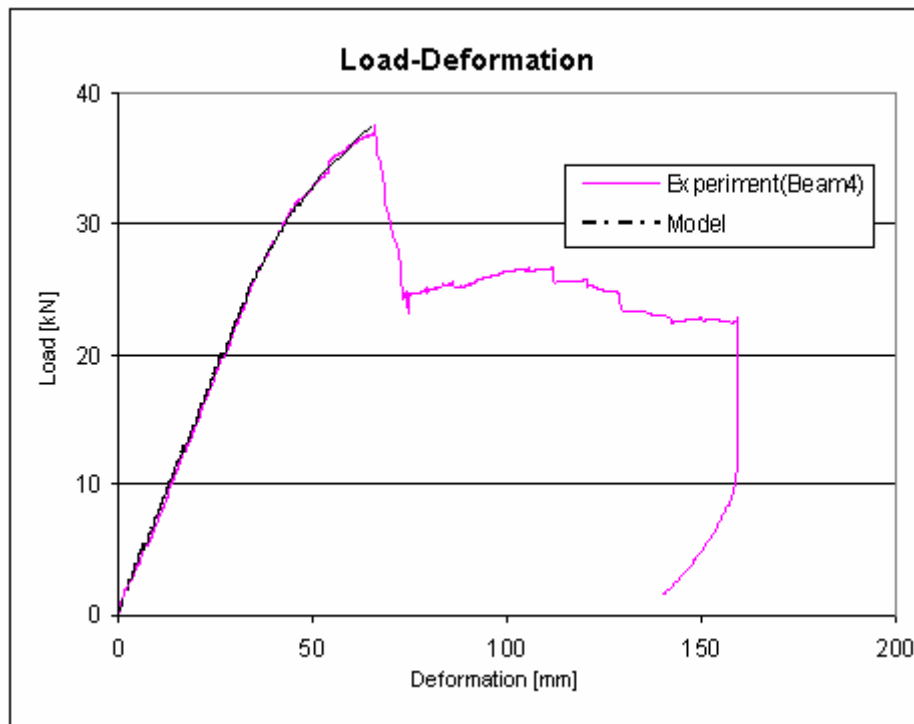
Figure 5.71 Comparison with model (Beam4)

c) Beam reinforced with steel on both sides

It could be seen that the model predicted the behaviour very good (*Figure 5.72*). The plastic behaviour due to steel yielding can be clearly seen at a load level of 24kN and the stiffness decreases dramatically.
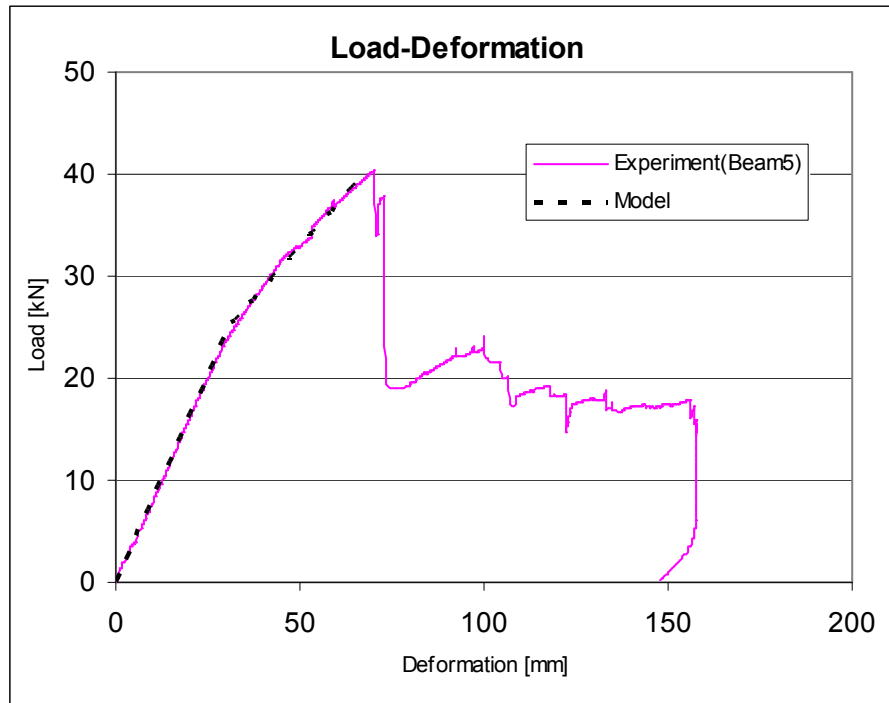
Figure 5.72 Comparison with model (Beam5)

d) Beam reinforced with CFRP(1.5% of gross cross section)

The model predicted the behaviour quite well in the linear elastic phase, but in the plastic phase the behaviour could not be followed very well as the model did not include the buckling behaviour of the fibers in the compressive region (see *Figure 5.73*). The model considered the behaviour of the CFRP in the compressive zone to be linear elastic- elastic plastic which might not have been the case while the CFRP fails due to fiber buckling. A more refined material model is required here in order to predict this behaviour accurately. But it is always advisable to use designs which do not allow buckling failures in the compressive region, as we know that buckling failure is catastrophic.
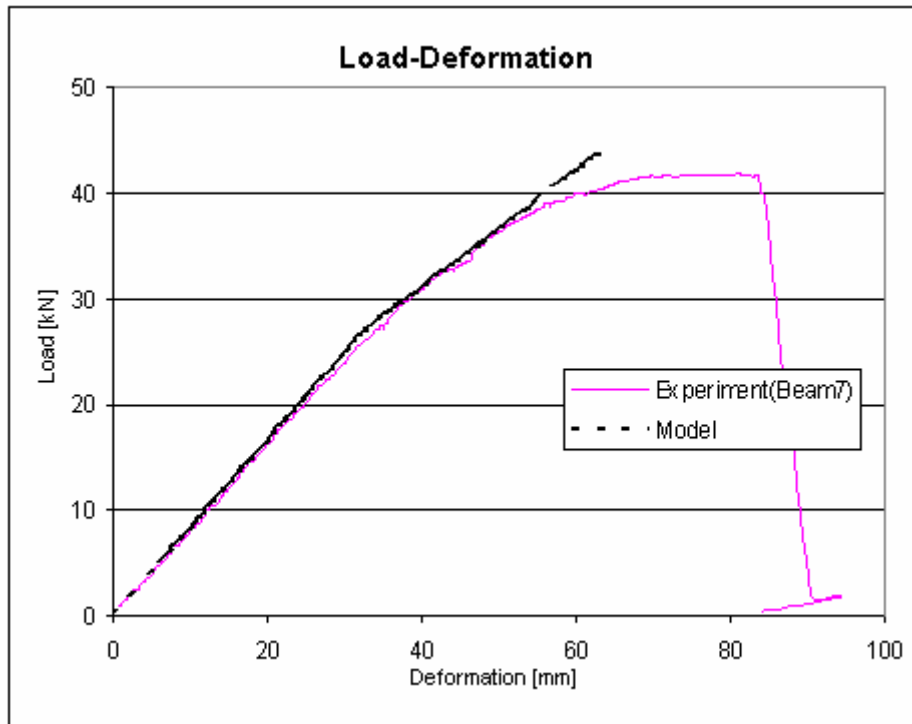
Figure 5.73 Comparison with model (Beam5)

e) Beam reinforced with CFRP(2.8% of the gross cross section)

The model was quite good in predicting this behaviour also. The shear failure was taken into consideration. It should be noted that the slight plastic behaviour of the beam due to the compressive failure of the timber also is predicted by the model.
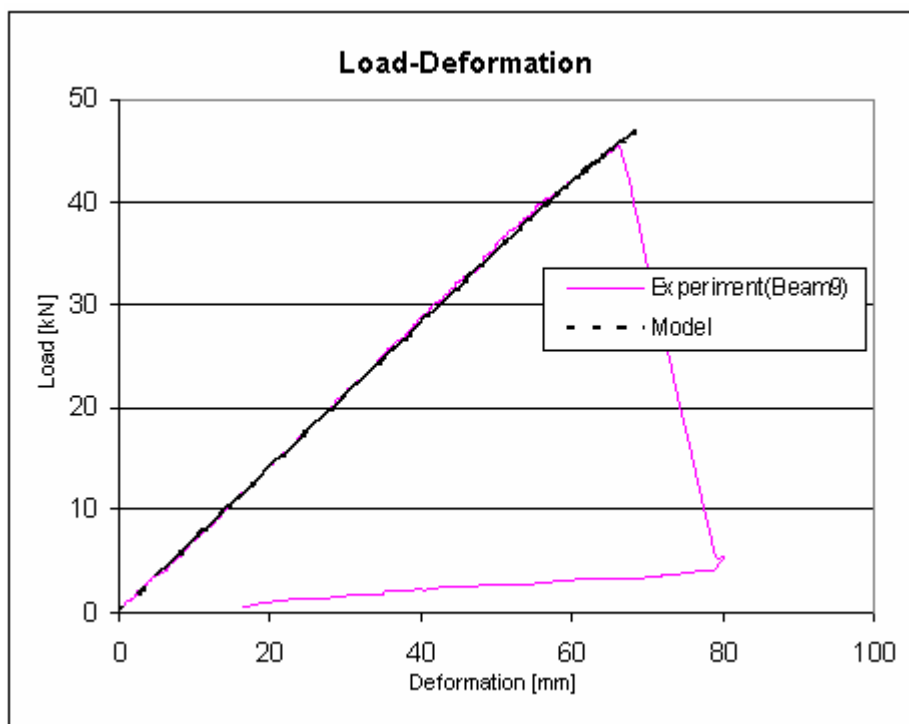
Figure 5.74 Comparison with model (Beam9)

6 CONCLUSIONS AND FUTURE RESEARCH

Conclusions

Although statistical significance could not be proved based on the low number of tests performed, the results show the viability of the reinforcing schemes as well as the working procedures. The major conclusions from our study are listed below.

All the interventions had resulted in considerable increase in the load bearing capacity as well as stiffness properties. The increase in the moment resistance was in the order of 57% to 96% and a stiffness increase of 80% to 107% could be achieved for different reinforcement schemes.

The amount of reinforcement in the cross section is decisive with regard to failure modes. It could be seen that increase in reinforcement may not necessarily result in increase in strength properties, as the shear failure mode becomes prominent for highly reinforced beams.

The reinforcement arrangement is also very important regarding strength, stiffness and failure modes. Controlling the amount of reinforcements in the tension and compressive zone can be done in order to achieve desired failure mode.

All the interventions had a positive effect on the variability of characteristic properties. The reinforced specimens were more consistent in their properties and behaviour. This is very decisive in design as it increases the predictability which can allow lesser partial safety factors.

The best configuration for reinforcement differs according to specific requirements envisaged by the load cases/ design situations. In our study, the optimum configuration was found to be the one having the reinforcements arranged 20-25% in the compressive zone and the rest in the tension zone. This configuration gave maximum moment resistance, with considerably high stiffness values allowing some plasticity in the compressive zone due to plastification of timber.

Selection of reinforcement material is basically demand driven. Both the reinforcing systems (steel and CFRP) have their advantages and disadvantages. So the selection criteria should be able to find a balance between the specific strength/stiffness needs of a particular design/load case and the economical/ production issues.

Steel reinforcements impart ductility to the overall behaviour of the beams. But steel reinforcements can be recommended only in concealed environments, where corrosion cannot be a problem. The stress levels in steel reinforcements are quite high in loaded beams because of the difference in the E modulus between steel and timber. Therefore, the loss of cross section, even in its feeble form due to corrosion can have catastrophic effects.

CFRP reinforcements, even though they are brittle, impart high stiffness/moment resistance to beams and are resistant to corrosion. But care should be taken while using FRP with thermoplastic matrix bases, as they have poor fire resistance. Ductility in the overall behaviour can be imparted by carefully arranging the reinforcements in the tension and compression zones.

Care should be taken while using unidirectional FRP in compressive zone as it can cause fiber buckling under compressive loads.

Future research

The long term behaviour of beams strengthened with steel and CFRP should be studied with particular attention to the fatigue performance, creep behaviour, and relaxation.

It would be possible to enhance the ultimate load carrying capacity of heavily reinforced sections beyond the shear limit, by an effective intervention which can safely transfer the shear forces to the supports without causing shear failure. A workable strut and tie model may be our suggestion for future research.

The conventional joinery details may not be workable on the reinforced specimens because of space constrains imparted by the reinforcements and also due to higher load levels than in conventional beams. So study of new joinery details for reinforced specimens can be proposed as a future research.

The buckling behaviour of unidirectional fibers in CFRP reinforcement is a problem that needs due consideration as it is a critical failure mode. Using conventional linear material models in design purposes will predict a higher load performance, which is practically in-achievable due to this buckling behaviour. So a new material model including this material behaviour should be studied in detail.

This study did not take into consideration the effect of varying material properties across the cross section among the laminates. A more specific study considering the variation of strength/stiffness properties among the laminates of glulam could be advantageous in better prediction of the overall behaviour.

An extensive parametric study considering the influence of using different material properties (of timber, reinforcements as well as adhesives) and different geometries can be done in order to understand their effects.

The change in moisture content and changes in temperatures which are inevitable in case of exposed structures can cause expansion/ contraction resulting in volume changes in the cross section. If this volume change is not occurring in a synchronised manner among the constituent materials (glulam, adhesive, reinforcement), it can result in residual stresses and eventually de-lamination under sustained loading. So the effect of alternating moisture content/ temperature on the bond properties need further focus.

A combined reinforcing system including Steel and CFRP in the cross section, in a favourable reinforcing configuration, may give better performance as it can combine the positive effects of both the reinforcements. The study may result in more economical cross section without compromising much on the strength/stiffness properties.

7 REFERENCES

Amy, K., and Svecova, D. (2004). "Strengthening of dapped timber beams using glass fiber reinforced polymer bars." *Can. J. Civ. Eng.*, 31, 943-955.

André, Alan (2006): "Fibres for Strengthening of Timber Structures." PhD Thesis .Department of Civil and Environmental Engineering, Luleå University of Technology, ISSN: 1402 -1528, Luleå, Sweden, 121pp.

Blaß, H. J., and Romani, M. (1998-2000). "Reinforcement of Glulam beams with FRP reinforcement.

Borri, A., Corradi, M., and Grazini, A. (2005). "A method for flexural reinforcement of old wood beams with CFRP materials." *Composites: Part B*, 36, 143-153.

Buell, T. W., and Saadatmanesh, H. (2005). "Strengthening timber bridge beams using carbon fibre." *Journal of Structural Engineering*, 131,173-187.

Dagher, H. J., Kimball, T. E., Shaler, S. M., and Abdel-Magid, B. "Effect of FRP reinforcement on low grade eastern hemlock Glulams." *National conference on wood transportation structures*.

Fiorelli, J., and Dias, A. A. (2003). "Analysis of the strength and stiffness of timber beams reinforced with carbon fibre and glass fibre." *Materials Research*, 6, 193-202.

Fletcher, A., (1994), Advanced Composites - A Profile of the International Advanced

Composites Industry, Elsevier Science, New York, NY.

Galloway, T. L., Fogstad, C., Dolan, C. W., and Puckett, J. A. "Initial tests of Kevlar prestressed timber beams." *National conference on wood transportation structures*.

Gentile, C., Svecova, D., and Rizkalla, S. H. (2002). "Timber beams strengthened with GFRP bars: development and applications." *Journal of Composites for Construction*.

Hernandez, R., Davalos, J. F., Sonti, S. S., Kim, Y., and Moody, R. C. (1997). "Strength and stiffness of reinforced yellow-poplar glued-laminated beams." *US Department of Agriculture, Forest Service, Forest Product Laboratory*.

John, K. C., and Lacroix, S. (2000). "Composite reinforcement of timber in bending." *Can. J. Civ. Eng.*, 27, 899-906.

Lopez-Anido, R., and Xu, H. (2002). "Structural characterization of hybrid fibre-reinforced polymer-Glulam panels for bridge decks." *Journal of Composites for Construction*.ASCE.

Lopez-Anido and Tarun R. (2000). "Emerging materials for civil infrastructure- State of the art." American Society of Civil Engineers (ASCE), ISBN: 0-7844-0538-7.

Micelli, F. (2005). "Flexural Reinforcement of Glulam Timber Beams and Joints with Carbon Fiber-reinforced Polymer Rods". *Journal of composites for construction, (ASCE),337-347.*

Ogawa, H. (2000). "Architectural application of carbon fibres, development of new carbon fibre reinforced Glulam." *Carbon*, 38, 211-226.

Steiger R. (2004): "Bonding of carbon fiber reinforced plastics (CFRP) with wood". In: Proceedings of COST E34 conference "Innovations in Wood Adhesives", Biel, Switzerland, 33 - 50.

Thomas G. Williamson, (2002): "APA Engineered Wood Handbook". The McGraw-Hill Companies, Inc. ISBN 0-07-136029-8

Douglas R. Rammer(1996) "Shear Strength of Glued-Laminated Timber Beams and Panels*" Forest Products Laboratory, USDA Forest Service*

8   APPENDICES

8.1 Appendix A: Linear Model (MathCAD)

Material Properties

Glulam

$f_{c\_elGl} := 44\text{MPa}$

$f_{t\_elGl} := 42\text{MPa}$

$E_{Gl} := 13500\text{MPa}$

$\varepsilon_{c\_elGl} := \dfrac{f_{c\_elGl}}{E_{Gl}}$

$\varepsilon_{t\_elGl} := \dfrac{f_{t\_elGl}}{E_{Gl}}$

CFRP

$f_{t\_elFRP} := 1300\text{MPa}$

$E_{FRP} := 165000\text{MPa}$

$\alpha := \dfrac{E_{FRP}}{E_{Gl}}$

$\alpha = 12.222$

Geometry Definition

$b_{Gl} := 115\text{mm}$

$h_{Gl} := 197\text{mm}$

$A_{Gl} := b_{Gl} h_{Gl}$

No. of FRP strips in the tension side= $n_t := 6$

$b_{FRP\_t} := 4\text{mm}$

$h_{FRP\_t} := 30\text{mm}$

$A_{FRP\_t} := n_t \cdot b_{FRP\_t} \cdot h_{FRP\_t}$

$A_{FRP\_t\_trans} := A_{FRP\_t} \cdot \alpha$

No. of FRP strips in the compression side= $n_c := 3$

$b_{FRP\_c} := 4mm$

$h_{FRP\_c} := 30mm$

$A_{FRP\_c} := n_c \cdot b_{FRP\_c} \cdot h_{FRP\_c}$

$A_{FRP\_c\_trans} := A_{FRP\_c} \cdot \alpha$

$$A_r := \begin{pmatrix} A_{Gl} \\ A_{FRP\_t\_trans} \\ A_{FRP\_c\_trans} \end{pmatrix}$$

Distance of the tension Reinforcement from the top of the beam= $d_t := 185mm$

Distance of Compression Reinforcement from the top of the beam= $d_c := 15mm$

$$y := \begin{pmatrix} \dfrac{h_{Gl}}{2} \\ d_t \\ d_c \end{pmatrix} \qquad y_1 := \dfrac{\displaystyle\sum_{n=0}^{2}\left(A_{r_n} \cdot y_n\right)}{\displaystyle\sum_{n=0}^{2}\left(A_{r_n}\right)} \qquad y_1 = 109.48313mm$$

$$b := \begin{pmatrix} b_{Gl} \\ b_{FRP\_t} \cdot n_t \cdot \alpha \\ b_{FRP\_c} \cdot n_c \cdot \alpha \end{pmatrix} \qquad h := \begin{pmatrix} h_{Gl} \\ h_{FRP\_t} \\ h_{FRP\_c} \end{pmatrix} \qquad h_0 := \begin{pmatrix} \left| y_1 - \dfrac{h_{Gl}}{2} \right| \\ d_t - y_1 \\ y_1 - d_c \end{pmatrix}$$

$$A_{r0} := \begin{pmatrix} A_{Gl} \\ A_{FRP\_t} \\ A_{FRP\_c} \end{pmatrix} \qquad b_0 := \begin{pmatrix} b_{Gl} \\ b_{FRP\_t} \cdot n_t \\ b_{FRP\_c} \cdot n_c \end{pmatrix} \qquad E := \begin{pmatrix} E_{Gl} \\ E_{FRP} \\ E_{FRP} \end{pmatrix}$$

$k := 0..2$

$$EI_{ef} := \sum_k \left[\dfrac{E_k \cdot b_{0_k} \cdot \left(h_k\right)^3}{12} + E_k \cdot A_{r0_k} \cdot \left(h_{0_k}\right)^2 \right] \qquad EI_{ef} = 2.247 \times 10^3 \, kN \cdot m^2$$

$$I_{xx} := \dfrac{b \cdot h^3}{12} + A_r \cdot h_0^2 \qquad I_{xx} = 1.664547 \times 10^8 \, mm^4$$

Deformation Criterion

$$L_{beam} := 4m$$

$$\delta_{lim} := \frac{L_{beam}}{300}$$

$$a := \frac{L_{beam}}{3}$$

$$\delta = \frac{P \cdot a \cdot \left(3 \cdot L_{beam}^2 - 4 \cdot a^2\right)}{24 \cdot EI_{ef}}$$ $$\delta_{lim} = 0.013 \, m$$

so

$$P := \frac{\delta_{lim} 24 \cdot EI_{ef}}{a \cdot \left(3 \cdot L_{beam}^2 - 4 \cdot a^2\right)}$$ $$P = 13.19 kN$$

Checking the governing failure mode

Enter the distance from the top of the beam to the point where the tensile strain to be limited

$$d_{t\_fail} := 180mm$$

Fixing the tensile strain just above the reinforcement to $$\varepsilon_{t\_Gl} := \varepsilon_{t\_elGl}$$

Checking compressive strain

$$\varepsilon_{c\_Gl} := \frac{\varepsilon_{t\_Gl}}{d_{t\_fail} - y_1} \cdot y_1$$ $$\varepsilon_{c\_Gl} = 4.83 \times 10^{-3}$$

$$\varepsilon_{t\_Gl} := \begin{vmatrix} \dfrac{\varepsilon_{c\_elGl}}{y_1} \cdot \left(d_{t\_fail} - y_1\right) & \text{if } \varepsilon_{c\_Gl} > \varepsilon_{c\_elGl} \\ \varepsilon_{t\_Gl} & \text{otherwise} \end{vmatrix}$$ $$\varepsilon_{t\_elGl} = 3.111 \times 10^{-3}$$

$$\varepsilon_{c\_Gl} := \begin{vmatrix} \varepsilon_{c\_elGl} & \text{if } \varepsilon_{c\_Gl} > \varepsilon_{c\_elGl} \\ \varepsilon_{c\_Gl} & \text{otherwise} \end{vmatrix}$$ $$\varepsilon_{c\_elGl} = 3.259 \times 10^{-3}$$

Limiting values

$$\varepsilon_{c\_Gl} = 3.259 \times 10^{-3}$$

$$\varepsilon_{t\_Gl} = 2.099 \times 10^{-3}$$

$$\sigma_c := \varepsilon_{c\_Gl} E_G \qquad\qquad \sigma_c = 4.4 \times 10^7 \ Pa$$

$$\sigma_t := \varepsilon_{t\_Gl} E_G \qquad\qquad \sigma_t = 2.834 \times 10^7 \ Pa$$

$$F_c := \frac{\sigma_c \cdot b_{Gl} y_1}{2} \qquad\qquad F_c = 276.992 kN$$

$$F_t := \frac{\sigma_t \cdot b_{Gl} \left(d_{t\_fail} - y_1 \right)}{2} \qquad\qquad F_t = 114.91 kN$$

Equilibrium

$$F_t := 0 \blacksquare$$

Force Equilibrium

$$F_{FRP\_t} + F_t = F_{FRP\_c} + F_c$$

If there is compression reinforcement

Applying Strain Compatibility

$$\frac{\varepsilon_{FRP.t}}{d_t - y_1} = \frac{\varepsilon_{FRP.c}}{y_1 - d_c}$$

i.e. $\varepsilon_{FRP.c} = \dfrac{\varepsilon_{FRP.t}}{d_t - y_1} \cdot \left(y_1 - d_c \right)$ .... valid only when there is compression reinforcement

Also from strain diagram

$$\varepsilon_{FRP.t} := \frac{\varepsilon_{t\_Gl}}{h_{Gl} - y_1} \cdot \left(d_t - y_1 \right)$$

$$\frac{\varepsilon_{FRP.t}}{d_t - y_1} = \frac{\varepsilon_{t\_Gl}}{h_{Gl} - y_1}$$

Therefore,

ie ,

$$F_{FRP\_t} := \varepsilon_{FRP.t} \cdot E_{FRP} \cdot A_{FRP\_t} \qquad F_{FRP\_t} = 215.196 kN$$

So

$$\varepsilon_{FRP.c} := \frac{\varepsilon_{FRP.t}}{d_t - y_1} \cdot (y_1 - d_c)$$

.......Valid only when there is compression reinforcement

$$F_{FRP\_c} := \begin{vmatrix} 0 & \text{if } n_c = 0 \\ \varepsilon_{FRP.c} \cdot E_{FRP} \cdot A_{FRP\_c} & \text{otherwise} \end{vmatrix}$$

$$F_{FRP\_c} = 134.621 \text{kN}$$

$$M_u := F_{FRP\_c} \cdot (y_1 - d_c) + F_t \cdot \frac{2}{3} \cdot (d_{t\_fail} - y_1) + F_c \cdot \frac{2}{3} \cdot y_1 + F_{FRP\_t} \cdot (d_t - y_1)$$

$$M_u = 54.59 \text{kN} \cdot \text{m}$$

we have

$$M_u = P \cdot a$$

$$P_{limit\_moment} := \frac{M_u}{a} \qquad\qquad P_{limit\_moment} = 40.942 \text{kN}$$

8.2 Appendix B: Nonlinear model

Matlab code for the Nonlinear Model

```
%Elastic-Plastic model for a Glulam beam reinforced with Steel and CFRP

clear all

clc;

%Geometry Defenitions

%Glulam

hgl=200;        %input('Height of the glulam=   ');    %[mm]

bgl=115;        %input('width of the glulam=   ');      %[mm]

Agl=hgl*bgl;    %[mm2]

L=4000-400;     % Length of the beam [mm]

%Laminate/Steel

blc=4;          %[mm]width of laminate in compression

hlc=30;         %[mm]height of laminate in compression
```

```matlab
nc=2                % number of parallel   laminates along width in compression side

blt=4;              %[mm]width of laminate in compression

hlt=30;             %[mm]height of laminate in tension

nt=2;               % number of parallel laminates along width in tension side

Alc=nc*blc*hlc;  %[mm2]

Alt=nt*blt*hlt;    %[mm2]

%Placement of the reinforcement

Zc=hlc/2;           %[mm]distance from the beam edge to the CG of compression reinforcement

Zt=hlt/2;            %[mm]distance from the beam edge to the CG of tension reinforcement

 %Material properties

 %Glulam

 Egl=10500;        %[MPa] Youngs modulus of Glulam

Ggl=850;           %[MPa]Shear modulus of Glulam

f_t=34;             %[MPa]tensile strength of glulam

eps_e_t=f_t/Egl;  % elastic strain limit in tension

f_c=35;            %[MPa]compressive strength of glulam

eps_e_c=f_c/Egl;       % elastic strain limit in compression

eps_p_c=3*eps_e_c;     % ultimate plastic strain

 %laminate

Ela=210000;             %[MPa]Youngs modulus of laminate

fy_t_la=350;            %[MPa]Yield strength of laminate in tension

fy_c_la=350;            %[MPa]Yield strength of laminate in tension

%Modular ratio

alpha=Ela/Egl           %transformation constant(for transforming c/s)

 %Linear Elastic Model

 %Neutral Axis

y_el_const=(Alc*alpha*Zc+ Alt*alpha*(hgl-Zt)+bgl*(hgl^2)/2)/(alpha*(Alc+Alt)+bgl*hgl);

y_el_prev=y_el_const;

%Assuming compressive strain is governing

eps_c0=eps_e_c/10;     %choosing a small initial value for the compressive strain
```

```
delta_eps_c=eps_e_c/100; % increment for compressive strain

%initialisation for plotting

N_la=hgl;                    %setting number of lamellas along height

eps_h=zeros(1,N_la+1); %strain across height

h_sec=zeros(1,N_la+1); %vector containing depth of each lamella

% initializing loop

ten=0;

eps_c=eps_c0;              %initial value of compressive strain

e(1)=eps_c;

i=2;                          %loop variable

while(eps_c<=eps_e_c) %if compressive strains in elastic range

    input_arg=[y_el_prev,Zc,eps_c,Ela,fy_t_la,fy_c_la,Zc,Zt,hgl,bgl,Egl,Alc,Alt,nc,nt];

    y_el=neut_el(input_arg)%Neural Axis when the timber is in linear elastic phase

    yel_prev=y_el;           %Saving for the next step

    eps_t=((hgl/y_el)-1)*eps_c;% finding corresponding tensile strains in the outermost fiber of
the timber

    if(eps_t>=eps_e_t);% checking if tensile strains exceed tensile strain limit

        display('tensile failure');

        ten=1;

        break;% if so exit loop

    end

    eps_lc=(1-Zc/y_el)*eps_c;% strains in the compressive reinforcement

    eps_lt=((hgl-y_el-Zt)/y_el)*eps_c;% strains in the tensile reinforcement

    sigma_t_lam=eps_lt*Ela;  %checking the tensile stresses in the laminate

    sigma_c_lam=eps_lc*Ela; %checking the compressive stresses in the laminate


    if (sigma_t_lam>=fy_t_la) %checking tensile yielding of laminate

            sigma_t_lam=fy_t_la;      %if so fixing the tensile stresses to yield stresses

    end

    if (sigma_c_lam>=fy_c_la)% checking compressive yielding of the laminate
```

```matlab
            sigma_c_lam=fy_c_la;%if so fixing the compressive stresses to yield stresses

      end

        phi(i)=eps_c/y_el;%Calculating Curvature

    %calculating resisting moment

    M(i)=eps_c*Egl*(bgl/3)*y_el^2+sigma_c_lam*Alc*(y_el-Zc)+eps_t*Egl*(bgl/3)*(hgl-
                y_el)^2+sigma_t_lam*Alt*(hgl-y_el-Zt);

    EI(i)=M(i)/phi(i);

    P(i)=M(i)/(L/3);

    Defle(i)=(P(i)*(L/3)*(3*L^2-4*(L/3)^2))/(24*EI(i))+M(i)/(Ggl*Agl);

     e(i)=eps_c;

    i=i+1;

    eps_c=eps_c+delta_eps_c;% strain increment

end

%Plotting Elastic Strains along depth

eps_h(1)=eps_c;

for k=2:N_la+1

    h_sec(k)=h_sec(k-1)+hgl/N_la;

    y1=y_el-k*hgl/N_la;

    eps_h(k)=eps_c/y_el*y1;

end

y_pl=0;

y_pl_prev=yel_prev;

eps_c=eps_c+0.00000001;% to avoid singularity at transition point

if (ten~=1)

%Plastic Model

while(eps_c<eps_p_c)

%      Finding neutral axis of plasticity

%                    a=f_c*bgl*(eps_c-eps_e_c)/eps_c+f_c*bgl/2*(1-(eps_c-eps_e_c)/eps_c)-
eps_c*bgl/2*Egl;

%      b=eps_c*(Ela*Alc+bgl*hgl*Egl+Alt*Ela);

%      c=eps_c*(Zt*Alt*Ela-Zc*Ela*Alc-(bgl/2)*Egl*hgl^2-hgl*Alt*Ela);
```

```matlab
%       y_pl=(-b+sqrt(b^2-4*a*c))/(2*a);

input_arg=[y_pl_prev,Zc,eps_c,Ela,fy_t_la,fy_c_la,Zc,Zt,hgl,bgl,Egl,Alc,Alt,nc,nt,f_c,eps_e_c];

    y_pl=neut_pl(input_arg)% neutral Axis when the timber is in Plastic phase

    ypl_prev=y_pl;%Saving for the next step

    eps_t=((hgl/y_pl)-1)*eps_c;% finding corresponding tensile strains

    if(eps_t>=eps_e_t);% checking if tensile strains in timber exceed tenisile strain limit

        display('tensile failure')

        break;% if so exit loop

    end

    eps_lc=(1-Zc/y_pl)*eps_c;% strains in the compressive reinforcement

    eps_lt=((hgl-y_pl-Zt)/y_pl)*eps_c;% strains in the tensile reinforcement




    sigma_t_lam=eps_lt*Ela;% checking the tensile stresses in the laminate

    sigma_c_lam=eps_lc*Ela;% checking the compressive stresses in the laminate




    if (sigma_t_lam>=fy_t_la)%checking tensile yielding of laminate

    sigma_t_lam=fy_t_la;%if so fixing the tensile stresses to yield stresses

    end




    if (sigma_c_lam>=fy_c_la)% checking compressive yielding of the laminate

    sigma_c_lam=fy_c_la;%if so fixing the compressive stresses to yield stresses

    end




    Zp=(1-(eps_e_c/eps_c))*y_pl;% depth of plastification

    phi(i)=eps_c/y_pl;% Calculating corresponding Curvature

    %calculating resisting moment

    M(i)=sigma_c_lam*Alc*(y_pl-Zc)+f_c*bgl*Zp*(y_pl-Zp/2)+1/2*f_c*(y_pl-Zp)*bgl*2/3*(y_pl-
            Zp)+sigma_t_lam*Alt*(hgl-y_pl-Zt)+1/2*(eps_t*Egl)*(hgl-y_pl)*bgl*2/3*(hgl-
            y_pl);
```

```matlab
        EI(i)=M(i)/phi(i);

        P(i)=M(i)/(L/3);

        Defle(i)=(P(i)*(L/3)*(3*L^2-4*(L/3)^2))/(24*EI(i))+M(i)/(Ggl*Agl);

        e(i)=eps_c;

        i=i+1;

        eps_c=eps_c+delta_eps_c;

    end

end

    phi_fail=phi(i-1);

    M_fail=M(i-1)/1e6;

%plotting Moment curvature relation

M(1)=0; phi(1)=0;

M=M/1e6;

P=P/1e3;

figure(1)

plot(phi,M,'r-');

title(['Moment Curvature Relation     h-la= ',num2str(hlc),'     E-la= ',num2str(Ela),'     t-la= ',num2str(blc),'   n-lc=',num2str(nc),'   n_lt=',num2str(nt)]);

legend(['% of Reinforcement=',num2str((Alc+Alt)/Agl*100)], 'location','north')

text(phi_fail,M_fail,'tension');

grid on;

Xlabel('\phi')

Ylabel('Moment [kNm]')

hold on

figure(2)

plot(Defle,P,'r-');

grid on;

Xlabel('\delta (mm)')

Ylabel('Load [kN]')
```

Finding the Neutral Axis

a) Elastic Neutral Axis

Function Nutel()

```matlab
function y_el=neut_el(input_arg)
```

%---

% PURPOSE

% To find the Neutral Axis when the timber is Linear Elastic

% Only Reinforcement Yields

% INPUT:

% y_el_prev   Neutral axis i the previous run

% eps_c   Compressive strain in the outermost timber fiber

% Ela   E-Modulus of Laminate/ reinforcement

% fy_t_la   Ultimate Tensile Strength of Reinforcement

% fy_c_la   Ultimate Tensile Strength of Reinforcement

% Zc   Depth till compression reinforcement

% Zt   Depth till Tension reinforcement

% hgl   Total Height of the beam

% bgl   Width of the beam

% Egl   E-Modulus of Glulam

% Alc   Area of compression reinforcement

% Alt   Area of tension Reinforcement

% nc   Number of laminates in compressive zone

% nt   Number of laminates in tension zone

% OUTPUT:

% yel   Depth of Neutral Axis when timber is in linear elastic phase

%--

%

% Copyright (c)   JOBIN JACOB & OLGA LUCIA GARZON

%   Department of Structural Engineering

%   Division of Steel and Timber Structures

%   CHALMERS UNIVERSITY OF TECHNOLOGY

```matlab
%-----------------------------------------------------------------------------------
y_el_prev=input_arg(1);

Zc=input_arg(2);

eps_c=input_arg(3);

Ela=input_arg(4);

fy_t_la=input_arg(5);

fy_c_la=input_arg(6);

Zc=input_arg(7);

Zt=input_arg(8);

hgl=input_arg(9);

bgl=input_arg(10);

Egl=input_arg(11);

Alc=input_arg(12);

Alt=input_arg(13);

nc=input_arg(14);

nt=input_arg(15);

flag=0;


eps_lc=(1-Zc/y_el_prev)*eps_c;              % strains in the compressive reinforcement
eps_lt=((hgl-y_el_prev-Zt)/y_el_prev)*eps_c;        % strains in the tensile reinforcement
for (i=1:5)
  sigma_t_lam=eps_lt*Ela;              %checking the tensile stresses in the laminate
  sigma_c_lam=eps_lc*Ela;              %checking the compressive stresses in the laminate
   if (sigma_t_lam>=fy_t_la)          %checkig tensile yielding of laminate
     sigma_t_lam=fy_t_la;                %if so fixing the tensile stresses to yield stresses
   end
   if (sigma_c_lam>=fy_c_la)        % checkig compressive yielding of the laminate
     sigma_c_lam=fy_c_la;            %if so fixing the compressive stresses to yield stresses
   end
   eps_lc_y=fy_c_la/Ela;
```

```matlab
    eps_lt_y=fy_t_la/Ela;

     % Nothing Yields!!!!

    if ((eps_lc<=eps_lc_y) & (eps_lt<=eps_lt_y))

        y_el=y_el_prev;

        if (flag ==1)

            y_el=y_el;

        end

        display('Nothing Yields');

end


    % only Compression Reinforcement yields


    if ((eps_lc>eps_lc_y) & (eps_lt<=eps_lt_y))

        a=eps_c*Egl*bgl;

        b=sigma_c_lam*Alc-1/2*eps_c*Egl*hgl*bgl+eps_c*Ela*Alt;

        c=eps_c*Ela*Alt*Zt-eps_c*Alt*hgl*Ela;

        y_el=(-b+sqrt(b^2-4*a*c))/(2*a);

        display('only Compression Reinforcement yields');

        flag=1;

end
    % only Tension Reinforcement yields

    if ((eps_lc<=eps_lc_y) & (eps_lt>eps_lt_y))

        a= eps_c*Egl*bgl;

        b= eps_c*Ela*Alc-1/2*eps_c*Egl*hgl*bgl-sigma_t_lam*Alt;

        c= -Zc*Ela*Alc*eps_c;

        y_el=(-b+sqrt(b^2-4*a*c))/(2*a);

        display('only Tension Reinforcement yields');

        flag=1;


    end
```

```matlab
    % Both Tension and Compression Reinforcements yields

  if ((eps_lc>eps_lc_y) & (eps_lt>eps_lt_y))

     y_el= (sigma_t_lam*Alt-sigma_c_lam*Alc)/(eps_c*Egl*bgl)+hgl/2;

     display('Both Tension and Compression Reinforcements yields');

     flag=1;

  end

  if (flag==1)

     eps_lc=(1-Zc/y_el)*eps_c;% strains in the compressive reinforcement

     eps_lt=((hgl-y_el-Zt)/y_el)*eps_c;% strains in the tensile reinforcement

  end

end
```

b) *Plastic Neutral Axis*

```matlab
function y_pl=neut_pl(input_arg)

%---------------------------------------------------------

% PURPOSE

%  To find the Neutral Axis when the timber is Linear Elastic

%  Only Reinforcement Yields

% INPUT:

% y_pl_prev     Neutral axis in the previous run

% Zc            Depth till compression reinforcment

% eps_c         Compressive strain in the outermost timber fiber

% Ela            E-Modulus of Laminate/ reinforcement

% fy_t_la       Ultimate Tensile Strength of Reinforcement

% fy_c_la       Ultimate Tensile Strength of Reinforcement

% Zc            Depth till compression reinforcment

% Zt            Depth till Tension reinforcement
```

% hgl   Total Height of the beam

% bgl   Width of the beam

% Egl   E-Modulus of Glulam

% Alc   Area of compression reinforcement

% Alt   Area of tension Reinforcement

% nc   Number of laminates in compressive zone

% nt   Number of laminates in tension zone

% f_c   Compresive strength of timber

% eps_e_c   Elastic strain limit for timber

% OUTPUT:

% yel   Depth of Neutral Axis when timber is in linear elstic phase

% OUTPUT:

% Depth of Neutral Axis

%---

%

% Copyright (c)   JOBIN JACOB & OLGA LUCIA GARZON

%   Department of Structural Engineering

%   Division of Steel and Timber Structures

%   CHALMERS UNIVERSITY OF TECHNOLOGY

%---

y_pl_prev=input_arg(1);

Zc=input_arg(2);

eps_c=input_arg(3);

Ela=input_arg(4);

fy_t_la=input_arg(5);

fy_c_la=input_arg(6);

Zc=input_arg(7);

Zt=input_arg(8);

hgl=input_arg(9);

```matlab
bgl=input_arg(10);

Egl=input_arg(11);

Alc=input_arg(12);

Alt=input_arg(13);

nc=input_arg(14);

nt=input_arg(15);

f_c=input_arg(16);

eps_e_c=input_arg(17);

flag=0;

eps_lc=(1-Zc/y_pl_prev)*eps_c;                % strains in the compressive reinforcement

eps_lt=((hgl-y_pl_prev-Zt)/y_pl_prev)*eps_c;  % strains in the tensile reinforcement

for (i=1:5)

    sigma_t_lam=eps_lt*Ela;       %checking the tensile stresses in the laminate

    sigma_c_lam=eps_lc*Ela;       %checking the compressive stresses in the laminate

    if (sigma_t_lam>=fy_t_la)      %checkig tensile yielding of laminate

        sigma_t_lam=fy_t_la;       %if so fixing the tensile stresses to yield stresses

    end

    if (sigma_c_lam>=fy_c_la)      % checkig compressive yielding of the laminate

        sigma_c_lam=fy_c_la;       %if so fixing the compressive stresses to yield stresses

    end

    eps_lc_y=fy_c_la/Ela;

    eps_lt_y=fy_t_la/Ela;

    % Only Timber Yields in compression!!!!

    if ((eps_lc<=eps_lc_y) & (eps_lt<=eps_lt_y))

        a=f_c*bgl*(eps_c-eps_e_c)/eps_c+f_c*bgl/2*(1-(eps_c-eps_e_c)/eps_c)-
eps_c*bgl/2*Egl;

        b=eps_c*(Ela*Alc+bgl*hgl*Egl+Alt*Ela);

        c=eps_c*(Zt*Alt*Ela-Zc*Ela*Alc-(bgl/2)*Egl*hgl^2-hgl*Alt*Ela);

        y_pl=(-b+sqrt(b^2-4*a*c))/(2*a);

    end
```

```matlab
% only Compression Reinforcement yields

if ((eps_lc>eps_lc_y) & (eps_lt<=eps_lt_y))

    a=1/2*f_c*bgl*(eps_c-eps_e_c)/eps_c+1/2*f_c*bgl-1/2*eps_c*Egl*bgl;

    b=eps_c*Ela*Alt+sigma_c_lam*Alc+1/2*eps_c*Egl*bgl*2*hgl;

    c=-1/2*eps_c*Egl*bgl*hgl*hgl-eps_c*Ela*Alc*(hgl-Zt);

    y_pl=(-b+sqrt(b^2-4*a*c))/(2*a);

    display('only Compression Reinforcement yields');

    flag=1;

end

% only Tension Reinforcement yields alongwith compressive

% plastification of timber

if ((eps_lc<=eps_lc_y) & (eps_lt>eps_lt_y))

    a=1/2*f_c*bgl*(eps_c-eps_e_c)/eps_c+1/2*f_c*bgl-1/2*eps_c*Egl*bgl;

    b=eps_c*Ela*Alc-sigma_t_lam*Alt+1/2*eps_c*Egl*bgl*2*hgl;

    c=-1/2*eps_c*Egl*bgl*hgl*hgl-eps_c*Ela*Alc*Zc;

    y_pl=(-b+sqrt(b^2-4*a*c))/(2*a);

    display('only Tension Reinforcement yields & compressive plastification');

    flag=1;

end

% Both Tension and Compression Reinforcements yields along with

% Compressive Plastification of timber

if ((eps_lc>eps_lc_y) & (eps_lt>eps_lt_y))

    a=1/2*f_c*bgl*(eps_c-eps_e_c)/eps_c+1/2*f_c*bgl-1/2*eps_c*Egl*bgl;

    b=sigma_c_lam*Alc-sigma_t_lam*Alt+1/2*eps_c*Egl*bgl*2*hgl;

    c=-1/2*eps_c*Egl*bgl*hgl*hgl;

    y_pl=(-b+sqrt(b^2-4*a*c))/(2*a);

    display('Both Tension and Compression Reinforcements yields & Compressive Plastification');

    flag=1;

end
```

```matlab
    if (flag==1)

        eps_lc=(1-Zc/y_pl)*eps_c;        % strains in the compressive reinforcement

        eps_lt=((hgl-y_pl-Zt)/y_pl)*eps_c;   % strains in the tensile reinforcement

    end

end
```



```matlab
    if (flag==1)
```

8.3 Appendix C: Calculating Stiffness of Glulam

Balk 1								
A	115*200	22655		Eglulam	8,20E+03			
Ahole	8*32	0						
Aglulam		22655						
ASteeltop		0		ECFRP	2,10E+05			
ASteelbottom		0		acfrp	25,61	(a-1)=	24,61	
Agluetop		0		Eglue	1,28E+04			
Agluebottom		0		aglue	1,56	(a-1)=	0,56	
	A [mm2]	z [mm]	a	ai*Ai	z*a*A	zeff	(a-1)*I	(a-1)*A*zeff^2
Glulam	22655	100	1	22655	2265500	0	73 268 158	0
Steeltop	0	15	25,61	0	0	-85	398 678	0
Steelbottom	0	185	25,61	0	0	85	797 356	0
Glue top	0	16	1,56	0	0	-84	64 337	0
Glue bottom	0	184	1,56	0	0	84	64 337	0
Σ				22655	2265500		74 592 866	0
z	100						Ieff	74592866,4
							Eieff=	6,12E+11
							Eieffreal=	6,12031E+11

Balk 2								
A	115*200	22655		Eglulam	9,49E+03			
Ahole	8*32	0						
Aglulam		22655						
ASteeltop		0		ECFRP	2,10E+05			
ASteelbottom		0		acfrp	22,13	(a-1)=	21,13	
Agluetop		0		Eglue	1,28E+04			
Agluebottom		0		aglue	1,35	(a-1)=	0,35	
	A [mm2]	z [mm]	a	ai*Ai	z*a*A	zeff	(a-1)*I	(a-1)*A*zeff^2
Glulam	22655	100	1	22655	2265500	0	73 268 158	0
Steeltop	0	15	22,13	0	0	-85	342 283	0
Steelbottom	0	185	22,13	0	0	85	684 565	0
Glue top	0	16	1,35	0	0	-84	40 002	0
Glue bottom	0	184	1,35	0	0	84	40 002	0
Σ				22655	2265500		74 375 009	0
z	100						Ieff	74375009,4
							Eieff=	7,06E+11
							Eieffreal=	7,06492E+11

<table>
<tr><td colspan="9" align="center">Balk 3</td></tr>
<tr><td>A</td><td>115*200</td><td>22655</td><td></td><td>Eglulam</td><td>8,38E+03</td><td></td><td></td><td></td></tr>
<tr><td>Ahole</td><td>8*32</td><td>256</td><td></td><td></td><td></td><td></td><td></td><td></td></tr>
<tr><td>Aglulam</td><td></td><td>21631</td><td></td><td></td><td></td><td></td><td></td><td></td></tr>
<tr><td>ASteeltop</td><td></td><td>240</td><td></td><td>ECFRP</td><td>2,10E+05</td><td></td><td></td><td></td></tr>
<tr><td>ASteelbottom</td><td></td><td>240</td><td></td><td>acfrp</td><td>25,06</td><td>(a-1)=</td><td>24,06</td><td></td></tr>
<tr><td>Agluetop</td><td></td><td>272</td><td></td><td>Eglue</td><td>1,28E+04</td><td></td><td></td><td></td></tr>
<tr><td>Agluebottom</td><td></td><td>272</td><td></td><td>aglue</td><td>1,53</td><td>(a-1)=</td><td>0,53</td><td></td></tr>
<tr><td></td><td></td><td></td><td></td><td></td><td></td><td></td><td></td><td></td></tr>
<tr><td></td><td>A [mm2]</td><td>z [mm]</td><td>a</td><td>ai*Ai</td><td>z*a*A</td><td>zeff</td><td>(a-1)*I</td><td>(a-1)*A*zeff^2</td></tr>
<tr><td>Glulam</td><td>21631</td><td>100</td><td>1</td><td>21631</td><td>2163100</td><td>0</td><td>73 268 158</td><td>0</td></tr>
<tr><td>Steeltop</td><td>240</td><td>15</td><td>25,06</td><td>6014,32</td><td>90214,8</td><td>-85</td><td>389 767</td><td>41 719 461</td></tr>
<tr><td>Steelbottom</td><td>240</td><td>185</td><td>25,06</td><td>6014,32</td><td>1112649</td><td>85</td><td>779 533</td><td>41 719 461</td></tr>
<tr><td>Glue top</td><td>272</td><td>16</td><td>1,53</td><td>415,4654</td><td>6647,446</td><td>-84</td><td>60 492</td><td>1 012 292</td></tr>
<tr><td>Glue bottom</td><td>272</td><td>184</td><td>1,53</td><td>415,4654</td><td>76445,63</td><td>84</td><td>60 492</td><td>1 012 292</td></tr>
<tr><td>Σ</td><td></td><td></td><td></td><td>34490,57</td><td>3449057</td><td></td><td>74 558 441</td><td>85 463 505</td></tr>
<tr><td></td><td></td><td></td><td></td><td></td><td></td><td></td><td></td><td></td></tr>
<tr><td>z</td><td>100</td><td></td><td></td><td></td><td></td><td></td><td>Ieff</td><td>160021946,1</td></tr>
<tr><td></td><td></td><td></td><td></td><td></td><td></td><td></td><td></td><td></td></tr>
<tr><td></td><td></td><td></td><td></td><td></td><td></td><td></td><td>Eieff=</td><td>1,34E+12</td></tr>
<tr><td></td><td></td><td></td><td></td><td></td><td></td><td></td><td>Eieffreal=</td><td>1,34113E+12</td></tr>
</table>

<table>
<tr><td colspan="9" align="center">Balk 4</td></tr>
<tr><td>A</td><td>115*200</td><td>22655</td><td></td><td>Eglulam</td><td>1,05E+04</td><td></td><td></td><td></td></tr>
<tr><td>Ahole</td><td>8*32</td><td>256</td><td></td><td></td><td></td><td></td><td></td><td></td></tr>
<tr><td>Aglulam</td><td></td><td>21631</td><td></td><td></td><td></td><td></td><td></td><td></td></tr>
<tr><td>ASteeltop</td><td></td><td>0</td><td></td><td>ECFRP</td><td>2,10E+05</td><td></td><td></td><td></td></tr>
<tr><td>ASteelbottom</td><td></td><td>480</td><td></td><td>acfrp</td><td>20,00</td><td>(a-1)=</td><td>19,00</td><td></td></tr>
<tr><td>Agluetop</td><td></td><td>0</td><td></td><td>Eglue</td><td>3,20E+03</td><td></td><td></td><td></td></tr>
<tr><td>Agluebottom</td><td></td><td>544</td><td></td><td>aglue</td><td>0,30</td><td>(a-1)=</td><td>-0,70</td><td></td></tr>
<tr><td></td><td></td><td></td><td></td><td></td><td></td><td></td><td></td><td></td></tr>
<tr><td></td><td>A [mm2]</td><td>z [mm]</td><td>a</td><td>ai*Ai</td><td>z*a*A</td><td>zeff</td><td>(a-1)*I</td><td>(a-1)*A*zeff^2</td></tr>
<tr><td>Glulam</td><td>21631</td><td>100</td><td>1</td><td>21631</td><td>2163100</td><td>-26,43348</td><td>73 268 158</td><td>15 829 701</td></tr>
<tr><td>Steeltop</td><td>0</td><td>15</td><td>20,00</td><td>0</td><td>0</td><td>-111,4335</td><td>307 800</td><td>0</td></tr>
<tr><td>Steelbottom</td><td>480</td><td>185</td><td>20,00</td><td>9600</td><td>1776000</td><td>58,56652</td><td>615 600</td><td>31 281 941</td></tr>
<tr><td>Glue top</td><td>0</td><td>16</td><td>0,30</td><td>0</td><td>0</td><td>-110,4335</td><td>-79 735</td><td>0</td></tr>
<tr><td>Glue bottom</td><td>544</td><td>184</td><td>0,30</td><td>165,7905</td><td>30505,45</td><td>57,56652</td><td>-79 735</td><td>- 1 253 350</td></tr>
<tr><td>Σ</td><td></td><td></td><td></td><td>31396,79</td><td>3969605</td><td></td><td>74 032 087</td><td>45 858 292</td></tr>
<tr><td></td><td></td><td></td><td></td><td></td><td></td><td></td><td></td><td></td></tr>
<tr><td>z</td><td>126,4335</td><td></td><td></td><td></td><td></td><td></td><td>Ieff</td><td>119890379</td></tr>
<tr><td></td><td></td><td></td><td></td><td></td><td></td><td></td><td></td><td></td></tr>
<tr><td></td><td></td><td></td><td></td><td></td><td></td><td></td><td>Eieff=</td><td>1,26E+12</td></tr>
<tr><td></td><td></td><td></td><td></td><td></td><td></td><td></td><td>Eieffreal=</td><td>1,26052E+12</td></tr>
</table>

Balk 5								
A	115*200	22655		Eglulam	9,05E+03			
Ahole	8*32	256						
Aglulam		21631						
ASteeltop		240		ECFRP	2,10E+05			
ASteelbottom		240		acfrp	23,20	(a-1)=	22,20	
Agluetop		272		Eglue	1,28E+04			
Agluebottom		272		aglue	1,41	(a-1)=	0,41	
	A [mm2]	z [mm]	a	ai*Ai	z*a*A	zeff	(a-1)*I	(a-1)*A*zeff^2
Glulam	21631	100	1	21631	2163100	0	73 268 158	0
Steeltop	240	15	23,20	5568,445	83526,68	-85	359 670	38 498 019
Steelbottom	240	185	23,20	5568,445	1030162	85	719 340	38 498 019
Glue top	272	16	1,41	384,6647	6154,635	-84	47 505	794 962
Glue bottom	272	184	1,41	384,6647	70778,3	84	47 505	794 962
Σ				33537,22	3353722		74 442 178	78 585 961
z	100						Ieff	153028138,6
							Eieff=	1,39E+12
							Eieffreal=	1,38879E+12

Balk 6								
A	115*200	22655		Eglulam	8,90E+03			
Ahole	8*32	256						
Aglulam		21631						
ASteeltop		0		ECFRP	2,10E+05			
ASteelbottom		480		acfrp	23,60	(a-1)=	22,60	
Agluetop		0		Eglue	3,20E+03			
Agluebottom		544		aglue	0,36	(a-1)=	-0,64	
	A [mm2]	z [mm]	a	ai*Ai	z*a*A	zeff	(a-1)*I	(a-1)*A*zeff^2
Glulam	21631	100	1	21631	2163100	-29,53408	73 268 158	19 761 088
Steeltop	0	15	23,60	0	0	-114,5341	366 047	0
Steelbottom	480	185	23,60	11325,84	2095281	55,46592	732 094	33 366 895
Glue top	0	16	0,36	0	0	-113,5341	-73 452	0
Glue bottom	544	184	0,36	195,5955	35989,57	54,46592	-73 452	-1 033 555
Σ				33152,44	4294370		74 219 396	52 094 429
z	129,5341						Ieff	126313824,5
							Eieff=	1,12E+12
							Eieffreal=	1,12233E+12

<table>
<tr><td colspan="8" align="center">Balk 7</td></tr>
<tr><td>A</td><td>115*197</td><td>22655</td><td></td><td>Eglulam</td><td>9,11E+03</td><td></td><td></td></tr>
<tr><td>Ahole</td><td>6*27</td><td>162</td><td></td><td></td><td></td><td></td><td></td></tr>
<tr><td>Aglulam</td><td></td><td>21035</td><td></td><td></td><td></td><td></td><td></td></tr>
<tr><td>ACFRPtop</td><td></td><td>175</td><td></td><td>ECFRP</td><td>3,00E+05</td><td></td><td></td></tr>
<tr><td>ACFRPbottom</td><td></td><td>175</td><td></td><td>acfrp</td><td>32,93</td><td>(a-1)=</td><td>31,93</td></tr>
<tr><td>Agluetop</td><td></td><td>635</td><td></td><td>Eglue</td><td>3,20E+03</td><td></td><td></td></tr>
<tr><td>Agluebottom</td><td></td><td>635</td><td></td><td>aglue</td><td>0,35</td><td>(a-1)=</td><td>-0,65</td></tr>
<tr><td></td><td></td><td></td><td></td><td></td><td></td><td></td><td></td></tr>
<tr><td></td><td>A [mm2]</td><td>z [mm]</td><td>a</td><td>ai*Ai</td><td>z*a*A</td><td>zeff</td><td>(a-1)*I</td><td>(a-1)*A*zeff^2</td></tr>
<tr><td>Glulam</td><td>21035</td><td>98,5</td><td>1</td><td>21035</td><td>2071947,5</td><td>0</td><td>73 268 158</td><td>0</td></tr>
<tr><td>CFRPtop</td><td>175</td><td>12,5</td><td>32,93</td><td>5762,898</td><td>72036,224</td><td>-86</td><td>517 280</td><td>41 328 093</td></tr>
<tr><td>CFRPbottom</td><td>175</td><td>184,5</td><td>32,93</td><td>5762,898</td><td>1063254,7</td><td>86</td><td>1 034 559</td><td>41 328 093</td></tr>
<tr><td>Glue top</td><td>635</td><td>16</td><td>0,35</td><td>223,0516</td><td>3568,8255</td><td>-82,5</td><td>-74 402</td><td>-2 803 824</td></tr>
<tr><td>Glue bottom</td><td>635</td><td>181</td><td>0,35</td><td>223,0516</td><td>40372,338</td><td>82,5</td><td>-74 402</td><td>-2 803 824</td></tr>
<tr><td>Σ</td><td></td><td></td><td></td><td>33006,9</td><td>3251179,6</td><td></td><td>74 671 192</td><td>77 048 538</td></tr>
<tr><td></td><td></td><td></td><td></td><td></td><td></td><td></td><td></td><td></td></tr>
<tr><td>z</td><td>98,5</td><td></td><td></td><td></td><td></td><td></td><td>Ieff</td><td>151719730,4</td></tr>
<tr><td></td><td></td><td></td><td></td><td></td><td></td><td></td><td></td><td></td></tr>
<tr><td></td><td></td><td></td><td></td><td></td><td></td><td></td><td>Eieff=</td><td>1,38E+12</td></tr>
<tr><td></td><td></td><td></td><td></td><td></td><td></td><td></td><td>Eieffreal=</td><td>1,38403E+12</td></tr>
</table>

<table>
<tr><td colspan="8" align="center">Balk 9</td></tr>
<tr><td>A</td><td>115*197</td><td>22655</td><td></td><td>Eglulam</td><td>9,26E+03</td><td></td><td></td></tr>
<tr><td>Ahole</td><td>14*32</td><td>448</td><td></td><td></td><td></td><td></td><td></td></tr>
<tr><td>Aglulam</td><td></td><td>19967</td><td></td><td></td><td></td><td></td><td></td></tr>
<tr><td>ACFRPtop</td><td></td><td>216</td><td></td><td>ECFRP</td><td>1,55E+05</td><td></td><td></td></tr>
<tr><td>ACFRPbottom</td><td></td><td>432</td><td></td><td>acfrp</td><td>16,75</td><td>(a-1)=</td><td>15,75</td></tr>
<tr><td>Agluetop</td><td></td><td>1128</td><td></td><td>Eglue</td><td>3,20E+03</td><td></td><td></td></tr>
<tr><td>Agluebottom</td><td></td><td>912</td><td></td><td>aglue</td><td>0,35</td><td>(a-1)=</td><td>-0,65</td></tr>
<tr><td></td><td></td><td></td><td></td><td></td><td></td><td></td><td></td></tr>
<tr><td></td><td>A [mm2]</td><td>z [mm]</td><td>a</td><td>ai*Ai</td><td>z*a*A</td><td>zeff</td><td>(a-1)*I</td><td>(a-1)*A*zeff^2</td></tr>
<tr><td>Glulam</td><td>19967</td><td>98,5</td><td>1</td><td>19967</td><td>1966749,5</td><td>-9,38612</td><td>73 268 158</td><td>1 995 888</td></tr>
<tr><td>CFRPtop</td><td>216</td><td>15</td><td>16,75</td><td>3617,426</td><td>54261,388</td><td>-92,88612</td><td>255 107</td><td>29 346 928</td></tr>
<tr><td>CFRPbottom</td><td>432</td><td>182</td><td>16,75</td><td>7234,852</td><td>1316743</td><td>74,11388</td><td>510 214</td><td>37 367 162</td></tr>
<tr><td>Glue top</td><td>1128</td><td>16</td><td>0,35</td><td>390,0078</td><td>6240,1245</td><td>-91,88612</td><td>-75 034</td><td>-6 230 912</td></tr>
<tr><td>Glue bottom</td><td>912</td><td>181</td><td>0,35</td><td>315,3254</td><td>57073,904</td><td>73,11388</td><td>-75 034</td><td>-3 189 607</td></tr>
<tr><td>Σ</td><td></td><td></td><td></td><td>31524,61</td><td>3401067,9</td><td></td><td>73 883 410</td><td>59 289 459</td></tr>
<tr><td></td><td></td><td></td><td></td><td></td><td></td><td></td><td></td><td></td></tr>
<tr><td>z</td><td>107,8861</td><td></td><td></td><td></td><td></td><td></td><td>Ieff</td><td>133172869,3</td></tr>
<tr><td></td><td></td><td></td><td></td><td></td><td></td><td></td><td></td><td></td></tr>
<tr><td></td><td></td><td></td><td></td><td></td><td></td><td></td><td>Eieff=</td><td>1,23E+12</td></tr>
<tr><td></td><td></td><td></td><td></td><td></td><td></td><td></td><td>Eieffreal=</td><td>1,23234E+12</td></tr>
</table>

Balk 10								
A	115*197	22655		**Eglulam**	9,30E+03			
Ahole	14*32	448						
Aglulam		19967						
ACFRPtop		216		**ECFRP**	1,55E+05			
ACFRPbottom		432		**acfrp**	16,67	(a-1)=	15,67	
Agluetop		1128		**Eglue**	3,20E+03			
Agluebottom		912		**aglue**	0,34	(a-1)=	-0,66	
	A [mm2]	z [mm]	a	ai*Ai	z*a*A	zeff	(a-1)*I	(a-1)*A*zeff^2
Glulam	19967	98,5	1	19967	1966749,5	-9,358069	73 268 158	1 983 977
CFRPtop	216	15	16,67	3600,387	54005,807	-92,85807	253 829	29 182 288
CFRPbottom	432	182	16,67	7200,774	1310540,9	74,14193	507 658	37 208 127
Glue top	1128	16	0,34	388,1708	6210,7323	-91,85807	-75 221	-6 242 609
Glue bottom	912	181	0,34	313,8402	56805,076	73,14193	-75 221	-3 200 001
Σ				31470,17	3394312		73 879 203	58 931 783
z	107,8581						**Ieff**	132810985,2
							Eieff=	1,24E+12
							Eieffreal=	1,24656E+12

8.4 Appendix D: Input Values for Non-Linear Model

	Beam 1	Beam 4	Beam 5	Beam 6	Beam 7	Beam 9
Egl	8200	10000	8800	8800	9000	9100
Ela	-	21000	21000	21000	300000	165000
fcugl	34	34	34	34	34	35
ftugl	35	40	35	40	35	63
fy_t_la	-	300	300	300	1200	275
fy_c_la	-	300	300	300	1200	275